Atmospheric Radiation II
("shortwave")

ATMS 533

Autumn 2013

Stephen Warren
Department of Atmospheric Sciences
University of Washington
sgw@uw.edu

BARROW. INTRO. TO MOLECULAR SPECTROSCOPY

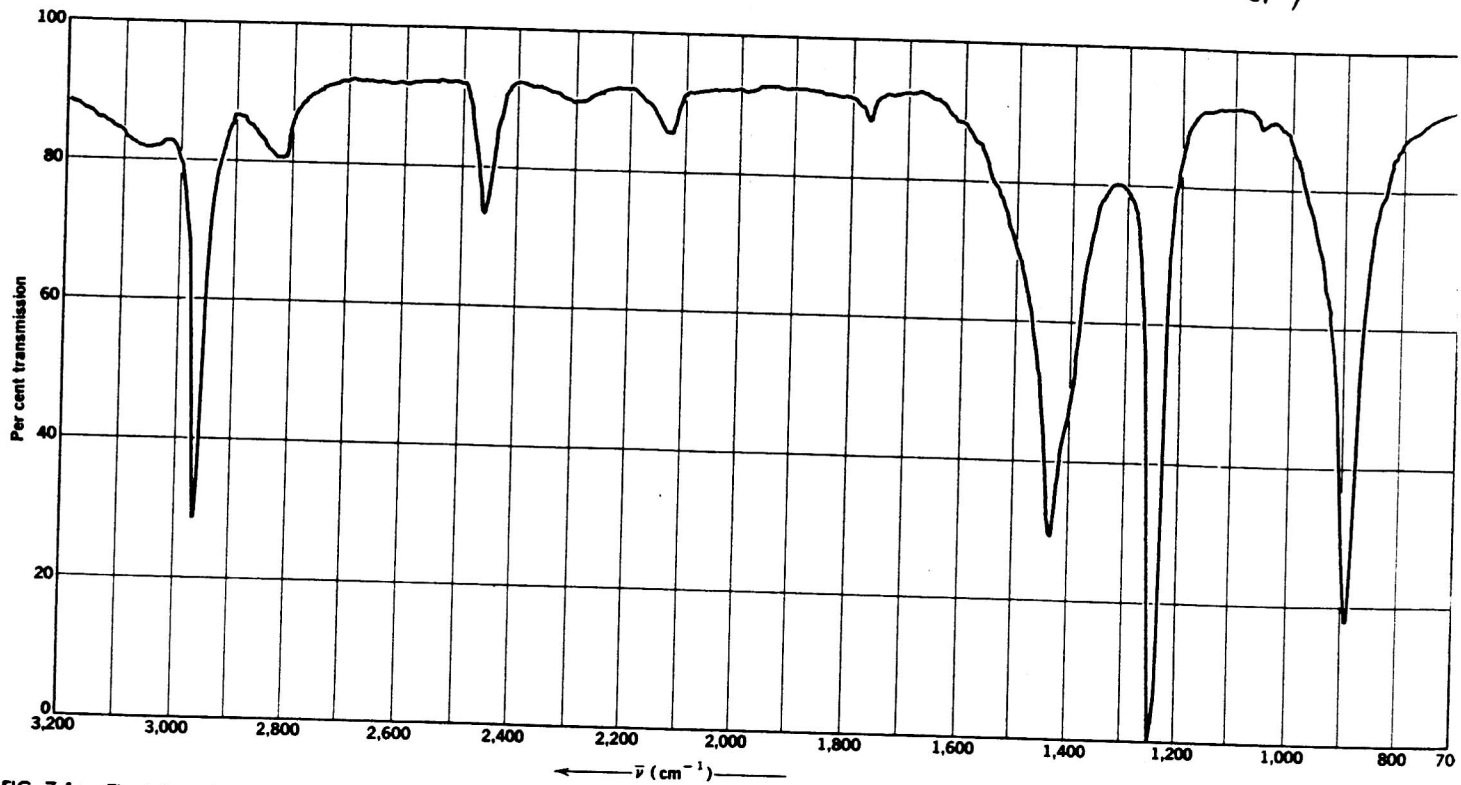

FIG. 7-1a The infrared spectrum of CH_3I as a liquid.

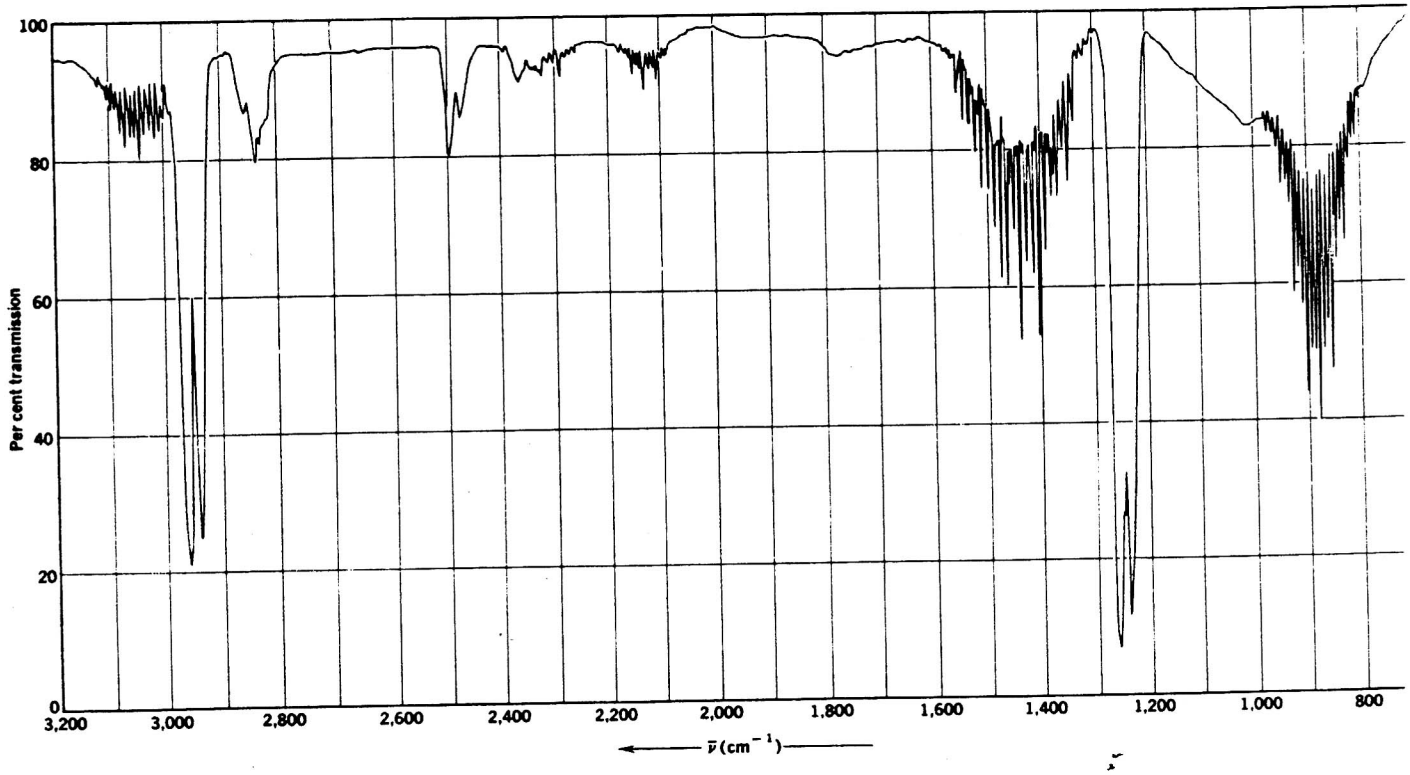

FIG. 7-1b The infrared spectrum of CH_3I as a vapor.

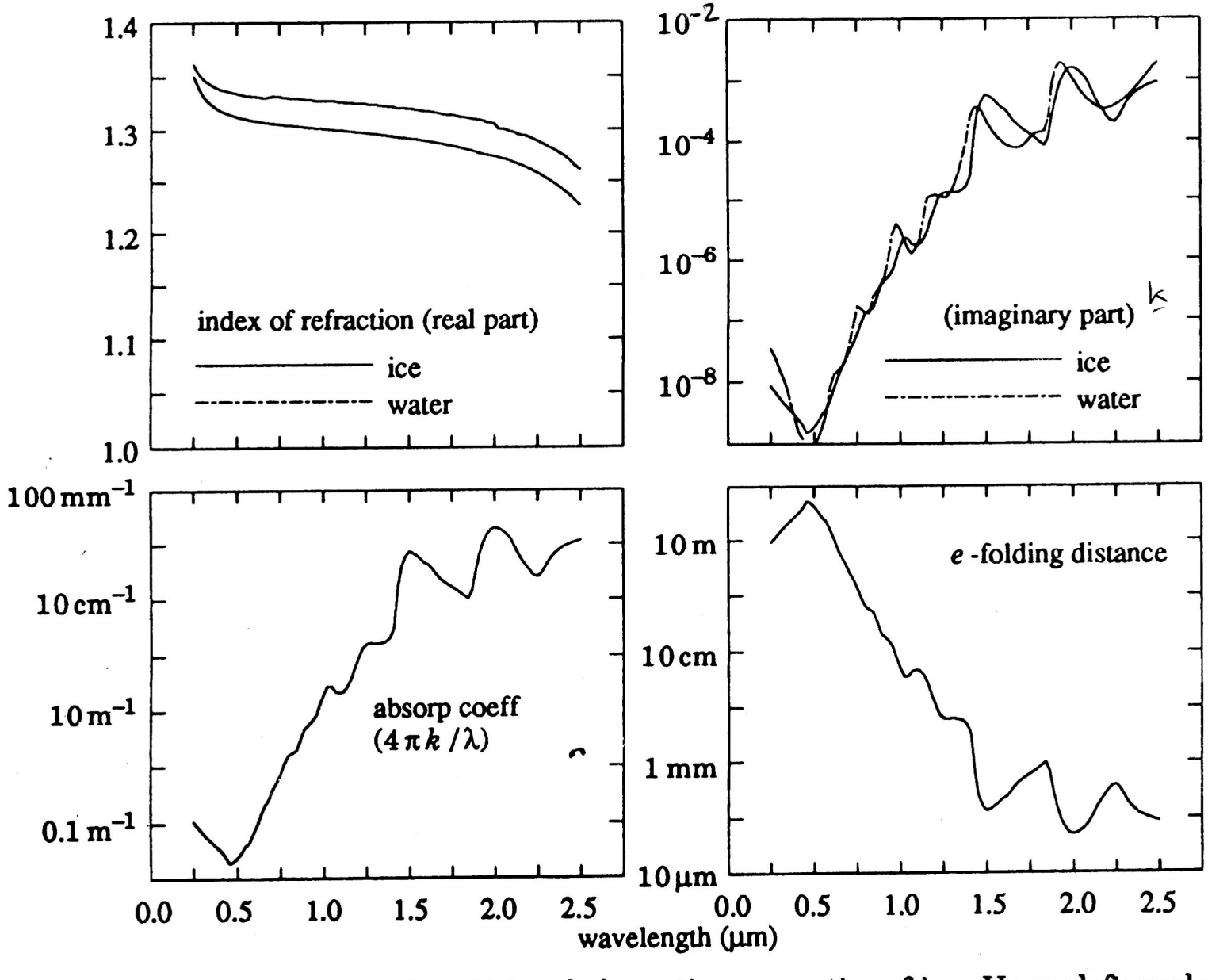

Figure 1. Complex refractive index ($n + i\,k$) and absorption properties of ice. Upper left: real part of refractive index (n). Upper right: imaginary part of refractive index (k). Lower left: absorption coefficient ($4\pi k/\lambda$). Lower right: e-folding distance, at which intensity is reduced to e^{-1}.

ATMS 533. Atmospheric Radiation II Autumn 2013

Instructor: Stephen Warren
room 524 ATG, tel. 543-7230. sgw@uw.edu

COURSE DESCRIPTION

(a) Radiative transfer: methods for solving the radiative transfer equation including scattering.

(b) Scattering and absorption of light by small atmospheric particles: Rayleigh scattering, Mie theory.

A particular application emphasized in the course is the interaction of clouds with solar radiation.

Prerequisite: (1) undergraduate electricity and magnetism.
(2) ATMS 532 is highly desirable.

COURSE OUTLINE

A. Radiative Transfer
1. Definitions and radiation quantities
2. Radiative transfer equation (r.t.e.)
3. Formal solution of r.t.e.
4. Plane-parallel form of r.t.e.
5. Azimuthally-averaged r.t.e.
6. Integral equation for source function
7. Monte-Carlo method
8. Representation of anisotropic phase functions in r.t.e.
9. r.t.e. for plane-parallel atmosphere illuminated by direct solar beam.
10. Two-stream method
11. Eddington method for multi-layer atmosphere
12. Phase function truncation
13. Doubling method
14. Discrete ordinates method

B. Single Scattering
1. Review of electromagnetic theory
2. Polarized light
3. Reflection at an interface
4. Theory of optical constants
5. Rayleigh scattering
6. Mie theory
7. Results of Mie theory
8. Nonspherical particles

TEXTBOOKS

Petty, G.W., 2006: *A First Course in Atmospheric Radiation.* Sundog Publishing.

Thomas, G., and K. Stamnes. *Radiative Transfer in the Atmosphere and Ocean.* Cambridge Univ. Press, 1999.

REFERENCE BOOKS

A. General

Liou, K.N. *An Introduction to Atmospheric Radiation* (second edition). Academic Press, 2002.

Goody and Yung. *Atmospheric Radiation* (second edition). Oxford, 1989.

Bohren, C.F., and E.E. Clothiaux, 2006: *Fundamentals of Atmospheric Radiation.* Wiley.

B. Radiative transfer

Menzel, D.H. (ed.) *Selected Papers on the Transfer of Radiation.* Dover, 1966.

Chandrasekhar, S. *Radiative Transfer.* Dover, 1966.

Mihalas, D. *Stellar Atmospheres.* Freeman, 1978.

Kourganoff. *Basic Methods in Transfer Problems.* 1950.

C. Single Scattering

van de Hulst, H.C. *Light Scattering by Small Particles.* Dover, 1981.

Bohren, D.F., and D.R. Huffman. *Absorption and Scattering of Light by Small Particles.* Wiley, 1983.

Hansen, J.E., and L.D. Travis. "Light Scattering in planetary atmospheres" *Space Science Reviews*, **16**, 527- 610 (1974).

McCartney, E.J. *Optics of the Atmosphere.* Wiley, 1976.

D. Applications

Paltridge, G.W., and C.M.R. Platt. *Radiation Processes in Meteorology and Climatology.* Elsevier, 1976.

These books will be on reserve in the Engineering Library for Atmos. Sci. 533, Autumn Quarter 2013.

510.8108 In8 v.1 Cashwell and Everett: *A Practical Manual on the Monte Carlo Method*

523 C361r Chandrasekhar, S. *Radiative Transfer.* Dover, 1966.

535.4 H879L van de Hulst, H.C. *Light Scattering by Small Particles.*

QB 817 M4 1966 Menzel: *Selected Papers on the Transfer of Radiation.*

QC 175.25.R3 T48 1999 Thomas, G., and K. Stamnes. *Radiative Transfer in the Atmosphere and Ocean.* Cambridge Univ. Press, 1999.

QC 882 B63 1983. Bohren, D.F., and D.R. Huffman. *Absorption and Scattering of Light by Small Particles.* Wiley, 1983.

QC912.3 .B64 2006 Bohren, C.F., and E.E. Clothiaux, 2006: *Fundamentals of Atmospheric Radiation.* Wiley.

QC 912.3 G66 Goody and Yung: *Atmospheric Radiation.* Oxford, 1989.

QC 912.3 L56. Liou: *An Introduction to Atmospheric Radiation.* (second edition). Academic Press, 2002.

QC 912.3 P34 Paltridge and Platt: *Radiative Processes in Meteorology and Climatology.* Elsevier, 1976.

QC 976 S3 M3 McCartney, E.J. *Optics of the Atmosphere.* Wiley, 1976.

JOURNALS

Journal of Quantitative Spectroscopy and Radiative Transfer
Astrophysical Journal
Journal of the Atmospheric Sciences
Applied Optics

ASSIGNMENTS

homework problems (60%)

computer project (30%)

class participation (10%)

Applications

reflection, transmission and absorption of light by clouds, snow, and aerosols
solar albedo of clouds and surfaces
microwave and infrared emissivity of surfaces
radar reflectivity of raindrops and hailstones
remote sensing of Earth's atmosphere and surface by reflected solar radiation
Earth radiation budget: problems of sampling in time and angle
climatic effects of aerosols
parameterization of solar radiation in the atmosphere

Detailed list of topics

A. Multiple Scattering

1. Introduction
   - Definition of terms: absorption, emission, scattering, incoherent radiation, plane-parallel atmosphere, direct problems and inverse problems
2. Radiative transfer equation
   - Absorption coefficient, optical depth, transmittance, mean-free-path, scattering coefficient, emission coefficient, source function, phase function
   - Examples of phase functions
   - Single-scattering albedo, examples
   - Examples of source function S
3. Formal solution of *r.t.e.*: solution of intensity in terms of source function
4. Plane-parallel form of r.t.e.
   - Solutions of emergent intensity for specified source functions
   - Limb brightening, limb darkening
5. Azimuthally-averaged r.t.e.
6. Milne's integral equation for source function
   - Exponential integrals
   - Iterative solution of integral equation (order-of-scattering series)
7. Monte-Carlo method; assign project.
8. Representation of anisotropic phase functions in r.t.e.
   - Examples of phase functions for molecules, aerosols, cloud droplets
   - Polynomial expansion of phase function
   - Moments of phase function
   - Henyey-Greenstein phase function
9. R.T.E. for plane-parallel atmosphere illuminated by direct solar beam
   - Sign of μ
   - Separation of direct and diffuse intensity
   - Average over azimuth
   - Polynomial expansion of azimuthally-averaged phase function
10. Two-stream method
    - Backscattered fraction, relation to asymmetry factor
    - Derivation of two-stream equations
    - Examples of results
11. Eddington method for multi-layer atmosphere
12. Phase-function truncation
    - Delta-Eddington method
    - Delta-M
13. Doubling method
14. Discrete Ordinates Method

B. Single Scattering

1. Review of electromagnetic theory
   - Coulomb's law, electric field, Gauss's law, dipole moment, polarizability, polarization, electric displacement, electric susceptibility, permittivity, dielectric constant
   - Magnetic field, Biot-Savart law, current, magnetization, bound currents, displacement current, magnetic susceptibility, magnetic permeability, conductivity
   - Maxwell's equations
   - EM wave solution to Maxwell's equations
     - Complex relative permittivity, complex refractive index
   - Energy stored in EM field, energy transported by EM field
2. Polarized light
3. Reflection at an interface
4. Theory of optical constants: frequency-dependence of permittivity and conductivity
   - Examples of optical constants; variation with wavelength
5. Rayleigh scattering: derivation of dependence on wavelength, angle, polarization
6. Mie theory
   - Outline of derivation
   - Methods of computation
   - Heterogeneous particles; mixing rules
7. Results of Mie theory: examples from van de Hulst, Hansen & Travis
8. Nonspherical particles; representation by "equivalent spheres"

Radiation crossing a surface.

Surface area element dA with normal $\hat{n}$

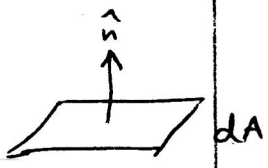

1. Flux F (Irradiance E)

$$F = \frac{d^2Q}{dA\,dt} \quad (W m^{-2}) \qquad (1)$$

where dQ is energy crossing face dA between time t and $t+dt$.

2. Spectral flux

$$F_\lambda = \frac{d^3Q}{dA\,dt\,d\lambda} \quad \left[W m^{-2} (\mu m)^{-1}\right]$$

or $$F_\nu = \frac{d^3Q}{dA\,dt\,d\nu} \quad \begin{bmatrix} W m^{-2} Hz^{-1} & \text{if } \nu \text{ in } Hz = sec^{-1} \\ W m^{-2} (cm^{-1})^{-1} & \text{if } \nu \text{ in } cm^{-1} \end{bmatrix}$$

Geometry of a sphere

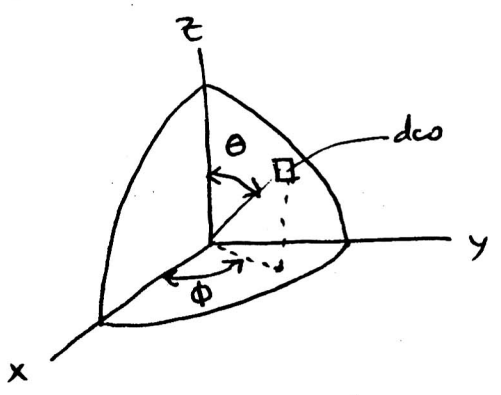

solid angle element:

$$d\omega = \sin\theta\, d\theta\, d\phi$$

θ = zenith angle

ϕ = azimuth angle.

$$\int_{\text{sphere}} d\omega = \int_0^{2\pi} d\phi \int_0^{\pi} \sin\theta\, d\theta = 4\pi \text{ steradians (sr)}$$

③ Intensity I (Radiance L)

Intensity is energy flow across a surface entering angular element $d\omega$.

Intensity is defined from the point of view of the detector; i.e., referred to a surface area perpendicular to the direction of view $\hat{\Omega}$. To express it in terms of a different surface (such as a horizontal surface), that surface must be projected onto the perpendicular surface, multiplying by the cosine of the zenith angle θ.

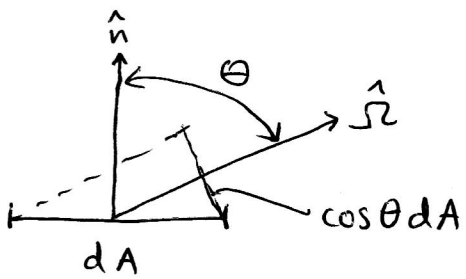

Intensity:

$$I = \frac{d^3Q}{dt\, d\omega \cos\theta\, dA} \qquad (W m^{-2} sr^{-1}) \qquad (2)$$

④ Spectral intensity I_λ, I_ν

Just as for spectral flux:

$$I_\lambda = \frac{dI}{d\lambda} \qquad I_\nu = \frac{dI}{d\nu}$$

$$F_\lambda = \frac{dF}{d\lambda} \qquad F_\nu = \frac{dF}{d\nu}$$

Relation of intensity to flux

Comparing (1), (2):

$$I = \frac{dF}{\cos\theta\, d\omega}$$

or $$F = \int I(\theta,\phi)\cos\theta\, d\omega$$

Separate the upward and downward fluxes, so the integral goes over one hemisphere. E.g. for the upward flux $F\uparrow$:

$$F\uparrow(z) = \int_{2\pi} I\uparrow(\theta,\phi,z)\cos\theta\, \underbrace{d\omega}_{\sin\theta\, d\theta\, d\phi}$$

$$= \int_0^{2\pi} d\phi \int_0^{\pi/2} I\uparrow(\mu,z)\, \underbrace{\cos\theta}_{\mu}\, \underbrace{\sin\theta\, d\theta}_{-d\mu}$$

if I indep. of ϕ or an average over ϕ

$$F_\uparrow(z) = 2\pi \int_0^1 I\uparrow(\mu,z)\,\mu\, d\mu$$

"vector irradiance" to oceanographers because of μ-weighting

Special case of I independent of μ in one hemisphere (e.g. upward emission from an isotropic emitter)

$$F(z) = 2\pi I(z) \underbrace{\int_0^1 \mu\, d\mu}_{1/2} = \pi I$$

5. Mean intensity

$$\bar{I} = \frac{1}{4\pi} \int_{4\pi} I \, d\omega$$ (no cosine-weighting)

"Scalar irradiance" $2\pi \int_0^1 I \, d\mu$ in one hemisphere (oceanography)

"Actinic flux" $4\pi \bar{I}$ (photochemistry)

6. Radiant energy density u (Joules/m^3)

$$u = \frac{4\pi}{c} \bar{I}$$

In general, radiance I can depend on
location (x,y,z)
angle (θ,ϕ)
time (t).

In the atmosphere and ocean, we assume I is independent of t ("steady") during the time it takes for a photon to transit the atmosphere.

We often assume I is independent of x,y ("plane-parallel", "horizontally homogeneous"), because in a planetary atmosphere I varies much more rapidly with z than with x,y.

The dependence is thus reduced to $I(z, \theta, \phi)$.

For thermal infrared radiation we can also usually assume that I is independent of ϕ ("azimuthally symmetric"). This approximation is also valid for solar radiation below or within a sufficiently thick cloud. In this case we have $I(z, \theta)$ or $I(z,\mu)$, where $\mu = \cos \theta$.

The special case of I independent of (θ, ϕ) is "isotropic".

Interaction of Radiation with Matter (ATMS 533)

Working definitions:

1. Absorption: A photon is destroyed. Its energy is distributed by collisions into other forms of energy (vibrational, rotational, etc.). The frequency of subsequently *emitted* radiation is independent of the frequency of the absorbed photon. [Assuming collision-dominated; i.e. that frequency of collisional transitions is much greater than frequency of radiation-induced transitions. This is the assumption of "local thermodynamic equilibrium".]

2. Scattering: The photon changes direction but not frequency.

3. Emission: A photon is created. The molecule emitting the photon loses internal energy (vibrational, rotational, etc.) equivalent to the energy of the photon.

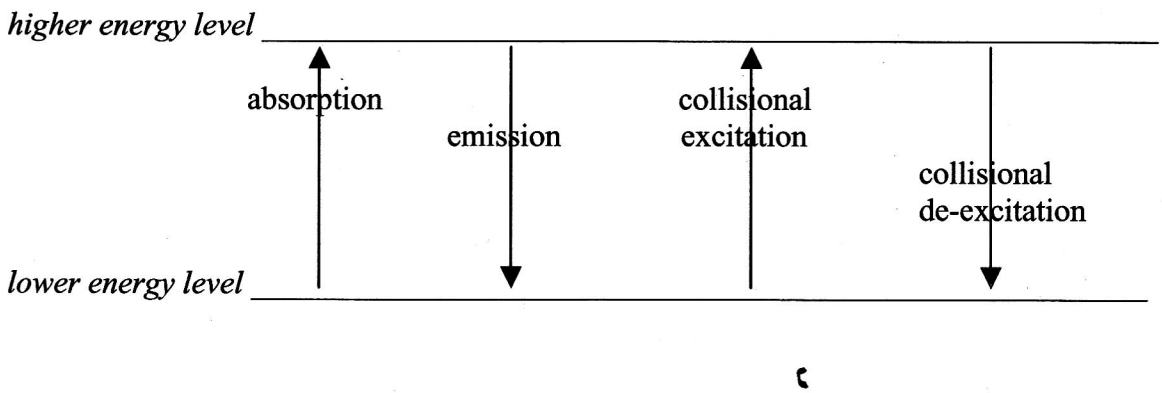

4. Extinction: All processes that remove photons from a beam of light. Extinction is the sum of scattering-out and absorption.

5. A beam of light passing through a medium can be:
Depleted by *scattering*-out-of-the-beam and by *absorption.*
Augmented by *scattering*-into-the-beam and by *emission.*

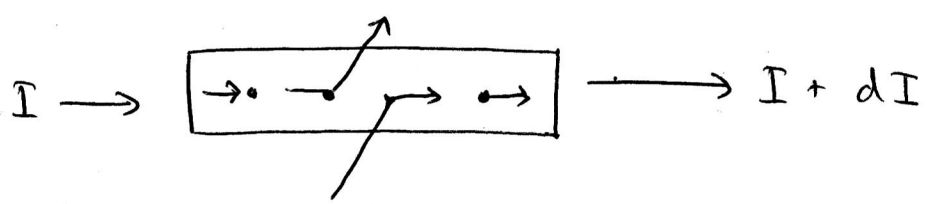

I. Radiative transfer equation for pure absorption (no scattering or emission)

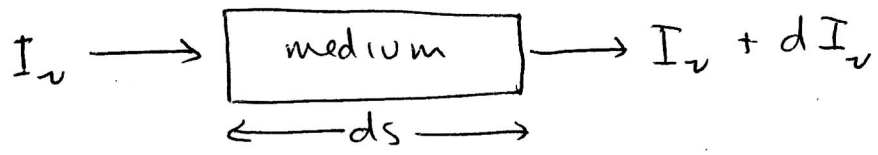

$$dI_\nu = -\sigma(\nu) I_\nu ds \qquad (1)$$

The minus-sign indicates that the intensity decreases. The change in intensity dI_ν is proportional to the intensity I_ν (assuming that photons do not interact with each other) and to the path increment *ds*. $\sigma(\nu)$ is the proportionality constant, the *linear absorption coefficient*, with units m^{-1}.

The dependence of dI_ν on the density of the absorbing material is contained within σ; it is often useful to write it this dependence explicitly, especially if density varies with s. There are then three ways of writing (1), with three different kinds of absorption coefficient:

$$dI_\nu = -\sigma(\nu) I_\nu ds$$

σ is the linear absorption coefficient (m^{-1}), used for bulk liquids and solids and also generally.

$$dI_\nu = -k_m(\nu)\rho(s) I_\nu ds$$

k_m is the mass absorption coefficient (m^2/g), used for gases; ρ is density (g/m^3).

$$dI_\nu = -k_n(\nu) n(s) I_\nu ds$$

k_n is the absorption cross-section (m^2/particle), used for aerosol particles and cloud droplets. n is number-density (particles/m^3). This form is also used sometimes for gases, where k_n is then the molecular absorption cross section (m^2/molecule).

We solve the r.t.e. (1) by integrating over a finite distance from s_1 to s_2:

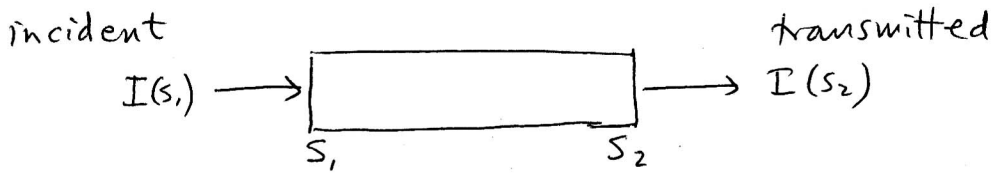

$$\int \frac{dI}{I} = -\int_{s_2}^{s_1} \sigma ds \quad \text{(dropping the subscript } \nu \text{ for simplicity).}$$

This results in the *Bouguer-Lambert law of absorption:*

$$I(s_2) = I(s_1) \exp\left[-\int_{s_1}^{s_2} \sigma ds \right]. \qquad (2)$$

The exponent (without the minus-sign) is called the *optical depth* τ (sometimes written δ); τ varies with ν because σ varies with ν:

$$\tau_\nu(s_1, s_2) = \left| \int_{s_1}^{s_2} \sigma(\nu) ds \right|.$$

For a gas, $\sigma = k_m \rho$, so

$$\tau_\nu(s_1, s_2) = \int_{s_1}^{s_2} k_\nu(s) \rho(s) ds, \qquad \text{or} \qquad d\tau_\nu = k_\nu \rho ds.$$

In terms of optical depth, (1) and (2) can be written as

$$\frac{dI_\lambda}{d\tau_\lambda} = -I_\lambda \quad , \quad \text{differential form of r.t.e. for pure absorption.} \qquad (1')$$

$$I_\lambda(s_2) = I_\lambda(s_1)\, e^{-\tau_\lambda(s_1, s_2)} \quad , \quad \text{solution of r.t.e. for pure absorption.} \qquad (2')$$

The <u>transmittance</u> (sometimes called <u>transmissivity</u>) t is the ratio of transmitted light to incident light.

$$t_\lambda(s_1, s_2) = \frac{I_\lambda(s_2)}{I_\lambda(s_1)} = e^{-\tau_\lambda(s_1, s_2)}$$

Thus, at an optical depth of 1.0, the intensity drops to $\frac{1}{e}$ of its initial value:

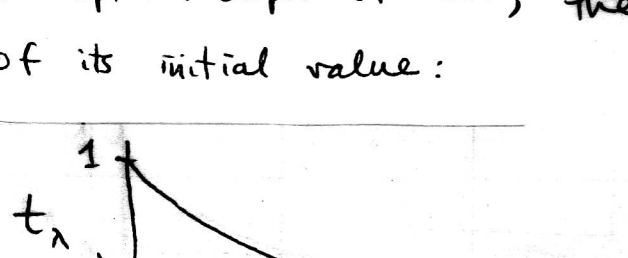

If the medium is homogeneous (k_λ, ρ independent of s), then $\tau_\lambda(s_1, s_2) = k_\lambda \rho\,(s_2 - s_1)$, and (2) becomes

$$I_\lambda(s_2) = I_\lambda(s_1)\, e^{-k_\lambda \rho (s_2 - s_1)}$$ <u>Beer's law</u>

In a <u>plane-parallel atmosphere</u> we use the vertical coordinate z instead of the path-coordinate s. Consider radiance along a direction (θ, ϕ) in the atmosphere. θ is the zenith angle.

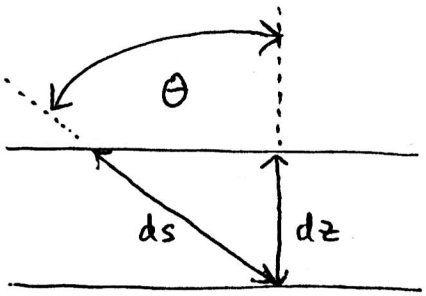

$$ds = \sec\theta\, dz = \frac{dz}{\cos\theta} = \frac{dz}{\mu}$$

Optical depth in the atmosphere is normally measured vertically unless otherwise specified. The optical depth along the path, $\tau(\text{path})$, will in general be larger than $\tau(\text{vertical})$:

$$\tau(\text{path}) = \tau(\text{vertical}) / \mu.$$

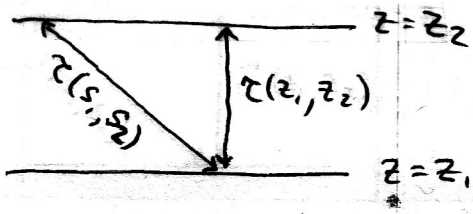

Using τ to mean $\tau(\text{vertical})$, our formulas become:

<u>Differential form of r.t.e.</u> $$\frac{dI(\theta)}{d\tau} = \frac{-I(\theta)}{\mu}$$

<u>Solution of r.t.e.</u> $$I(z_2, \theta) = I(z_1, \theta)\, e^{-\tau(z_1, z_2)/\mu}$$

<u>Transmittance</u> $$t_\lambda(z_1, z_2, \theta) = e^{-\tau(z_1, z_2)/\mu}$$

II. Radiative transfer equation including scattering

A. Depletion of the beam.

By analogy to the absorption coefficient, we can also have a scattering coefficient. For scattering out of the beam, an equation similar to (1) applies:

$$dI_\lambda = -k_\lambda^s \rho I_\lambda ds \quad , \text{ where } k_\lambda^s \text{ is a}$$

mass scattering coefficient at this wavelength.

If both absorption and scattering occur, we have

$$dI_\lambda^s = -k_\lambda^s \rho I_\lambda ds$$

$$dI_\lambda^a = -k_\lambda^a \rho I_\lambda ds \quad ,$$

where the superscripts are added to distinguish depletion due to absorption, dI_λ^a, from that due to scattering, dI_λ^s. The total depletion is just the sum:

$$dI_\lambda = dI_\lambda^a + dI_\lambda^s = -(k_\lambda^s + k_\lambda^a) \rho I_\lambda ds$$

The sum of absorption and scattering coefficients which appears is called the mass extinction coefficient k_λ^e:

$$k_\lambda^e = k_\lambda^s + k_\lambda^a \; .$$

We will now drop the λ-subscript for convenience (but remembering that we are still referring only to a particular wavelength).

Summarizing, we have

mass extinction coeff. $k_e = k_a + k_s$ $(m^2 g^{-1})$

linear extinction coeff. $\sigma_e = \sigma_a + \sigma_s$ (m^{-1}), where $\sigma_e = k_e \rho$

extinction optical depth $\tau = \tau_e = \tau_a + \tau_s$

where τ_a = absorption optical depth

and τ_s = scattering optical depth.

If "optical depth" is used without a qualifier, it means extinction optical depth.

B. Additions to the beam.

Define a mass "emission" coefficient j_λ, which includes all gains, not just emission:

$j = j_{em} + j_s$ (emission + scattering-into-the-beam).

The full r.t.e. is

$$dI = -\text{losses} + \text{gains}$$

$$dI = -k_e \rho I ds + j\rho\, ds \qquad (3)$$

Units of j are $(W m^{-2} sr^{-1})(m^2 g^{-1})$

↑ units of I ↑ units of k

To make the r.t.e. symmetric, we define a source function

$S_\lambda = S_\lambda^s + S_\lambda^{em}$, as

$$S_\lambda = \frac{J_\lambda}{k_\lambda^e} \quad \text{or} \quad S = \frac{J}{k_e} .$$

S will have units of intensity.

Then the r.t.e. (3) becomes

$$dI = -k_e \rho I ds + k_e \rho S ds .$$

Since $d\tau = k_e \rho ds$, this simplifies to

$$\frac{dI}{d\tau} = -I + S \qquad (4)$$

[So S is intensity added to the beam per unit optical depth.]
The source function contains both

emission (which depends on temperature but not on intensity field)

and scattering-in (which depends on intensity field).

The emission source function S^{em} we will specify later as proportional to Planck's blackbody function. For now we will just note that it is a function of temperature: $S^{em} = S^{em}(T)$.

The scattering source function S^s is a sum over contributions from all directions. Energy removed from a beam $I(\hat{\Omega}')$ by scattering is redirected in angle according to the phase function $P(\hat{\Omega}', \hat{\Omega})$, defined as follows:

Given a photon that was incident from solid angle $d\omega'$ about $\hat{\Omega}'$ and has been scattered, then $\frac{1}{4\pi} P(\hat{\Omega}', \hat{\Omega})\, d\omega$ is the probability that the photon will reappear in solid angle element $d\omega$ about $\hat{\Omega}$.

The average value of P is 1: $\int_{4\pi} \frac{1}{4\pi} P(\hat{\Omega}', \hat{\Omega})\, d\omega = 1$.

Now we can write the explicit form of the additions to the beam $\hat{\Omega}$ due to scattering:

$$J_s(z, \hat{\Omega}) = \int_{4\pi} d\omega'\, k_s\, I(z, \hat{\Omega}')\, \frac{1}{4\pi} P(\hat{\Omega}', \hat{\Omega}) \qquad (5)$$

and the scattering source function is

$$S^s = \frac{J_s}{k_e} = \int_{4\pi} \frac{d\omega'}{4\pi}\, \frac{k_s}{k_e}\, I(\hat{\Omega}')\, P(\hat{\Omega}', \hat{\Omega}).$$

[The quantity $\frac{k_s}{k_e}$ which appears in this integral is called the single-scattering albedo $\tilde{\omega}$. It is the probability, given extinction, that a photon is scattered rather than absorbed.]

The total source function is

$$S = S^s + S^{em} = \frac{J^s}{k^e} + \frac{J^{em}}{k^e} \quad ,$$

which we now incorporate into the r.t.e. (4), putting back the subscripts to remind us of the dependences on z and λ:

$$\frac{dI_\lambda(z,\hat{\Omega})}{d\tau_\lambda} = -I_\lambda(z,\hat{\Omega}) + S_\lambda^{em}(T(z)) + \int_{4\pi} \frac{d\omega'}{4\pi} \frac{k_\lambda^s(z)}{k_\lambda^e(z)} I_\lambda(z,\hat{\Omega}') P(\hat{\Omega}', \hat{\Omega})$$

This is an integro-differential equation because I appears both differentiated and under an integral. The last term on the right vanishes if $k_\lambda^s = 0$, i.e. no scattering.

radiative transfer equation. Derivation of (5). (p.21)

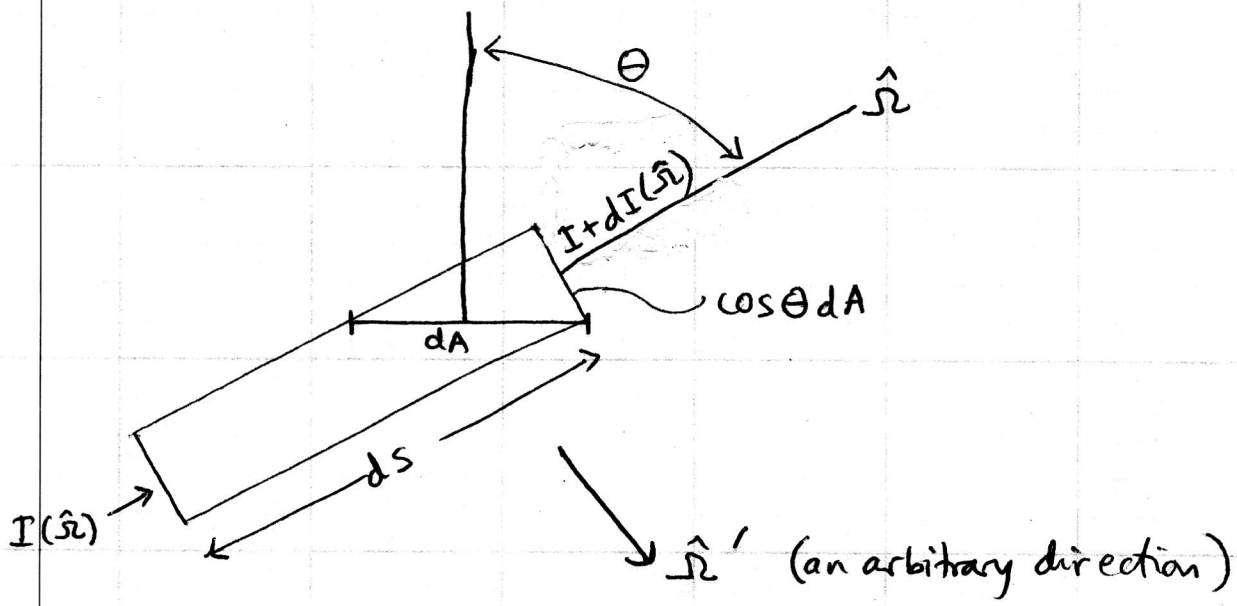

volume element $dV = \cos\theta\, dA\, ds$ (m^3)

mass in this volume $dm = \rho dV = \rho \cos\theta\, dA\, ds$ (g)

Intensity in direction $\hat{\Omega}$ (Q is energy):

$$I = \frac{dQ}{\cos\theta\, dA\, d\omega\, d\nu\, dt} \quad \text{units} \quad \frac{J}{m^2\, sr\, Hz\, sec}, \text{ or } W m^{-2} sr^{-1} Hz^{-1}$$

Energy δQ scattered out of $\hat{\Omega}$ (solid angle $d\omega$ about $\hat{\Omega}$) due to interaction with this mass dm (in time dt in frequency interval $d\nu$)

$$\delta Q_{\substack{\text{loss} \\ \text{from } \hat{\Omega}}} = k_s \, dm \, I(\hat{\Omega}) \, d\omega \, d\nu \, dt$$

$\frac{m^2}{g}$	g	$\frac{J}{m^2 \text{ sec sr Hz}}$	sr	Hz	sec

$$= k_s \overbrace{\rho \cos\theta \, dA \, ds} \; I(\hat{\Omega}) \, d\omega \, d\nu \, dt$$

And the corresponding $dI(\hat{\Omega})$ is

$$dI(\hat{\Omega}) \underset{\substack{\text{due to} \\ \text{scattering-out}}}{=} \frac{-\delta Q_{\text{loss from } \Omega}}{\cos\theta \, dA \, d\omega \, d\nu \, dt} = \frac{-k_s \rho \cos\theta \, dA \, ds \, I \, d\omega \, d\nu \, dt}{\cos\theta \, dA \, d\omega \, d\nu \, dt}$$

$$= -k_s \rho I \, ds$$

so

$$\boxed{dI(\hat{\Omega}) = -k_s \rho I \, ds \quad \begin{pmatrix} \text{due to} \\ \text{scattering-out} \end{pmatrix}}$$

Now consider energy scattered out of a <u>different</u> direction $\hat{\Omega}'$ due to interaction with this <u>same</u> mass:

* If k_s is independent of direction (when might this <u>not</u> be true?), then

$$\delta Q_{\substack{\text{loss} \\ \text{from } \hat{\Omega}'}} = k_s \underbrace{dm}_{\updownarrow} I(\hat{\Omega}')\, d\omega'\, dv\, dt$$

$$= k_s \overbrace{\rho \cos\theta\, dA\, ds}\ I(\hat{\Omega}')\, d\omega'\, dv\, dt$$

note θ not θ'.

Some of this energy lost from $\hat{\Omega}'$ is redirected into $\hat{\Omega}$:

$$\delta Q_{\hat{\Omega}' \to \hat{\Omega}} = \delta Q_{\substack{\text{loss} \\ \text{from } \hat{\Omega}'}} \cdot P(\hat{\Omega}', \hat{\Omega}) \frac{d\omega}{4\pi} .$$

The corresponding change in $I(\hat{\Omega})$ due to scattering from $\hat{\Omega}'$ is

$$dI(\hat{\Omega}) = \frac{\delta Q_{\hat{\Omega}' \to \hat{\Omega}}}{\cos\theta\, dA\, d\omega\, dv\, dt} = k_s \rho\, ds\, I(\hat{\Omega}')\, d\omega' \frac{P(\hat{\Omega}', \hat{\Omega})}{4\pi}$$

(due to scattering-in from $\hat{\Omega}'$)

Now sum the contributions scattered in from

<u>all</u> angles $\hat{\Omega}'$.

$$dI(\hat{\Omega}) = k_s \rho ds \int_{4\pi} I(\hat{\Omega}') P(\hat{\Omega}', \hat{\Omega}) \frac{d\omega'}{4\pi} \quad (6)$$

(due to scattering in from all angles)

Now, the "<u>mass emission coefficient</u>" j is defined as

$$dI_{gains} = j \rho ds \quad (7)$$

Then, from (6) and (7), the scattering component of j

is $$j_s(\hat{\Omega}) = k_s \int_{4\pi} I(\hat{\Omega}') P(\hat{\Omega}', \hat{\Omega}) \frac{d\omega'}{4\pi} \quad (5)$$

(see page 21 above)

There is also an emission component of j:

$$j = j_s + j_{em}$$

NOTES ON SOURCE FUNCTION

The r.t.e. with τ measured vertically is

$$\mu \frac{dI(\hat{\Omega}, \tau)}{d\tau} = -I(\hat{\Omega}, \tau) + S(\hat{\Omega}, \tau) \qquad (1)$$

where S is the source function:

$$S(\hat{\Omega}, \tau) = (1-\tilde{\omega}) B + \frac{\tilde{\omega}}{4\pi} \int d\omega' P(\hat{\Omega}', \hat{\Omega}) I(\hat{\Omega}', \tau) \qquad (1a)$$

emission + scattering

Eq(1) cannot be solved explicitly unless we know the source function. But we can solve it "formally" to get I as a function of S. This is instructive, and also is useful

(a) in cases where S is known independent of I ($\tilde{\omega} = 0$), and

(b) in an iterative solution for the source function.

We'll use the path coordinate s, and the linear extinction coefficient σ; where

$$\frac{d\tau}{\mu} = d\tau_{path} = k_e \rho ds = \sigma ds \quad ; \quad ds = \frac{dz}{\mu}$$

Use "J" for source function, to avoid confusion with path s. Then (1) becomes

$$\frac{1}{\sigma} \frac{dI}{ds} = -I + J \qquad (2)$$

Now we want to solve the R.T.E. (2); i.e. to find $I(b)$, given $I(a)$.

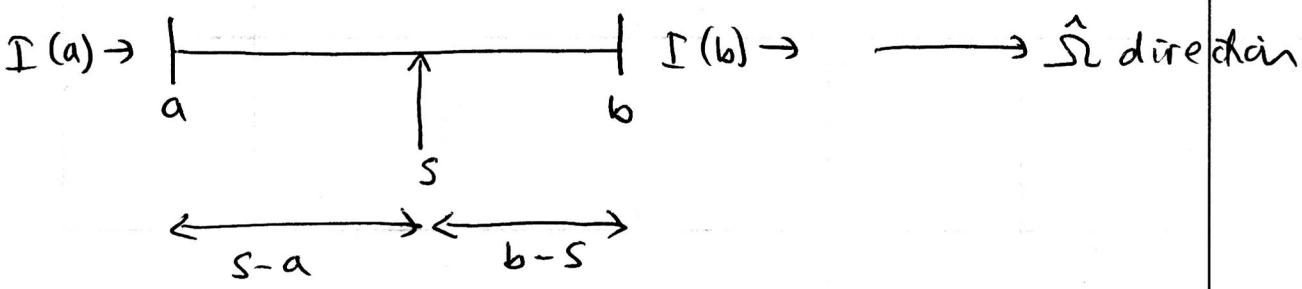

optical depth: $\sigma(s-a)$ $\sigma(b-s)$

s is the variable of integration which starts at a and goes to b.

To solve (2): $\frac{1}{\sigma}\frac{dI(s)}{ds} = -I(s) + J(s)$ (2)

we use the INTEGRATING FACTOR $e^{+\sigma(s-a)} = e^{+\tau(a,s)}$

Multiply both sides of (2) by $e^{+\sigma(s-a)}$.

$$\underbrace{e^{\sigma(s-a)}\frac{dI(s)}{\sigma ds}}_{\text{group these terms:}} = \underbrace{-e^{\sigma(s-a)}I(s)}_{\text{group these terms:}} + e^{\sigma(s-a)}J(s)$$

$$\frac{1}{\sigma}\frac{d}{ds}\left[e^{\sigma(s-a)}I(s)\right] = e^{\sigma(s-a)}J(s).$$

This differential equation can now be solved just by integration.

Integrate along $\hat{\Omega}$ from $s=a$ to $s=b$:

$$\frac{1}{\sigma}\left[e^{\sigma(s-a)}I(s)\right]_{s=a}^{s=b} = \int_a^b e^{\sigma(s-a)}J(s)\,ds$$

$$\frac{1}{\sigma}e^{\sigma(b-a)}I(b) = \frac{1}{\sigma}I(a) + \int_a^b e^{\sigma(s-a)}J(s)\,ds.$$

Now multiply through by $\sigma e^{-\sigma(b-a)}$, to get $I(b)$ on the L.H.S.:

$$I(b) = e^{-\sigma(b-a)}I(a) + \int_a^b \sigma \underbrace{e^{-\sigma(b-a)}e^{\sigma(s-a)}}_{e^{-\sigma(b-s)}} J(s)\,ds$$

Rewriting in terms of τ_{path}: $\tau(x,y) = \sigma(y-x)$, and $d\tau = \sigma ds$:

$$I(b) = \underbrace{e^{-\tau(a,b)}I(a)}_{\text{attenuated incident beam}} + \underbrace{\int_{\tau(a)}^{\tau(b)} e^{-\tau(s,b)}J(s)\,d\tau}_{\text{contributions to } I \text{ from sources along the path between } a \text{ and } b, \text{ attenuated along the remaining distance to } b.} \qquad (3)$$

The intensity at b is thus given by the attenuated initial intensity and the sources along the way.

Now rewrite (2) using plane-parallel coordinate system.

→ τ is vertical

→ μ is positive. $\mu = |\cos\theta|$

→ average over azimuth.

→ Replace all τ in (2) by τ/μ

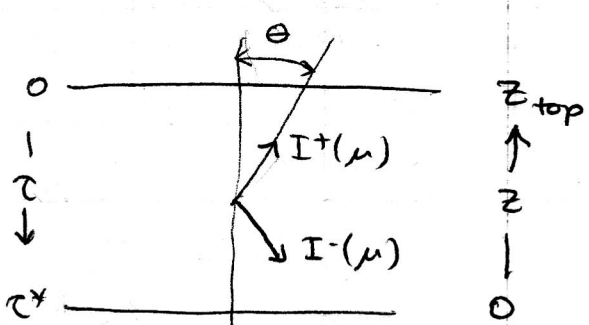

Then the solution for I in terms of S is

Downward ($a = 0$)

$$I^-(\tau,\mu) = I^-(0,\mu)\, e^{-\tau/\mu} + \int_0^{\tau} \frac{d\tau'}{\mu}\, S(\tau',-\mu)\, e^{-(\tau-\tau')/\mu} \qquad (3a)$$

upward ($a = \tau^*$)

$$I^+(\tau,\mu) = I^+(\tau^*,\mu)\, e^{-(\tau^*-\tau)/\mu} + \int_{\tau}^{\tau^*} \frac{d\tau'}{\mu}\, S(\tau',\mu)\, e^{-(\tau'-\tau)/\mu} \qquad (3b)$$

You should be able to write down Eqs (3) just by looking at the diagram at top of this page and thinking about the processes involved.

Special cases (done in class)

① Isothermal emitting slab with no radiation incident at top or bottom.

$$I^+(\tau^*,\mu) = 0$$

so (3b) reduces to

$$I^+(0,\mu) = B(T) \int_0^{\tau^*} e^{-\tau/\mu}\, \frac{d\tau}{\mu}$$

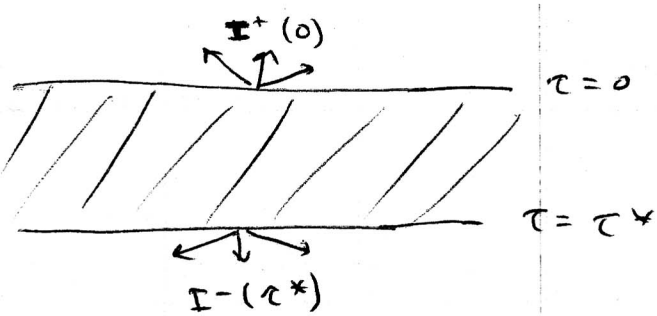

This describes the emergent radiation at the top of the slab, as a function of viewing angle. The radiation emerging from the bottom is the same.

As an exercise, do this integration and plot the slab emissivity $\epsilon(\theta)$ as a function of viewing angle θ, for $\tau^* = 0.05$, $\tau^* = 0.5$, and $\tau^* = 5$ [different total slab thicknesses].

The emissivity is $\epsilon = I^+ / B$

Note also the limits

a) optically thick slab $\tau^* \gg 1$

$I^+(0, \mu) = B$, independent of μ

b) optically thin slab $\tau^* \ll 1$

$$I^+(0, \mu) = \frac{B\tau^*}{\mu} - \frac{B\tau^{*2}}{2\mu^2} + \cdots \approx \frac{B\tau^*}{\mu} .$$

Intensity is proportional to the amount of material along the line-of-sight path, τ^*/μ.

② Radiation emerging from a star whose temperature varies with depth.

Consider two cases: T increasing with depth or decreasing with depth.

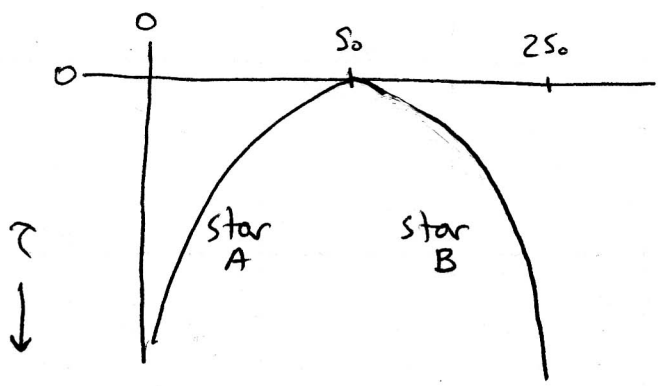

$$S = S_0 \pm S_0(1 - e^{-\tau})$$

As an exercise, solve for $I^+(0, \mu)$ in these cases and evaluate I^+ at $\mu = 1$ (normal) and $\mu = 0$ (limb).

The sun exhibits limb darkening so is more like Star B.

Azimuthal averaging of r.t.e.

For computing fluxes and heating rates, the azimuthal variation of intensity is not needed.

$$F = \int_0^{2\pi} \int_0^1 I(\mu, \phi)\, \mu\, d\mu\, d\phi$$

In the integral there is weighting by μ but no weighting by ϕ.

The r.t.e. is an equation for $I(\mu, \phi)$.
But we can derive an azimuthally-averaged form of the r.t.e. to solve for azimuthally-averaged intensity $I_0(\mu)$; then we can use I_0 to compute F, thus:

$$I_0(\mu) \equiv \frac{1}{2\pi} \int_0^{2\pi} I(\mu, \phi)\, d\phi$$

$$\text{then } F^+ = \int_\Delta I \mu\, d\omega = \int_0^1 \mu\, d\mu \underbrace{\int_0^{2\pi} I(\mu, \phi)\, d\phi}_{2\pi I_0(\mu)}$$

$$F^+ = 2\pi \int_0^1 I_0(\mu)\, \mu\, d\mu$$

Derivation of r.t.e. for I_0 :

Start with the full r.t.e. for I :

$$\mu \frac{dI(\tau,\mu,\phi)}{d\tau} = -I(\tau,\mu,\phi) + (1-\tilde{\omega})B(\tau) + \frac{\tilde{\omega}}{4\pi}\int d\omega' P(\mu,\phi,\mu',\phi') I(\tau,\mu',\phi') \quad (4)$$

Apply the ϕ-averaging operator $\left[\frac{1}{2\pi}\int_0^{2\pi} d\phi\right]$ to both sides:

$$\mu \frac{dI_0(\tau,\mu)}{d\tau} = -I_0(\tau,\mu) + (1-\tilde{\omega})B(\tau) + \underbrace{\frac{1}{2\pi}\int_0^{2\pi} d\phi \left[\frac{\tilde{\omega}}{4\pi}\int d\omega' P\cdot I\right]}_{\text{scattering source}} \quad (5)$$

expanding the scattering source term:

$$\frac{1}{2\pi}\int_0^{2\pi} d\phi \;\; \frac{\tilde{\omega}}{4\pi}\int_0^{2\pi} d\phi' \int_{-1}^{1} d\mu' \, P(\mu,\phi,\mu',\phi') \, I(\tau,\mu',\phi')$$

Here P depends on ϕ but I does not. We define the azimuthally-averaged phase function P_0:

$$P_0(\mu,\mu') = \frac{1}{2\pi}\int_0^{2\pi} d\phi \, P(\mu,\phi,\mu',\phi')$$

Integration over ϕ also removed the ϕ'-dependence, because if P depends only on Θ then the (ϕ,ϕ') dependence of P appears only as $\cos(\phi-\phi')$ [shown on Homework 2.]

Then

$$\text{Scat. source term} = \frac{\tilde{\omega}}{4\pi}\int_0^{2\pi} d\phi' \int_{-1}^{1} d\mu' \, P_0(\mu,\mu') \, I(\tau,\mu',\phi')$$

The only thing now dependent on ϕ' is I, so interchange the order of integration:

$$\text{scat. source} = \frac{\tilde{\omega}}{2}\int_{-1}^{1} d\mu' P_0(\mu,\mu') \underbrace{\frac{1}{2\pi}\int_0^{2\pi} d\phi' I(\tau,\mu',\phi')}_{I_0(\tau,\mu')}$$

$$= \frac{\tilde{\omega}}{2}\int_{-1}^{1} d\mu' P_0(\mu,\mu') I_0(\tau,\mu')$$

Then (5) becomes:

$$\mu \frac{dI_0(\tau,\mu)}{d\tau} = -I_0(\tau,\mu) + (1-\tilde{\omega})B(\tau) + \frac{\tilde{\omega}}{2}\int_{-1}^{1} d\mu' P_0(\mu,\mu') I_0(\tau,\mu')$$

Now drop the subscripts 0 [writing $I(\tau,\mu)$ implies no ϕ-dependence]

$$\boxed{\mu \frac{dI(\tau,\mu)}{d\tau} = -I(\tau,\mu) + (1-\tilde{\omega})B + \frac{\tilde{\omega}}{2}\int_{-1}^{1} d\mu' P(\mu,\mu') I(\tau,\mu')} \quad (6)$$

This is the azimuthally-averaged r.t.e.

Note that we have separately averaged P and I over azimuth; it turned out that their azimuthal dependences don't interact in a way that affects the ~~r.t.e.~~ azimuthally-averaged r.t.e. So we can average P in advance to P_0, then solve for I_0.

Later we will show how to express P and I as Fourier series in ϕ; again the terms will separate so that we obtain a set of non-interacting r.t.e's, one for each Fourier component. This is the way we will solve the r.t.e. when we are not satisfied with just fluxes but do desire the complete solution $I(\tau,\mu,\phi)$.

MILNE'S INTEGRAL EQUATION FOR SOURCE FUNCTION

(To reduce complexity of notation we'll use the azimuthally-averaged r.t.e. for this derivation, but that simplification is not necessary.) Start with azim-avg r.t.e:

$$\mu \frac{dI(\tau,\mu)}{d\tau} = -I(\tau,\mu) + (1-\tilde{\omega})B + \frac{\tilde{\omega}}{2}\int_{-1}^{1} d\mu' P(\mu',\mu) I(\tau,\mu') \qquad (6)$$

The last term on the right is the scattering source function:

$$S_s(\tau,\mu) = \frac{\tilde{\omega}}{2}\int_{-1}^{1} d\mu' P(\mu,\mu') I(\tau,\mu') \qquad (7)$$

Breaking up I into upward and downward parts,

$$\int_{-1}^{1} I\, d\mu' = \int_{0}^{1} (I^+ + I^-)\, d\mu' \text{, then (5) becomes}$$

$$\left.\begin{aligned} S_s(\tau,\mu) = {} & \frac{\tilde{\omega}}{2}\int_0^1 d\mu' P(\mu,\mu') I^+(\tau,\mu') \\ & + \frac{\tilde{\omega}}{2}\int_0^1 d\mu' P(\mu,-\mu') I^-(\tau,\mu') \end{aligned}\right\} \qquad (8)$$

Now we can obtain an integral equation for S by substituting (3) into (8) and adding $S_{emission}$:

↓

(solution for I, p. 28), replacing μ by μ'

This leads to Milne's Integral Equation

(Thomas–Stamnes sec. 6.12)

$$
\begin{aligned}
S(\tau,\mu) = \quad & (1-\tilde{\omega})B(\tau) \\
& + \frac{\tilde{\omega}}{2}\int_0^1 d\mu'\, p(\mu,\mu')\, I^+(\tau^*,\mu')\, e^{-(\tau^*-\tau)/\mu'} \\
& + \frac{\tilde{\omega}}{2}\int_0^1 d\mu'\, p(\mu,\mu')\, I^-(0,\mu')\, e^{-\tau/\mu'} \qquad \Big\} S_0 \\
& + \frac{\tilde{\omega}}{2}\int_0^1 d\mu'\, p(\mu,\mu') \int_\tau^{\tau^*} \frac{d\tau'}{\mu'}\, S(\tau',\mu')\, e^{-(\tau'-\tau)/\mu'} \\
& + \frac{\tilde{\omega}}{2}\int_0^1 d\mu'\, p(\mu,-\mu') \int_0^{\tau} \frac{d\tau'}{\mu'}\, S(\tau',-\mu')\, e^{-(\tau-\tau')/\mu'}
\end{aligned}
\tag{9}
$$

The first three terms depend on the boundary conditions and thermal emission; they can be calculated immediately. Call their sum S^0. S^0 represents the photons that are just now being scattered for the first time or being emitted here; i.e. the "single-scattering" part of S. The last two terms are "multiple-scattering" terms, representing photons that have already been scattered or emitted at τ' and are now being scattered again at τ.

Call the last two terms "$M(S)$" (the "multiple-scattering" contribution)

so $S = S_0 + M(S)$.

This is an integral equation: S on left, integral of S on right

We know S_0 but not S.

<u>Solution by iteration</u>: "multiple-scattering series"

If $\tilde{\omega}\tau^* \ll 1$ then $S \approx S_0$

(photons scattered only once)

First approximation:

$$S_1 = S_0 + M(S_0)$$

S_0 contains photons scattered once

S_1 contains photons scattered once or twice

$$S_2 = S_0 + M(S_1)$$

S_2 contains photons scattered once, twice, three times.

... continue until $|S_{n+1} - S_n|$ is small.

This process is what Thomas calls "Λ-iteration" (p. 220)

It is practical for $\tilde{\omega}\tau^* \lesssim 1$.

Thus we obtain $S(\tau, \mu)$; it can be put into Eq 3 on p. 28 to get $I(\tau, \mu)$. For example:

$$I^+(\tau, \mu) = I^+(\tau^*, \mu)\, e^{-|\tau^* - \tau|/\mu} + \int_{\tau}^{\tau^*} \frac{d\tau'}{\mu} S(\tau', \mu)\, e^{-|\tau' - \tau|/\mu}$$

National Brand 42-381 50 SHEETS EYE-EASE® - 5 SQUARES 42-382 100 SHEETS EYE-EASE® - 5 SQUARES 42-389 200 SHEETS EYE-EASE® - 5 SQUARES

Radiative Transfer Project (from Prof. Gary Thomas, Univ. Colorado)

This problem is a computer exercise that is designed to teach several things:
(1) it emphasizes the statistical nature of radiative transfer; (2) it helps to relate the elementary RT concepts, such as scattering cross-sections, to the integro-differential RT equation; and (3) it introduces the student to a modern technique for obtaining approximate, but accurate, solutions.

Solve the following problem by a *Monte-Carlo* method. A beam with flux πI_o (normal to the beam) is incident onto a plane-parallel slab at zenith angle $\theta_o = 60°$. The slab scatters isotropically and conservatively. The total vertical optical thickness is $\tau^* = 2$; $I_o = 1.0$ W m^{-2}sr^{-1}.

(a) Plot successive approximations to the source function: $S_0(\tau)$, $S_1(\tau)$, $S_2(\tau)$, ...
(b) Obtain the reflected and transmitted diffuse intensities as functions of θ (or μ) by counting the photons exiting the medium into each angular bin. [The "diffuse" intensity excludes the directly transmitted beam.]
(c) Compute the intensity $I(\theta)$ by integrating the source function over τ, to verify consistency with (b).
(d) Obtain the 'exact" solution for the intensity using X- and Y-function tables by Sobouti in Eq. 16 on page 211 of Chandrasekhar (supplemental pages provided) and check your results. They should lie within the "statistical error", which you should define carefully.
(e) Time permitting, run your program for a different set of conditions. [If you use a non-isotropic phase function, you will need to incorporate an additional angle ϕ, and this will increase the computer time required to achieve comparable accuracy.]

Use a random-number generator available as a utility subroutine on the computer. Find out how the numbers are generated and how 'random' they actually are.

For your debugging runs, 1000 photons should suffice for determining whether your answers are reasonable. Use 10^6 photons or more for your 'production' run.

Your writeup should include not just the results but also
- a description of the algorithms
- explanation of the results

References:

House, L, and Avery, L, 1969: The Monte-Carlo technique applied to radiative transfer. *J. Quant. Spect. Rad. Trans., 9,* 1579-1591. Available at http://www.atmos.washington.edu/~sgw/Papers_for_class/HouseAvery1969.pdf

Cashwell, E.D., and C.J. Everett, 1959: *A Practical Manual on the Monte Carlo Method for Random Walk Problems.* Pergamon Press, 153 pp. On reserve in Engineering library for this class.

CHANDRASEKHAR'S X-, Y-, AND RELATED FUNCTIONS*

YOUSEF SOBOUTI
Yerkes Observatory
Received August 29, 1962

ABSTRACT

Chandrasekhar's X- and Y-functions and four additional functions derived from them have been tabulated for the values of optical depth in the range 0.1–3.0, the values of albedo in the range of 0.10–1.00, and the values of argument μ in the range 0–20.

I. INTRODUCTION

Chandrasekhar's X- and Y-functions are encountered in the study of multiple scattering of light by optically finite atmospheres. For isotropic scattering they satisfy the following simultaneous integral equations:

$$X(\mu) = 1 + \tfrac{1}{2}\mu\varpi\int_0^1 \frac{d\mu'}{\mu+\mu'}[X(\mu)X(\mu') + Y(\mu)Y(\mu')] \tag{1}$$

and

$$Y(\mu) = e^{-\tau/\mu} + \tfrac{1}{2}\mu\varpi\int_0^1 \frac{d\mu'}{\mu-\mu'}[Y(\mu)X(\mu') - X(\mu)Y(\mu')], \tag{2}$$

where τ is the optical depth of the atmosphere, ϖ is the albedo of scattering, and μ is the cosine of the angle between the normal to the plane of the atmosphere and the direction to which the scattered or transmitted radiation refers.

In the study of scattering and transmission of fluorescent radiation from planetary atmospheres (Chamberlain and Sobouti 1962) we encountered the X- and Y-functions with arguments greater than unity, which were defined to satisfy the same equations (1) and (2) as do the X- and Y-functions with arguments less than unity. In considering the coupled fluorescent radiation (Sobouti 1962), we introduced two pairs of ξ- and ζ-functions defined as follows:

$$\xi^{\pm}(\mu) = \tfrac{1}{2}\mu\varpi\int_0^1 \frac{X(\mu')}{\mu\pm\mu'}\,d\mu' \tag{3}$$

and

$$\zeta^{\pm}(\mu) = \tfrac{1}{2}\mu\varpi\int_0^1 \frac{Y(\mu')}{\mu\pm\mu'}\,d\mu'. \tag{4}$$

In the present work we tabulate the functions X, Y, $\xi^{\pm}$, and $\zeta^{\pm}$ for arguments μ both smaller and greater than unity.

Some tabulations of X- and Y-functions, for $\mu \leq 1$ and for certain values of τ and ϖ, have been published by Chandrasekhar, Elbert, and Franklin (1952), Chandrasekhar and Elbert (1952), and Mayers (1962). The plan of this project, however, is to present somewhat less accurate data than the first two works mentioned above (only four figures compared with five figures of Chandrasekhar *et al.*), but to cover larger ranges of optical depth and albedo.

Computation has been done on an IBM 1620 computer and the program was written in *Fortran* language.

II. COMPUTATION OF X- AND Y-FUNCTIONS FOR $\mu \leq 1$

This part of the program, which is the most essential of the lot, was carried out by an iteration process. An account of the procedure is given in *Radiative Transfer* by

* The research reported in this paper was supported in part by the National Aeronautics and Space Administration through research grant NsG 118-61.

Chandrasekhar (1950, p. 202, which hereafter, for brevity, will be referred to as "*R.T.*"). Each iteration was corrected by means of formulas (124) and (126) of *R.T.* (p. 204), before proceeding to the next higher iterate. These corrections proved to be exceedingly efficient in making the iterations converge rapidly.

The succession of iterations was interrupted whenever the difference between two consecutive iterates of $X(1)$ became less than 10^{-4}. On the basis of this criterion for terminating the computations, we might expect our data to have an accuracy of 10^{-4} throughout the ranges of the parameters μ, τ, and ϖ. This accuracy was achieved for small values of τ and ϖ with as few as three iterations; for large values of τ and ϖ, as many as seven iterations were needed. To economize on time, lower-order iterates were computed with less accuracy than the higher ones. That is, for the lower-order iterates, the integrals were approximated by summations of either 5 or 10 terms, for the higher-order iterates, the summations had 25 terms.

The integrand of equation (2), the defining equation for $Y(\mu)$, is indeterminate for $\mu = \mu'$. To find the value of the integrand at $\mu = \mu'$, a second-order interpolation formula was employed. The integrand was then obtained from three points preceding and following the point $\mu = \mu'$.

The X- and Y-functions for the conservative case.—It is well known that solutions of equations (1) and (2), corresponding to $\varpi = 1$, are not unique. We have chosen those solutions which give the correct expressions for the scattered and transmitted radiations in an actual physical situation. The method of obtaining such solutions is developed by Chandrasekhar (*R.T.*, pp. 212–214). These solutions were calculated from equations (5)–(7) below, once "a solution" of X and Y was known:

$$X(\mu) = X'(\mu) + Q\mu[X'(\mu) + Y'(\mu)] \tag{5}$$

and

$$Y(\mu) = Y'(\mu) - Q\mu[X'(\mu) + Y'(\mu)]\,. \tag{6}$$

Here $X'(\mu)$ and $Y'(\mu)$ are any solutions of equations (1) and (2) and

$$Q = \frac{1}{a_1' + \beta_1}\left[\beta_0' - \tfrac{4}{3}\frac{1}{(a_1' + \beta_1')\tau + 2(a_2' + \beta_2')}\right], \tag{7}$$

where a_n' and β_n' are the moments of $X'(\mu)$ and $Y'(\mu)$. This expression for Q is derived from equations (25), (26), (43), and (46) of *R.T.* (pp. 212–215). We have also made use of the fact that in the conservative case the quantities $X(\mu) + Y(\mu)$ and $a_n + \beta_n$ are invariants of equations (1) and (2) (see Chandrasekhar *et al.* 1952).

It was found that, for $\tau \leq 1.5$, the $X(\mu)$ and $Y(\mu)$ calculated from equations (5) and (6) were the same as $X'(\mu)$ and $Y'(\mu)$ which were obtained by our previously described method. For $\tau \geq 2$, however, the difference between the primed functions and the unprimed functions extended to the third decimal figures.

III. COMPUTATION OF ξ- AND ζ-FUNCTIONS

The functions $\xi^+(\mu)$ and $\zeta^+(\mu)$ for all values of μ and $\xi^-(\mu)$ and $\zeta^-(\mu)$ for $\mu > 1$ were computed directly from equations (3) and (4) by numerical integrations. When $\mu < 1$, however, these equations for $\xi^-(\mu)$ and $\zeta^-(\mu)$ contain singular integrands. These functions were then computed from the following equations, which are equivalent forms of equations (3) and (4):

$$\xi^-(\mu) = -\tfrac{1}{2}\mu\varpi\left\{X(\mu)\log\left(\frac{1}{\mu} - 1\right) + \int_0^1 \frac{d\mu'}{\mu - \mu'}[X(\mu) - X(\mu')]\right\} \tag{8}$$

and

$$\zeta^-(\mu) = -\tfrac{1}{2}\mu\varpi\left\{Y(\mu)\log\left(\frac{1}{\mu} - 1\right) + \int_0^1 \frac{d\mu'}{\mu - \mu'}[Y(\mu) - Y(\mu')]\right\}. \tag{9}$$

The integrands in equations (8) and (9) are no longer singular but are indeterminate at $\mu = \mu'$. This indeterminacy was dealt with in the same manner as the indeterminacy of the Y-equation.

IV. COMPUTATION OF X- AND Y-FUNCTIONS FOR $\mu > 1$

These functions were calculated from the following forms of equations (1) and (2), once ξ- and ζ-functions were known:

$$X(\mu) = 1 + X(\mu)\,\xi^+(\mu) + Y(\mu)\,\zeta^+(\mu) \tag{10}$$

and

$$Y(\mu) = e^{-\tau/\mu} + Y(\mu)\,\xi^-(\mu) + X(\mu)\,\zeta^-(\mu)\,. \tag{11}$$

V. MOMENTS OF X- AND Y-FUNCTIONS

These moments are defined by the equations

$$\alpha_n = \int_0^1 X(\mu)\,\mu^n d\mu \tag{12}$$

and

$$\beta_n = \int_0^1 Y(\mu)\,\mu^n d\mu\,. \tag{13}$$

Moments of order zero, 1, and 2 were integrated numerically and are listed in Table 2.

The present tables of X- and Y-functions and their moments overlap with those published previously and may be checked against them.

VI. A TEST OF THE ACCURACY OF THE COMPUTATIONS

Sobouti (1962) has derived the following equation relating the four functions $\xi^{\pm}(\mu)$ and $\zeta^{\pm}(\mu)$:

$$\xi^+(\mu) + \xi^-(\mu) - \xi^+(\mu)\,\xi^-(\mu) + \zeta^+(\mu)\,\zeta^-(\mu) + \frac{\varpi\mu}{2}\ln\left|\frac{1-\mu}{1+\mu}\right| = 0\,. \tag{14}$$

This equation was used to check the computations. Column 8 of Table 1, which bears the heading "$E(.10^{-4})$" is the left side of equation (14) multiplied by 10^4. This column might be considered as an indicator of the magnitude of error committed in the computation of X, Y, $\xi^{\pm}$, and $\zeta^{\pm}$. Most of the entries in column 8 had $E < 10^{-4}$ and have not been listed. The value of E corresponding to $\mu = 1.02$ is always very large. This is caused by the large errors in $\xi^-(\mu)$ and $\zeta^-(\mu)$, which have singularities at $\mu = 1$. In any case, not much significance may be attached to the values of functions at $\mu = 1.02$.

Another test is provided by the moments of X- and Y-functions. In the conservative case, $\varpi = 1$, the expression $\alpha_0 + \beta_0$ has the value 1.9999 for all values of τ, in agreement with the theoretical value of $\alpha_0 + \beta_0 = 2$.

I am indebted to Dr. J. W. Chamberlain for his continued interest and guidance in the course of this project.

REFERENCES

Chamberlain, J. W., and Sobouti, Y. 1962, *Ap. J.*, **135**, 925 (Paper I).
Chandrasekhar, S. 1950, *Radiative Transfer* (Oxford: Clarendon Press).
Chandrasekhar, S., and Elbert, D. 1952, *Ap. J.*, **115**, 269.
Chandrasekhar, S., Elbert, D., and Franklin A. 1952, *Ap. J.*, **115**, 244.
Mayers, D. F. 1962, *M.N.*, **123**, 471.
Sobouti, Y. 1962, *Ap. J.*, **135**, 938 (Paper II).

Table I

$\tau = 2.0$ $\varpi = 1.00$

μ	$X(\mu)$	$Y(\mu)$	$\xi^+(\mu)$	$\xi^-(\mu)$	$\zeta^+(\mu)$	$\zeta^-(\mu)$	E(10⁻⁹)
.00	1.0000	.0000	.0000	.0000	.0000	.0000	
.02	1.0564	.0063	.0530	-.0556	.0055	-.0063	
.04	1.0998	.0131	.0908	-.0979	.0106	-.0131	
.06	1.1392	.0205	.1224	-.1350	.0153	-.0205	
.08	1.1759	.0285	.1500	-.1684	.0196	-.0283	
.10	1.2107	.0369	.1747	-.1985	.0237	-.0365	
.12	1.2439	.0458	.1971	-.2259	.0275	-.0451	
.14	1.2758	.0551	.2175	-.2506	.0311	-.0540	
.16	1.3065	.0650	.2363	-.2728	.0344	-.0633	
.18	1.3363	.0753	.2537	-.2925	.0376	-.0728	
.20	1.3651	.0861	.2700	-.3097	.0407	-.0826	
.22	1.3931	.0975	.2852	-.3245	.0436	-.0926	
.24	1.4203	.1093	.2995	-.3368	.0463	-.1027	
.26	1.4468	.1217	.3129	-.3466	.0490	-.1130	
.28	1.4725	.1346	.3256	-.3539	.0515	-.1232	
.30	1.4976	.1481	.3375	-.3585	.0539	-.1335	
.32	1.5220	.1621	.3489	-.3605	.0562	-.1437	
.34	1.5458	.1767	.3597	-.3598	.0584	-.1536	
.36	1.5690	.1918	.3700	-.3562	.0605	-.1633	
.38	1.5916	.2074	.3798	-.3498	.0625	-.1727	
.40	1.6136	.2236	.3891	-.3404	.0645	-.1815	
.42	1.6350	.2401	.3981	-.3280	.0663	-.1898	
.44	1.6559	.2571	.4066	-.3124	.0681	-.1973	
.46	1.6763	.2745	.4148	-.2935	.0699	-.2041	
.48	1.6961	.2922	.4227	-.2713	.0716	-.2099	
.50	1.7155	.3102	.4303	-.2454	.0732	-.2146	
.52	1.7343	.3286	.4375	-.2159	.0748	-.2180	
.54	1.7527	.3471	.4445	-.1825	.0763	-.2201	
.56	1.7706	.3659	.4512	-.1451	.0777	-.2208	1
.58	1.7880	.3849	.4577	-.1033	.0792	-.2197	1
.60	1.8050	.4040	.4640	-.0569	.0805	-.2168	1
.62	1.8216	.4232	.4700	-.0058	.0819	-.2118	1
.64	1.8377	.4425	.4759	.0505	.0832	-.2047	1
.66	1.8535	.4618	.4815	.1125	.0844	-.1950	1
.68	1.8689	.4811	.4869	.1805	.0856	-.1827	1
.70	1.8838	.5004	.4922	.2551	.0868	-.1673	1
.72	1.8985	.5196	.4973	.3369	.0880	-.1487	1
.74	1.9127	.5387	.5023	.4268	.0891	-.1263	1
.76	1.9267	.5579	.5071	.5258	.0902	-.0999	1
.78	1.9402	.5771	.5118	.6350	.0912	-.0688	1
.80	1.9535	.5961	.5163	.7560	.0922	-.0324	1
.82	1.9665	.6152	.5207	.8910	.0932	.0102	1
.84	1.9791	.6349	.5250	1.0426	.0942	.0603	1
.86	1.9914	.6544	.5291	1.2146	.0952	.1196	1
.88	2.0035	.6732	.5331	1.4125	.0961	.1900	1
.90	2.0152	.6918	.5371	1.6447	.0970	.2751	1
.92	2.0267	.7102	.5409	1.9253	.0979	.3803	1
.94	2.0379	.7284	.5446	2.2801	.0987	.5160	1
.96	2.0489	.7465	.5482	2.7665	.0995	.7043	
.98	2.0597	.7644	.5518	3.5652	.1004	1.0151	
1.00	2.0702	.7821	.5552		.1012		
1.02	2.0808	.7992	.5585	3.8114	.1019	1.1474	42
1.04	2.0909	.8164	.5618	3.1692	.1027	.9169	
1.06	2.1008	.8336	.5650	2.8205	.1034	.7945	
1.08	2.1104	.8505	.5681	2.5861	.1042	.7135	
1.10	2.1199	.8673	.5712	2.4127	.1049	.6545	
1.12	2.1291	.8839	.5741	2.2770	.1056	.6089	
1.14	2.1382	.9003	.5770	2.1668	.1063	.5722	
1.16	2.1471	.9165	.5799	2.0749	.1069	.5419	
1.18	2.1558	.9326	.5826	1.9967	.1076	.5163	
1.20	2.1643	.9485	.5854	1.9290	.1082	.4944	
1.25	2.1848	.9873	.5919	1.7932	.1097	.4509	
1.30	2.2043	1.0250	.5980	1.6902	.1112	.4188	
1.35	2.2229	1.0616	.6039	1.6087	.1126	.3929	
1.40	2.2406	1.0971	.6095	1.5423	.1139	.3724	
1.45	2.2576	1.1315	.6148	1.4870	.1152	.3556	
1.50	2.2737	1.1649	.6198	1.4401	.1164	.3414	
1.55	2.2892	1.1972	.6246	1.3998	.1175	.3293	
1.60	2.3039	1.2285	.6292	1.3647	.1186	.3188	
1.65	2.3181	1.2589	.6336	1.3338	.1197	.3096	
1.70	2.3316	1.2883	.6378	1.3065	.1207	.3016	
1.75	2.3447	1.3168	.6418	1.2820	.1217	.2944	
1.80	2.3571	1.3445	.6457	1.2601	.1226	.2880	
1.85	2.3691	1.3714	.6494	1.2402	.1235	.2822	
1.90	2.3807	1.3974	.6529	1.2221	.1244	.2770	
1.95	2.3918	1.4227	.6564	1.2056	.1252	.2722	
2.00	2.4024	1.4472	.6597	1.1905	.1260	.2678	
2.10	2.4226	1.4941	.6659	1.1637	.1275	.2602	
2.20	2.4414	1.5384	.6716	1.1406	.1289	.2536	
2.30	2.4590	1.5802	.6770	1.1206	.1303	.2479	
2.40	2.4754	1.6198	.6821	1.1031	.1315	.2430	
2.50	2.4907	1.6572	.6868	1.0876	.1327	.2386	
2.60	2.5051	1.6927	.6912	1.0737	.1337	.2348	
2.70	2.5186	1.7264	.6953	1.0613	.1348	.2313	
2.80	2.5314	1.7584	.6992	1.0502	.1357	.2282	
2.90	2.5434	1.7888	.7029	1.0400	.1367	.2254	
3.00	2.5548	1.8178	.7064	1.0308	.1375	.2228	
3.20	2.5758	1.8718	.7129	1.0146	.1391	.2184	
3.40	2.5947	1.9222	.7187	1.0008	.1406	.2146	
3.60	2.6118	1.9658	.7239	.9890	.1419	.2114	
3.80	2.6273	2.0072	.7287	.9787	.1431	.2086	
4.00	2.6415	2.0452	.7331	.9697	.1442	.2061	
4.20	2.6546	2.0804	.7371	.9617	.1452	.2039	
4.40	2.6666	2.1130	.7408	.9546	.1461	.2020	
4.60	2.6776	2.1433	.7442	.9482	.1470	.2003	
4.80	2.6879	2.1715	.7473	.9424	.1478	.1987	
5.00	2.6974	2.1979	.7503	.9372	.1485	.1973	
5.50	2.7184	2.2566	.7568	.9261	.1502	.1943	
6.00	2.7363	2.3070	.7623	.9171	.1516	.1919	
6.50	2.7517	2.3507	.7671	.9096	.1528	.1899	
7.00	2.7650	2.3889	.7712	.9033	.1538	.1883	
7.50	2.7766	2.4226	.7749	.8980	.1548	.1868	
8.00	2.7869	2.4525	.7781	.8934	.1556	.1856	
8.50	2.7961	2.4793	.7810	.8894	.1563	.1846	
9.00	2.8043	2.5034	.7835	.8858	.1570	.1836	
9.50	2.8117	2.5252	.7858	.8827	.1576	.1828	
10.00	2.8183	2.5450	.7879	.8799	.1581	.1820	
11.00	2.8299	2.5797	.7916	.8751	.1590	.1808	
12.00	2.8397	2.6089	.7947	.8712	.1598	.1797	
13.00	2.8480	2.6340	.7973	.8679	.1605	.1789	
14.00	2.8552	2.6558	.7996	.8651	.1611	.1781	
15.00	2.8614	2.6748	.8016	.8627	.1616	.1775	
16.00	2.8669	2.6915	.8033	.8606	.1621	.1770	
17.00	2.8717	2.7065	.8049	.8588	.1625	.1765	
18.00	2.8761	2.7197	.8063	.8572	.1628	.1761	
19.00	2.8800	2.7317	.8075	.8557	.1631	.1757	
20.00	2.8832	2.7429	.8086	.8544	.1634	.1753	

$\xi^-(1) = \zeta^-(1) = \infty$

MENDENHALL

DUXBURY PRESS 1981

(45)

3.29 Simulate the experiment described in Exercise 3.28 by marking six marbles, or coins, so that two represent defectives and four represent nondefectives. Place the marbles in a hat, mix, draw three, and record Y, the number of defectives observed. Replace the marbles and repeat the process until a total of $n = 100$ observations on Y has been recorded. Construct a relative frequency histogram for this sample and compare it with the population probability distribution, Exercise 3.28.

*3.30 The sizes of animal populations are often estimated by using a capture-tag-recapture method. In this method k animals are captured, tagged, and then released into the population. Some time later n animals are recaptured, and Y, the number of tagged animals among the n, is noted. The probabilities associated with Y are a function of N, the number of animals in the population, and the observed value of Y contains information on this unknown N. Suppose $k = 4$ animals are tagged and then released. A sample of $n = 3$ animals is then selected at random from the same population. Find $P(Y = 1)$ as a function of N. What value of N will *maximize* $P(Y = 1)$?

3.6 The Poisson Probability Distribution

Suppose that we want to find the probability distribution of the number of automobile accidents at a particular intersection during a time period of 1 week. At first glance this random variable, the number of accidents, may not seem even remotely related to a binomial random variable, but we will see that there is an interesting relationship.

Think of the time period, 1 week in the example above, as being split up into n subintervals, *each of which is so small that at most one accident could occur in it with probability different from zero.* Denoting the probability of an accident in any subinterval by p, we have, for all practical purposes,

$$P(\text{no accidents in a subinterval}) = 1 - p$$

$$P(\text{one accident in a subinterval}) = p$$

and

$$P(\text{more than one accident in a subinterval}) = 0$$

Then the total number of accidents in the week is just the total number of subintervals that contain one accident. If the occurrence of accidents can be regarded as independent from interval to interval, the total number of accidents has a binomial distribution.

Although there is no unique way to choose the subintervals, and we therefore know neither n nor p, it seems reasonable that as we divide the week into a greater number n of subintervals, the probability p of one accident in one of these shorter subintervals will decrease. Letting $\lambda = np$ and taking the limit of the binomial probability $p(y) = \binom{n}{y} p^y (1 - p)^{n-y}$ as $n \to \infty$, we have

* Exercises preceded by an asterisk are optional.

MENDENHALL, MATHEMATICAL STATISTICS WITH APPLICATIONS

46

$$\lim_{n\to\infty}\binom{n}{y}p^y(1-p)^{n-y} = \lim_{n\to\infty}\frac{n(n-1)\cdots(n-y+1)}{y!}\left(\frac{\lambda}{n}\right)^y\left(1-\frac{\lambda}{n}\right)^{n-y}$$

$$= \lim_{n\to\infty}\frac{\lambda^y}{y!}\left(1-\frac{\lambda}{n}\right)^n\frac{n(n-1)\cdots(n-y+1)}{n^y}\left(1-\frac{\lambda}{n}\right)^{-y}$$

$$= \frac{\lambda^y}{y!}\lim_{n\to\infty}\left(1-\frac{\lambda}{n}\right)^n\left(1-\frac{\lambda}{n}\right)^{-y}\left(1-\frac{1}{n}\right)\left(1-\frac{2}{n}\right)\cdots\left(\frac{y-1}{n}\right)$$

Noting that $$\lim_{n\to\infty}\left(1-\frac{\lambda}{n}\right)^n = e^{-\lambda}$$

and all other terms to the right of the limit have a limit of 1, we obtain

$$p(y) = \frac{\lambda^y}{y!}e^{-\lambda}$$

(Note: $e = 2.718\ldots$.) Random variables possessing this distribution are said to be Poisson random variables. Hence Y, the number of accidents per week, should possess the Poisson distribution given above.

The convergence of the binomial probability function to the Poisson is of practical value, because the Poisson probabilities can be used to approximate their binomial counterparts for large n, small p, and $\lambda = np$ less than, roughly, 7. Exercise 3.37 will require the calculation of corresponding binomial and Poisson probabilities and will demonstrate the adequacy of the approximation.

The Poisson probability distribution often provides a good model for the probability distribution of the number Y of rare events that occur infrequently in space, time, volume, or any other dimension, where λ is the average value of y. As we have noted, it provides a good model for the probability distribution of the number Y of automobile accidents, industrial accidents, or other types of accidents in a given unit of time. Other examples of random variables with approximate Poisson distributions are the number of telephone calls handled by a switchboard in a time interval, the number of radioactive particles that decay in a particular time period, and the number of errors a typist makes in typing a page.

Poisson Probability Distribution

$$p(y) = \frac{\lambda^y}{y!}e^{-\lambda}, \qquad y = 0, 1, 2, \ldots$$

POISSON DISTRIBUTION

① Probability of observing n random events in a time interval is $p(n) = \frac{\lambda^n}{n!} e^{-\lambda}$, with a mean value of λ.

② Show that $\sum_{n=0}^{\infty} p(n) = 1$.

$$\sum_{n=0}^{\infty} p(n) = \sum_{n=0}^{\infty} \frac{\lambda^n}{n!} e^{-\lambda} = e^{-\lambda} \sum_{n=0}^{\infty} \frac{\lambda^n}{n!} = e^{-\lambda} e^{\lambda} = 1 \quad \checkmark$$

because the series expansion for e^x is $\sum_{n=0}^{\infty} \frac{x^n}{n!}$

③ Show that the expected value of n is λ.

Expected value $E(n) = \frac{\sum n\,p(n)}{\sum p(n)} = \sum n\,p(n)$.

$$E(n) = \sum_{n=0}^{\infty} \frac{n\lambda^n}{n!} e^{-\lambda} = \lambda e^{-\lambda} \sum_{n=0}^{\infty} \frac{n\lambda^{n-1}}{n!}$$

$$= \lambda e^{-\lambda} \left[\frac{0 \cdot \lambda^{-1}}{0!} + \sum_{n=1}^{\infty} \frac{\lambda^{n-1}}{(n-1)!} \right]. \quad \text{Now let } k = n-1.$$

$$= \lambda e^{-\lambda} \sum_{k=0}^{\infty} \frac{\lambda^k}{k!} = \lambda e^{-\lambda} e^{\lambda} = \lambda = E(n) = \mu \text{ [mean]}. \quad \text{QED.}$$

④ Show that the variance of n is λ.

Variance of n is expected value of $(n-\mu)^2 = (n-\lambda)^2$.

$$V(n) = E\left[(n-\mu)^2\right] = \frac{\sum (n-\mu)^2 p(n)}{\sum p(n)} = \sum_{n=0}^{\infty} (n-\lambda)^2 \frac{\lambda^n}{n!} e^{-\lambda} = \lambda$$

↑ using tricks as in ③

HOW TO BUILD THE IGLOO

We want to divide the hemisphere into bins of exactly equal solid angle and approximately square dimensions.
i.e. $\Delta\theta \approx \sin\theta \, \Delta\phi$

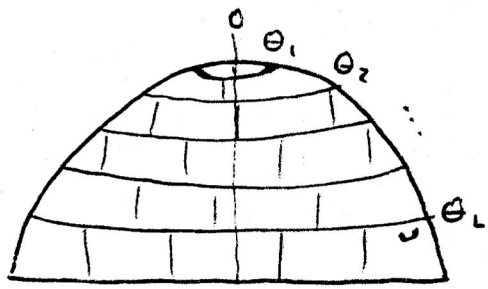

Rules

1. One bin to cover the cap
2. $\Delta\theta$ for other bins $\approx$ full-θ-width of cap, not half-width
3. Start at bottom to ensure roughly equidimensional bins.

Algorithm

1. Select N = number of bins
2. $\Delta\omega = 2\pi / N$
3. Find θ_1: $\Delta\omega = 2\pi \int_0^{\theta_1} \sin\theta \, d\theta$, so $\theta_1 = \cos^{-1}\left(1 - \frac{\Delta\omega}{2\pi}\right)$
4. $\Delta\theta_{try} = 2\theta_1$. This is a first approximation to $\Delta\theta$
5. Find n_θ = number of θ-strips, or "zones", not counting cap:

   $n_\theta + \frac{1}{2} = \frac{\pi/2}{\Delta\theta_{try}}$ (round, don't truncate. The $\frac{1}{2}$ is for the cap.)

   $\Delta\theta = (\pi/2)/(n_\theta + \frac{1}{2})$
6. Start at bottom and work up. Find θ_L

   (a) First find θ_L approximately as θ_{try}:

$\theta_{try} = 90 - \Delta\theta$

$\S$ solid angle of zone (approximate) $= 2\pi \int_{\theta_{try}}^{90} \sin\theta \, d\theta = 2\pi \cos\theta_{try}$

(b) Find number of boxes in zone; n_ϕ

$$n_\phi = \frac{2\pi \cos\theta_{try}}{\Delta\omega} \quad \text{(round.)}$$

(c) Now find θ_L exactly:

$$\theta_L = \cos^{-1}\left(n_\phi \frac{\Delta\omega}{2\pi}\right)$$

7. Next-to-lowest zone.

Find θ_{L-1} approximately: $\theta_{try} = \theta_L + \Delta\theta$

$$n_\phi = \frac{2\pi[\cos\theta_{try} - \cos\theta_L]}{\Delta\omega} \text{ (round), etc. as in 6.}$$

8. Continue until $\Delta\theta < \theta < 2\Delta\theta$.
Now only one zone remains in addition to the cap.
Put all remaining boxes but 1 into top zone,
leaving 1 for the cap.

e.g. $N = 20$ bins.

$$\Delta\omega = \frac{2\pi}{20}. \qquad \cos\theta_1 = \left(1 - \frac{1}{20}\right) = \frac{19}{20}$$

$$\theta_1 = 18.19°$$

$$\Delta\theta_{tny} = 2 \times 18.19° = 36.39°$$

$$n_\theta + \tfrac{1}{2} = \frac{90}{36.39} = 2.47, \text{ round to } 2.5$$

$$\Delta\theta = \frac{90°}{2.5} = 36°$$

$$\theta_{tny} = 90 - 36 = 54$$

$$n_\phi = \frac{2\pi \cos 54°}{\Delta\omega} = \frac{(2\pi)(0.59)}{(2\pi/20)} = 11.76. \text{ round to } 12.$$

$$\theta_1 = \theta_2 = \cos^{-1}\left(\frac{12}{20}\right) = 53.13°.$$

12 in bottom row, 1 for cap, leaves 7 for top row.

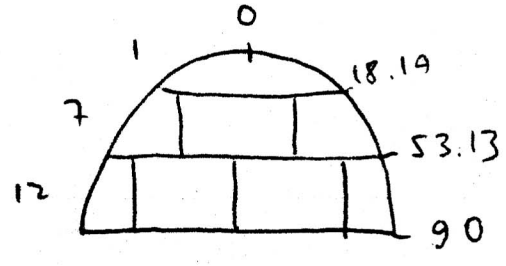

Try 4 boxes.

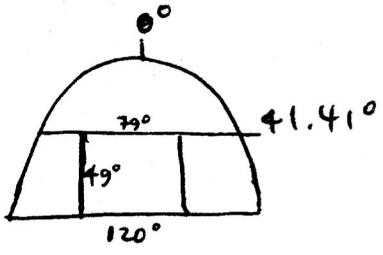

$\cos\theta_1 = 3/4$ $\theta_1 = 41.41°$

Try 7 boxes

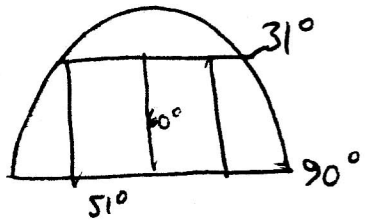

$\cos\theta_1 = \frac{6}{7}$ $\theta_1 = 31.00°$

Try 10 boxes $\cos\theta_1 = 9/10$ $\theta_1 = 25.84.$

$\frac{90}{2 \times 25.84} = 1.74$ round to 1.5

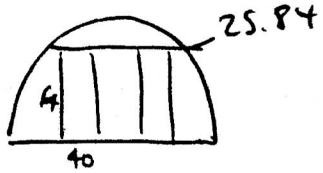

pages 52-53. Units in Monte-carlo project.
Look at these pages after doing the project;
then correct your analysis if necessary.

UNITS IN MONTE-CARLO PROJECT

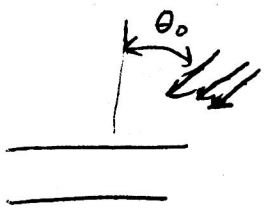

$\mu_0 = \cos\theta_0$

Flux of beam is

πI_0 normal to beam

or $\pi I_0 \mu_0$ normal to surface $(W m^{-2})$

Our πI_0 is Chandrasekhar's πF (Ch. page 20)

Conversion factor from photons to intensity :

N_0 photons total in the incident beam (eg. $N_0 = 10000$)

N_0 photons represent $\pi I_0 \mu_0$ $W m^{-2}$ } where m^2 means area of surface.

so 1 photon represents $\left(\frac{\pi I_0 \mu_0}{N_0}\right) W m^{-2}$ }

(a) Counting

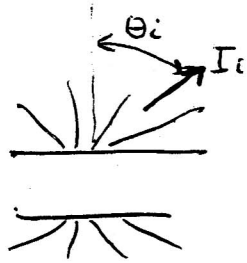

The number of photons emerging in bin i is N_i ; convert this to intensity I_i.

N_i photons represents $N_i \left(\frac{\pi I_0 \mu_0}{N_0}\right) W m^{-2}$

Definition of I is watts per unit solid angle per unit area $\perp$ beam.

so 1) convert from surface area to area $\perp$ beam (factor of μ_i)

2) divide by solid angle of bin $\Delta\omega_i$

$$\therefore \quad I_i = \frac{N_i}{\mu_i \Delta\omega_i}\left(\frac{\pi I_0 \mu_0}{N_0}\right) \qquad W m^{-2} sr^{-1}$$

For accurate computation :

$$I_i = \left(\frac{\pi I_0 \mu_0}{N_0}\right)\left(\frac{N_i}{\Delta\omega_i}\right)\left(\frac{1}{\mu_i}\right).$$

This last factor, $\frac{1}{\mu_i}$, is the average value of $\frac{1}{\mu}$ for all the photons exiting in ~~the~~ angular bin i.

(b) Source function from counting of scattered photons

We can compute Intensity by integrating over the source function.

$$I_i = \int S(\tau)\, e^{-\tau/\mu_i} \frac{d\tau}{\mu_i} = \sum_{j=1}^{n} S(\tau_j)\, e^{-\tau_j/\mu_i} \frac{\Delta\tau}{\mu_i} \qquad (1)$$

where i denotes a bin and j is a layer.

The source function has a value at every point in the medium. It cannot change if we change the size of the layers.

① When we count photons in a layer, then to get the source function we must divide by the size of the layer.

In other words to compute $I_i = \int S(\tau) \ldots d\tau$

we want I_i in units $W m^{-2} sr^{-1}$

so we need S in units $W m^{-2} sr^{-1}$ per unit optical depth

② In converting from photons to source function we must also convert from units of flux to units of intensity. The photons are distributed (scattered) into 4π steradians.

The source function in layer j is then computed as

$$S_j = \frac{N_{scat}(j)}{(\Delta\tau_j)(4\pi)} \left(\frac{\pi I_0 \mu_0}{N_0} \right)$$

Improving accuracy of integral of source function:

$$I(\mu) = \sum_{j=1}^{n} S(\tau_j) \underbrace{e^{-(\tau_j - \tau_{bound.})/\mu}}_{\text{this is the transmittance from layer } j \text{ to the surface.}} \frac{\Delta\tau}{\mu}$$

[where $\Delta\tau$ is the layer thickness, and τ_{bound} is 0 or τ^*, the top or bottom boundary.]

The accuracy can be improved by making $\Delta\tau$ smaller (subdividing into more layers). But accuracy for any number of layers can be improved by using not the average value of τ for the layer but rather the average t_j

i.e. use $\bar{t} = \langle e^{-\tau_j/\mu} \rangle$ not $e^{-\langle\tau_j\rangle/\mu}$

e.g.

① transmittance from level 2 to top surface.

$$\bar{t}_2 = \frac{1}{\tau_2 - \tau_1} \int_{\tau_1}^{\tau_2} e^{-\tau/\mu} d\tau = \frac{\mu}{\tau_2 - \tau_1} \left[e^{-\tau_1/\mu} - e^{-\tau_2/\mu} \right]$$

② transmittance from level 2 to bottom:

$$\bar{t}_2 = \frac{1}{\tau_2 - \tau_1} \int_{\tau_1}^{\tau_2} e^{-(\tau^* - \tau)/\mu} d\tau$$

supplementary notes

For ATMS 533 Monte-Carlo project:

Computation of reflected and transmitted intensities from the X and Y functions is given by Chandrasekhar (Ch):
for $\varpi<1$ on page 211, eq. 16
for $\varpi=1$ on page 213, eq. 27.

These two equations are related by Sobouti's equations 5 & 6. If Sobouti's (5,6) are inserted into Ch (16), then Ch (27) results. The values tabulated by Sobouti for $\varpi=1$ are therefore to be used in Ch (16).

In summary, take values of X and Y from Sobouti's tables and put them directly into Chandrasekhar's Eq. 16.

In the statement of our problem (notes, page 40) we specify the flux normal to the beam as πI_o; Chandrasekhar calls this flux πF.

RADIATIVE TRANSFER

BY

S. CHANDRASEKHAR

MORTON D. HULL DISTINGUISHED SERVICE PROFESSOR

UNIVERSITY OF CHICAGO

1950
reprinted 1960

DOVER PUBLICATIONS, INC.
NEW YORK

ATMS 533 Notes by Stephen Warren

1. Representation of anisotropic phase functions in the radiative transfer equation
    - 1.1 Polynomial expansion of the phase function
    - 1.2 Moments of the phase function
    - 1.3 Henyey-Greenstein phase function

2. R.T.E. for plane-parallel atmosphere illuminated by direct solar beam
    - 2.1 Sign of μ
    - 2.2 Separation of scattered and direct radiation
    - 2.3 Averaging over azimuth
    - 2.4 Polynomial expansion of azimuthally-averaged phase function

3. Two-stream method
    - 3.1 Backscattered fraction; relation to asymmetry factor
    - 3.2 Derivation of two-stream equations, including direct beam
    - 3.3 Solution for diffuse incidence
    - 3.4 Examples of results

Hansen & Travis A74

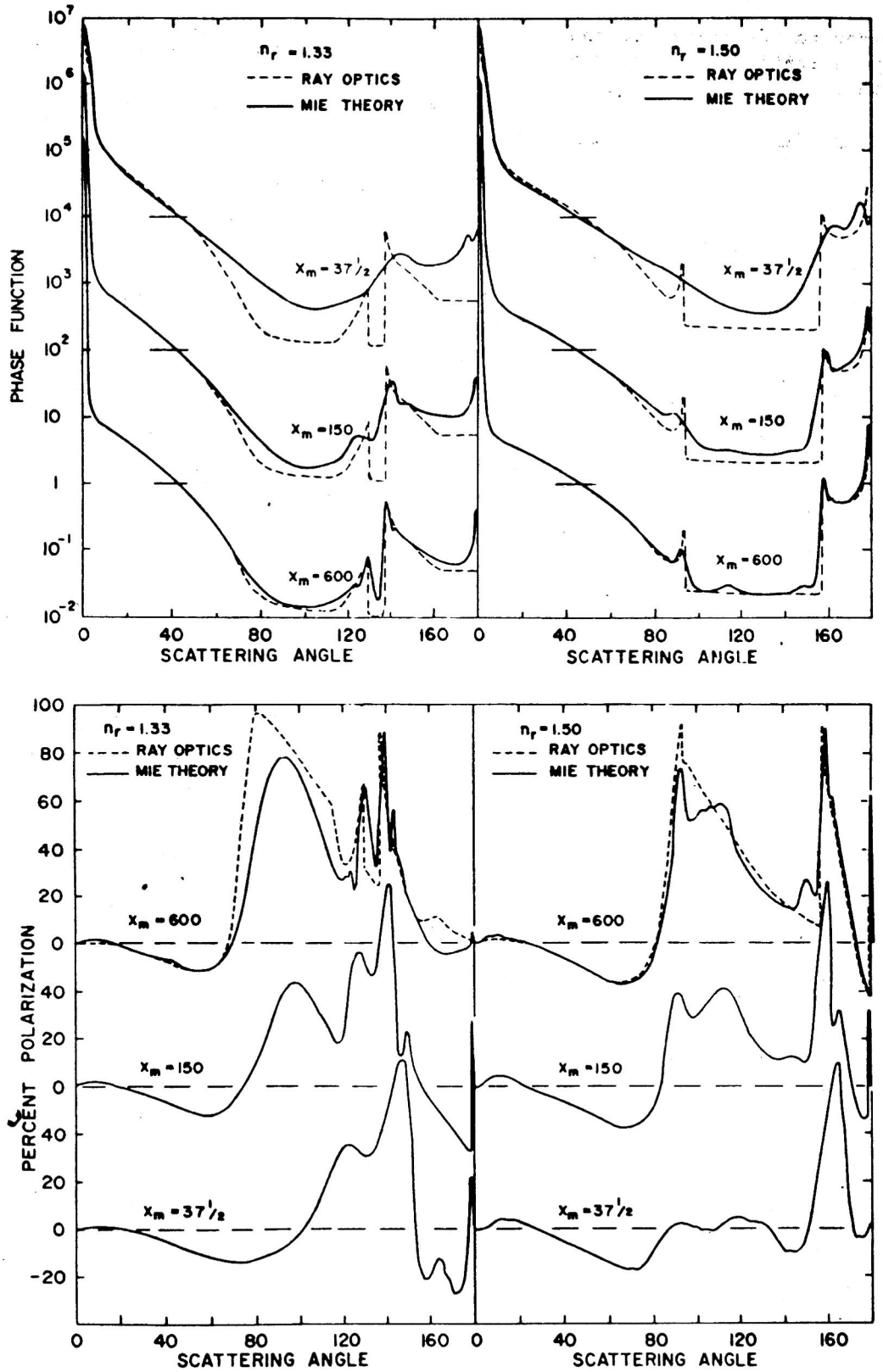

Fig. 4. Comparison of ray optics (geometrical optics and diffraction) and Mie theory for the percent polarization (upper figure) and phase function (lower figure) for scattering by spheres. The size distribution is $n(x) = x^{(1-3b)/b}\, e^{-x/x_m b}$ with $b = 1/9$. Results are shown for two refractive indices and three values of the effective mean size parameter, x_m. For the phase function the scale applies to the curves for $x_m = 600$, the other curves being successively displaced upwards by factors of 100.

1. Representation of anisotropic phase functions in R.T.E.

1.1. Polynomial expansion of phase function

$$P(\cos\Theta) = \sum_{l=0}^{\infty} (2l+1)\, \chi_l\, P_l(\cos\Theta) \qquad (1)$$

[The coefficients χ_l will be shown to be "moments" of phase function]

The Legendre polynomials P_l are orthogonal to each other and form a complete set of basis functions for the interval $[-1, 1]$, which is the range of values for $\cos\Theta$.

The first few Legendre polynomials P_l are

$P_0(x) = 1$

$P_1(x) = x$

$P_2(x) = \frac{1}{2}(3x^2 - 1)$

$P_3(x) = \frac{1}{2}(5x^3 - 3x)$

$P_4(x) = \frac{1}{8}(35x^4 - 30x^2 + 3)$

$P_5(x) = \frac{1}{8}(63x^5 - 70x^3 + 15x)$

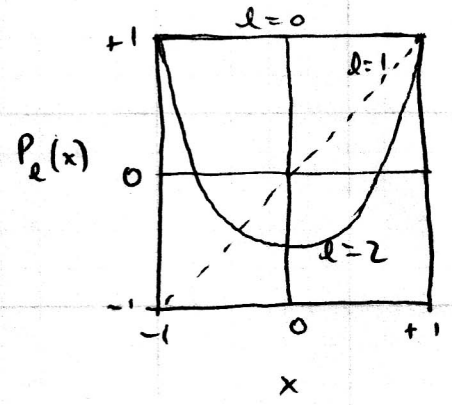

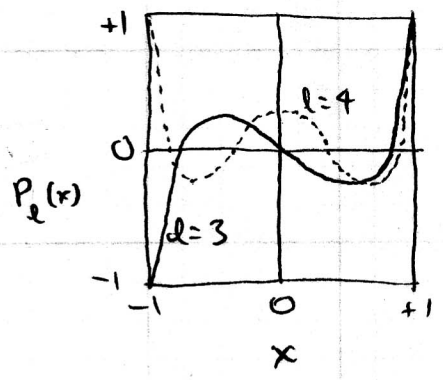

Orthogonality property:

$$\int_{-1}^{1} P_n(x)\, P_m(x)\, dx = \begin{cases} 0, & n \neq m \\ \dfrac{2}{2n+1}, & n = m \end{cases} \qquad (2)$$

1.2 Moments of phase function

These moments will be used in derivation of the Eddington method because we will take moments of the R.T.E. in order to solve it.

The nth moment is defined as the average value of $P_n(\cos\Theta)$, weighted by the phase function:

$$\langle P_n(\cos\Theta)\rangle = \frac{\int_{4\pi} \frac{P(\cos\Theta)}{4\pi} P_n(\cos\Theta)\, d\omega}{\int_{4\pi} \frac{P(\cos\Theta)}{4\pi}\, d\omega} \qquad (3)$$

[The denominator = 1.] For integration, center the local coordinate system on the scatterer such that the Φ-angle is around the incident direction, so

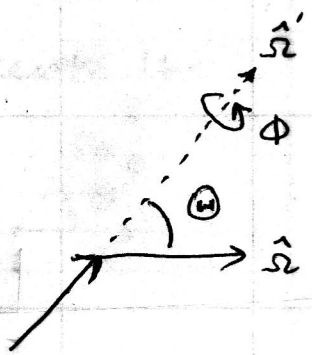

$$d\omega = \sin\Theta\, d\Theta\, d\Phi = d\Phi\, d(\cos\Theta).$$

Then (3) becomes

$$\langle P_n(\cos\Theta)\rangle = 2\pi \int_{-1}^{1} P_n(\cos\Theta)\, \frac{P(\cos\Theta)}{4\pi}\, d\cos\Theta.$$

Let $x \equiv \cos\Theta$.

Then $$\langle P_n(x)\rangle = \frac{1}{2}\int_{-1}^{1} P_n(x)\, P(x)\, dx \qquad (4)$$

$P_n(x)$: Legendre polynomial; $P(x)$: Phase function

Zeroth moment is $\bar{P} = 1$ because $P_0(x) = 1$

First moment is $\langle \cos\Theta \rangle \equiv g$ "asymmetry factor" "asymmetry parameter"

because $P_1(x) = x = \cos\Theta$

Given $P(\cos\Theta)$, now evaluate g, using the Legendre polynomial expansion of P:

$$g = \frac{1}{2}\int_{-1}^{1} P_1(x)\, P(x)\, dx$$

$P_1(x) = x$

$$P(x) = \sum_{\ell} (2\ell+1)\chi_\ell P_\ell(x)$$

$$= \frac{1}{2}\int_{-1}^{1} P_1(x) \sum_{\ell} (2\ell+1)\chi_\ell P_\ell(x)\, dx$$

Only $P_1(x)$ will survive in the Σ because of orthogonality. $2\ell+1 = 3$

$$= \frac{1}{2}\int_{-1}^{1} x \cdot 3\chi_1 \cdot x\, dx = \chi_1 \cdot \frac{3}{2}\underbrace{\int_{-1}^{1} x^2 dx}_{2/3}$$

So $g = \chi_1$ as expected.

So the first two terms in the polynomial expansion of the phase function are

$$P(\cos\Theta) = 1 + 3g\cos\Theta + \cdots . \qquad (5)$$

These first two terms are all we will need for the Eddington method.

g is the average value of $\cos\Theta$, weighted by P.

Its value is between -1 and +1.

$g = 0$ for isotropic or Rayleigh

$g = 1$ for pure forward scattering

$g = -1$ for pure backward scattering.

For Mie scattering by cloud droplets at visible wavelengths, g is typically between 0,8 and 0.9. For flux computation it is usually sufficient just to know g (no higher moments).

1.3 Henyey – Greenstein (HG) phase function

Some modelers replace the true phase function by the HG phase function for simplicity of modeling. It represents some of the character of realistic phase functions. It was introduced in 1941 by the astronomers Henyey and Greenstein. By adjusting the one parameter (g), a variety of shapes can be obtained:

$$P_{HG}(\cos\Theta) = \frac{1-g^2}{(1+g^2-2g\cos\Theta)^{3/2}} \qquad (6)$$

The asymmetry factor of P_{HG} is g.

Welch & Zdunkowski (1982) evaluated the accuracy of P_{HG} for atmospheric radiative transfer. Fluxes are obtained accurately for optically thick atmospheres ($\tau^* \gg 1$); less accurately for optically thin atmospheres.

(61)

Astrophysical Journal 93, 70-83 (1941)

DIFFUSE RADIATION IN THE GALAXY

L. G. HENYEY AND J. L. GREENSTEIN[1]

Little information concerning the nature of the phase function for interstellar scattering is now available. We have carried out our computations, using a phase function of the form

$$\Phi(a) = \frac{\gamma(1 - g^2)}{4\pi} \frac{1}{(1 + g^2 - 2g \cos a)^{3/2}} . \qquad (2)$$

The phase angle is a, defined as the deviation of the ray from the forward direction; γ is the spherical albedo; the parameter g measures the asymmetry of the phase function, according to the expression

$$\gamma g = \int \Phi(a) \cos a \, d\omega . \qquad (3)$$

For $g = 0$ we have an isotropic distribution of the scattered radiation; for $g = +1$ all the radiation is thrown forward. A representation of the cases $g = +\frac{1}{3}$ and $g = +\frac{2}{3}$, with $\gamma = 1$, is given in Figure 3. Such forward-throwing functions resemble those com-

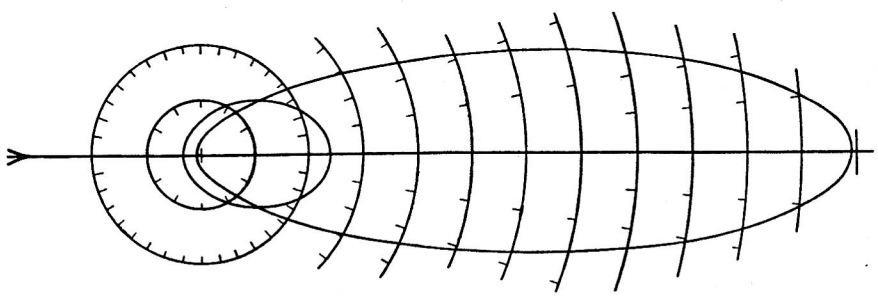

FIG. 3.—Polar diagram of the phase function of equation (2), for $\gamma = 1$. The more elongated curve is for $g = +\frac{2}{3}$; the other, for $g = +\frac{1}{3}$. The radiation is incident on the particle from the left, as shown by the arrow.

puted on the basis of the Mie theory for particles whose radius is near a wave length. If the sign of g is negative, we have backward-throwing phase functions of the same form as those in Figure 3. Suitable combinations of forward and backward phase functions of the form of (2) can also be used.

Henyey-Greenstein phase function $p_{HG}(\Theta) = \dfrac{1-g^2}{(1+g^2-2g\cos\Theta)^{3/2}}$

MODEL DATE

(62)

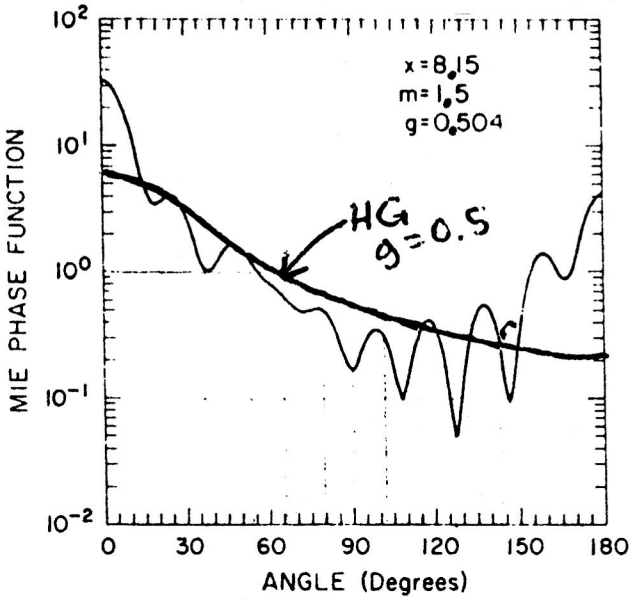

FIG. 1. Mie phase function vs angle for size parameter $x = 8.15$ and index of refraction $m = 1.5$.

P_{HG}

1000
100
10
1
0.1
0.01

$g = 0.9$
$g = 0$
$g = 0.2$
$g = 0.5$
$g = 0.8$
$g = 0.9$

0 15 30 45 60 75 90 105 120 135 150 165 180

scattering angle (degrees) Θ

46 6460

SEMI-LOGARITHMIC 7 CYCLES X 60 DIVISIONS
KEUFFEL & ESSER CO. MADE IN U.S.A.

(63)

Beiträge zur Physik der Atmosphäre 55, 28-42.

Backscattering Approximations and their Influence on Eddington-Type Solar Flux Calculations

R. M. Welch and W. G. Zdunkowski

Institut für Meteorologie, Johannes Gutenberg-Universität, D 6500 Mainz

(Manuscript received 04.06.1981, in revised form 21.09.1981)

1982

VI Summary and Conclusions

Difficulties in solving the RTE by approximate methods may be traced to the fact that the highly asymmetric phase function cannot be represented by polynomials of low order. However, it has been demonstrated during the last decade that reasonably accurate values of radiative fluxes can be obtained using relatively small numbers of expansion terms. The primary purpose of the present paper is to give some details of this behavior.

This is accomplished using expansions of backscattering coefficients β_0 and $\beta(\mu_0)$ in conjunction with the recently unified treatment of two-stream radiative transfer methods developed by ZDUNKOWSKI et al. (1980) and MEADOR and WEAVER (1980). The contributions by each term in the $\beta(\mu_0)$ expansion are $(3C_1/2, 7C_3/8, 11C_5/16, \ldots)$, while contributions by each term in the β_0 expansion drop off very quickly as $(3C_1/4, 7C_3/64, 11C_5/256, \ldots)$ with increasing order of expansion (j). Therefore, very few terms are required for accurate values of β_0, while higher order expansions are required for accurate values of $\beta(\mu_0)$. The quantity β_0 determines the scattering field in optically thick atmospheres, while $\beta(\mu_0)$ controls the scattering field developing at cloud tops and in optically thin atmospheres. The reason why radiative transfer methods produce relatively accurate flux values with low orders of expansion is that the backscattering coefficients approach their asymptotic limits very quickly with increasing order. Errors in the values of $\beta(\mu_0)$ generally are larger than those for β_0; however, these errors have negligible effect in optically dense media.

The Henyey-Greenstein approximation has identical values for the C_1 phase function expansion term, with increasingly divergent values at higher orders of expansion. However, since the contributions from higher order terms to β_0 decrease so rapidly, the HG approximation produces excellent values of radiative fluxes in optically thick atmospheres; because contributions from higher order terms to $\beta(\mu_0)$ decrease more slowly, the HG approximation produces less accurate values in optically thin atmospheres.

For asymmetry factors with $g < 0.5$, both β_0 and $\beta(\mu_0)$ are very near their asymptotic limits even for the $j = 0$ order of expansion. It is for this reason that the two-stream methods produce accurate fluxes for such values of g. $\beta(1)$ becomes very small for $g = 0.6$ and negative for $g > 2/3$ in the Eddington method. For such values of g, such two-stream methods may produce negative (nonphysical) values of upward flux and values of downward flux larger than those incident to the medium.

At larger solar zenith angles the $j = 0$ expansion (two-stream) produces poor but at least positive estimates for $\beta(\mu_0)$, even for large asymmetry factors. However, the approximation to $\beta(\mu_0)$ rapidly improves for $j > 1$, especially for large values of μ_0.

The preceeding analysis shows how various orders of expansion, asymmetry factors, optical thickness, and solar zenith angles effect resulting values of diffuse radiative fluxes. Therefore, paradoxical and even nonphysical behavior previously reported in the literature is seen to be a consequence of the various approximations to backscattering coefficients.

2. R.T.E. for plane-parallel atmosphere illuminated by direct solar beam.

2.1 Sign of μ $\mu = \cos\theta$, where θ is the angle from vertical to the forward direction.

R.T.E along path is $\frac{dI}{d\tau_{path}} = -I + S$.

Some define μ as the cosine of the angle to the forward direction from the upward normal; others from the downward normal:

(a) If

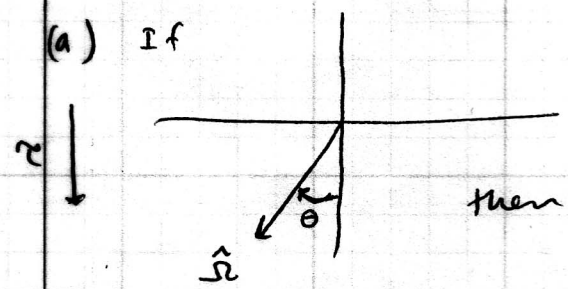

then $\mu \frac{dI}{d\tau} = -I + S$

Shettle & Weinman
Wiscombe

(b) If

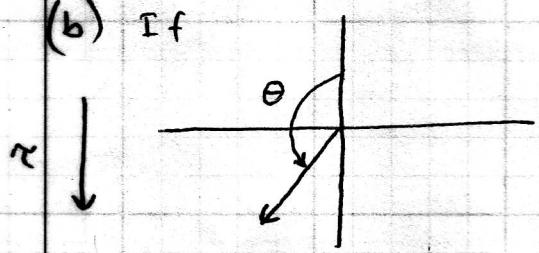

then $-\mu \frac{dI}{d\tau} = -I + S$

or $\mu \frac{dI}{d\tau} = I - S$

Liou
Thomas
Petty

Petty, Liou, Thomas use (b). $0 \le \mu \le 1$ for I^+; $-1 \le \mu \le 0$ for I^-

We'll use (b) for 2-stream
(a) for Eddington

Let's verify that the same equation applies to both I^+ and I^-, using convention (b).

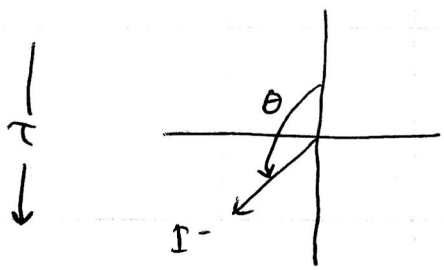

For I^-, $d\tau_{path} = \frac{-d\tau}{\mu}$

because $-\mu$ is positive

$$-\mu \frac{dI^-}{d\tau} = -I^- + S$$

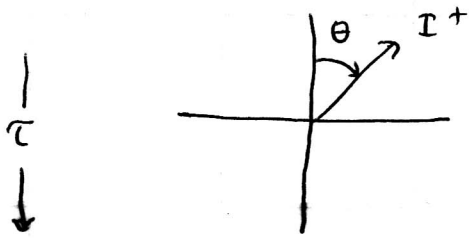

For I^+, μ is ⊕

but path is in $-\tau$-direction.

So $d\tau_{path} = \frac{-d\tau}{\mu}$

$\frac{dI^+}{d\tau}$ is the change of upward intensity with increasing τ, i.e. going backward along the beam.

So extinction causes I^+ to increase with τ,

and sources cause I^+ to decrease with τ.

In summary, we have the same equation for I^+, I^-:

$$\mu \frac{dI^+}{d\tau} = I^+ - S$$

$$\mu \frac{dI^-}{d\tau} = I^- - S$$

JOURNAL OF GEOPHYSICAL RESEARCH, VOL. 99, NO. D9, PAGES 18,669–18,684, SEPTEMBER 20, 1994

Reflection of solar radiation by the Antarctic snow surface at ultraviolet, visible, and near-infrared wavelengths

Thomas C. Grenfell and Stephen G. Warren
Department of Atmospheric Sciences, University of Washington, Seattle

Peter C. Mullen[1]
Geophysics Program, University of Washington, Seattle

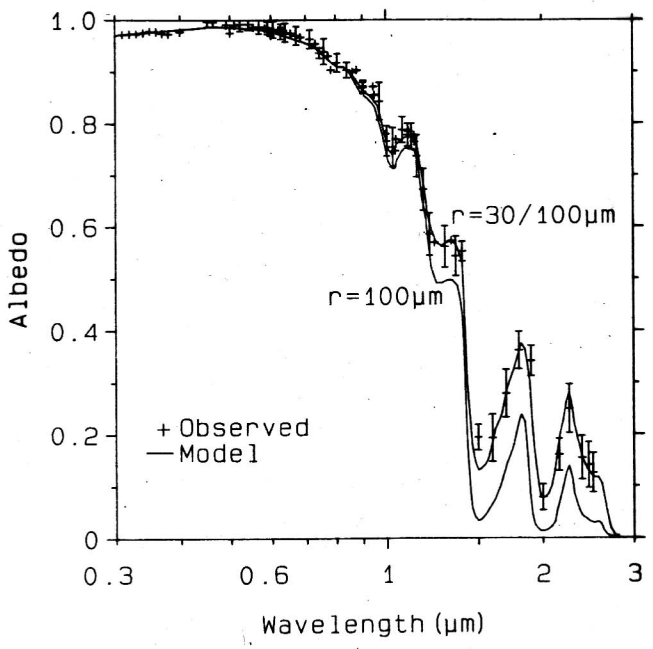

Figure 4. The observed spectral albedo for diffuse incident radiation versus wavelength for January 23, 1986, near South Pole Station [$\langle\alpha\rangle$ = 0.83]. The error bars show the standard deviation of three scans. Where they are not shown, the standard deviation is smaller than the height of the symbol. The solid lines are model results for a homogeneous layer with a grain radius of 100 μm [$\langle\alpha\rangle$ = 0.81] and for a two-layer model with a 0.25-mm thick layer of 30-μm grains over a thick layer of 100-μm grains [$\langle\alpha\rangle$ = 0.83]. NOAA's average albedo for this day was $\langle\alpha\rangle$ = 0.839.

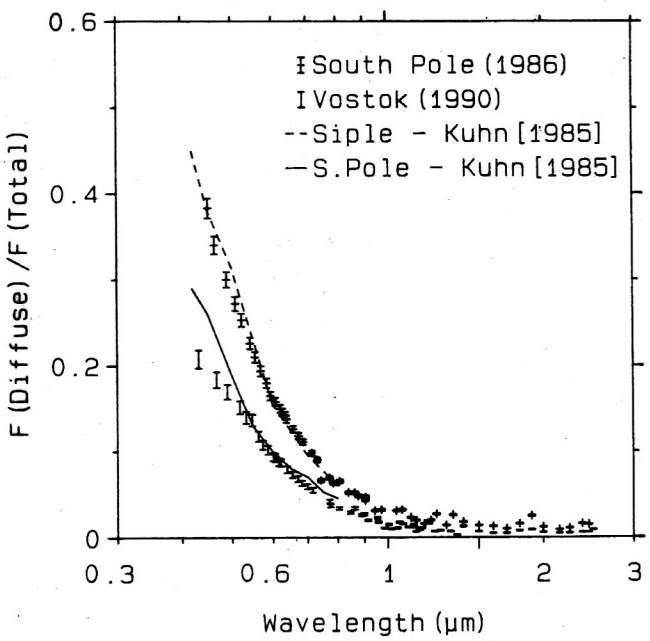

Figure 8. Observations of the ratio of diffuse to total (D/T) radiation under clear sky conditions. Results of *Kuhn* [1985] are included for reference. Station elevations are as follows: South Pole, 2835 m; Vostok, 3488 m; Siple Station, 1054 m. We apparently used a smaller shade than did Kuhn, so we measured a larger fraction of diffuse radiation.

RTE for plane-parallel atmosphere illuminated by direct solar beam, for use in 2-stream, Eddington, δ-Eddington methods; i.e. for flux.

2.2 Separation of (scattered / diffuse) and (direct / solar) radiation

$I = I_s + I_d$ $\quad$ I_s "solar" (direct)

I_d "diffuse" (scattered)

Obtain separate r.t.e.s for each. The rte for I_s can be solved immediately; it's just Beer's law:

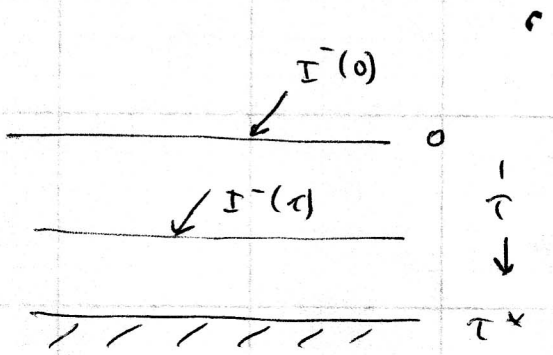

$$I_s^-(\tau,\mu,\phi) = I_s^-(0,\mu,\phi)e^{-\tau/|\mu|}, \text{ or } \mu\frac{dI_s^-}{d\tau} = I_s^- \quad (7)$$

(μ is negative for I^-)

$I_s^+(\tau,\mu,\phi) = 0$ for all τ if no specular reflection from bottom

Complete rte (without emission), using upward-normal convention for μ, is

$$\mu\frac{dI}{d\tau} = I - \frac{\bar{\omega}}{4\pi}\int I \cdot P\, d\omega'$$

$$\mu\frac{d}{d\tau}(I_s + I_d) = I_s + I_d - \frac{\bar{\omega}}{4\pi}\int (I_s + I_d)\, P\, d\omega'$$

these cancel by eq (7)

What remains is rte for I_d (diffuse intensity):

$$\mu \frac{dI_d(\tau,\mu,\phi)}{d\tau} = I_d(\tau,\mu,\phi) - \underbrace{\frac{\varpi}{4\pi}\int_{4\pi} I_d(\tau,\mu',\phi') P(\mu,\phi,\mu',\phi')\, d\omega'}_{S_d(\tau,\mu,\phi)}$$

$$- \underbrace{\frac{\varpi}{4\pi}\int I_s(\tau,\mu',\phi') P(\mu,\phi,\mu',\phi')\, d\omega'}_{S_s(\tau,\mu,\phi)} . \qquad (8)$$

Now specify I_s as incident "parallel-beam" radiation from the sun in direction $(-\mu_0, \phi_0)$. Define F^s as incident solar flux perpendicular to the beam.

Then $I_s^-(0,\mu',\phi') = F^s \delta(\mu'+\mu_0)\delta(\phi'-\phi_0)$ (9)

[Flux on a horizontal surface at TOA is

$$\int I_s^- \mu\, d\omega = \mu_0 F^s .]$$

I_s^- is attenuated exponentially:

$$I_s^-(\tau,\mu',\phi') = I_s^-(0,\mu',\phi')\, e^{-\tau/|\mu'|}$$

Putting (9) into (7) and (7) into (8):

$$S_s(\tau,\mu,\phi) = \frac{\tilde{\omega}}{4\pi}\int_0^{2\pi} d\phi' \int_{-1}^{1} d\mu' \, \overline{F^s}\, \delta(\mu'+\mu_0)\,\delta(\phi'-\phi_0)\, e^{-\tau/|\mu'|}\, P(\mu,\phi,\mu',\phi')$$

μ_0 $\quad -\mu_0$ $\quad \phi_0$

$$\int_0^{\infty} \delta(x-x_0)\,dx = 1$$

and $\int_0^{\infty} f(x)\,\delta(x-x_0)\,dx = f(x_0)$ } so

so

$$\boxed{S_s(\tau,\mu,\phi) = \frac{\tilde{\omega}}{4\pi}\,\overline{F^s}\, e^{-\tau/\mu_0}\, P(\mu,\phi,-\mu_0,\phi_0)} \qquad (10)$$

The physical meaning of this can readily be seen as the product of a series of probabilities:

	[Contributions to scattered intensity in direction (μ,ϕ) due to sources in layer $d\tau$ from scattering of direct beam]	$S_s(\tau,\mu,\phi)\,d\tau$
=	incident flux	$\mu_0 \overline{F^s}$
×	transmittance to τ	$e^{-\tau/\mu_0}$
×	attenuation in $d\tau$	$1-e^{-d\tau/\mu_0} = d\tau/\mu_0$
×	probability of scattering given extinction	$\tilde{\omega}$
×	probability density of going to direction μ,ϕ given scattering out of $(-\mu_0,\phi_0)$	$\frac{P(\mu,\phi,-\mu_0,\phi_0)}{4\pi}$

2.3 Averaging over azimuth.

Now average the r.t.e. (8) over azimuth: Apply $\frac{1}{2\pi}\int d\phi$ to both sides. As we showed earlier in class, the S_d term will became

$$\frac{1}{2\pi}\int_0^{2\pi} S_d \, d\phi = \frac{\omega}{2}\int_{-1}^{1} d\mu' \, P(\mu,\mu') \, I(\tau,\mu'),$$

where $p(\mu,\mu')$ is the azimuthally averaged phase function:

$$p(\mu,\mu') \equiv \frac{1}{2\pi}\int_0^{2\pi} p(\mu,\phi,\mu',\phi') \, d\phi .$$

The azimuthally-averaged r.t.e. for the diffuse intensity is then

$$\mu \frac{dI(\tau,\mu)}{d\tau} = I(\tau,\mu) - \overbrace{\frac{\omega}{2}\int_{-1}^{1} d\mu' \, p(\mu,\mu') I(\tau,\mu')}^{S_d} - \underbrace{\frac{\omega}{4\pi} F^s \, e^{-\tau/\mu_0} \, p(\mu,-\mu_0)}_{S_s} \qquad (11)$$

where here $I \equiv$ azimuthally averaged scattered (diffuse) intensity, we have dropped the subscript **d**.

This is eq. 6.1.12 of Liou. [Liou writes $F_\odot$ for F^s.]

Eq (11) will be used for derivation of the two-stream method.

2.4 Polynomial expansion of the azimuthally-averaged phase function.

If the phase function is expressed as a polynomial expansion, then the conversion from $P(\cos\Theta)$ to $p(\mu,\mu')$ requires azimuthal averaging of the polynomial expansion.

We have $P(\cos\Theta) = \sum_l (2l+1)\chi_l P_l(\cos\Theta)$.

The relation between $\cos\Theta$ and μ, μ', ϕ, ϕ' was derived in homework:

$$\cos\Theta = \mu\mu' + (1-\mu^2)^{1/2}(1-\mu'^2)^{1/2}\cos(\phi-\phi') \qquad (12)$$

Given (12), then by the "addition theorem" (proven by Liou ~~p. 367~~ Appendix E, p. 534)

$$P_l(\cos\Theta) = P_l(\mu)P_l(\mu') + 2\sum_{m=1}^{l}\frac{(l-m)!}{(l+m)!}P_l^m(\mu)P_l^m(\mu')\cos[m(\phi'-\phi)] \qquad (13)$$

The P_l^m are "associated Legendre functions":

$$P_l^m(\mu) \equiv (1-\mu^2)^{m/2}\frac{d^m P_l(\mu)}{d\mu^m}, \text{ where } \frac{d^m}{d\mu^m} \text{ is the } m^{th} \text{ derivative}$$

But these all disappear when we average over ϕ because

$$\int_0^{2\pi}\cos m(\phi'-\phi)\,d\phi = 0 \quad \text{for} \quad m \neq 0 \quad [m = \text{integer}]$$

so for each P_l: $\frac{1}{2\pi}\int_0^{2\pi} P_l(\cos\Theta)\,d\phi = P_l(\mu)P_l(\mu')$

Now we're ready to average the phase function over azimuth:

$$P(\mu,\mu') = \frac{1}{2\pi}\int_0^{2\pi} P(\cos\Theta)\,d\phi$$

$$= \frac{1}{2\pi}\int_0^{2\pi} d\phi \sum_l (2l+1)\chi_l P_l(\cos\Theta)$$

$$= \sum_l (2l+1)\chi_l P_l(\mu) P_l(\mu') \qquad (14)$$

Putting (14) into (11), S_d becomes

$$S_d = \frac{\omega}{2}\int_{-1}^{1} d\mu' \left[\sum_l (2l+1)\chi_l P_l(\mu) P_l(\mu')\right] I(\tau,\mu')$$

$$= \frac{\omega}{2}\sum_l \chi_l(2l+1) P_l(\mu)\int_{-1}^{1} d\mu' P_l(\mu') I(\tau,\mu')$$

Similarly, S_s becomes

$$S_s = \frac{\omega}{4\pi} F^s e^{-\tau/\mu_0}\sum_l (2l+1)\chi_l P_l(\mu) P_l(-\mu_0)$$

S_0 (11) becomes

$$\mu\frac{dI(\tau,\mu)}{d\tau} = I(\tau,\mu) - \frac{\omega}{2}\sum(2l+1)\chi_l P_l(\mu)\int_{-1}^{1} d\mu' P_l(\mu') I(\tau,\mu')$$

$$-\frac{\omega}{4\pi} F^s e^{-\tau/\mu_0}\sum_l (2l+1)\chi_l P_l(\mu) P_l(-\mu_0) \qquad (15)$$

This is eq. 6.1.6 of Liou.
(Liou's coefficients are $\omega_l \equiv (2l+1)\chi_l$.)
We will use (15) in derivation of the Eddington method and Discrete Ordinates method.

3. TWO-STREAM METHOD

Intensity variation with angle is represented by just two 'streams' of radiation: I^+ constant over upward hemisphere and I^- constant over downward hemisphere.

3.1 Backscattered fraction; relation to asymmetry factor.

Break phase function $p(\mu,\mu')$ into two parts:

$$\int \frac{p}{4\pi} d\omega = \frac{1}{4\pi}\int_0^{2\pi} d\phi \int_{-1}^{1} p\, d\mu = \frac{1}{2}\int_{-1}^{1} p(\mu,\mu')\, d\mu \quad ; \text{ break into upward \& downward hemispheres.}$$

$$= \frac{1}{2}\int_0^1 p(\mu,\mu')\, d\mu + \frac{1}{2}\int_{-1}^{0} p(\mu,\mu')\, d\mu$$

$$= \underbrace{\frac{1}{2}\int_0^1 p(\mu,\mu')\, d\mu}_{\substack{\text{fraction of } \mu' \text{ radiation} \\ \text{scattered into the} \\ +\mu \text{ hemisphere} \\ \text{(forward if } \mu'>0\text{)}}} + \underbrace{\frac{1}{2}\int_0^1 p(-\mu,\mu')\, d\mu}_{\substack{\text{fraction of } \mu' \text{ radiation} \\ \text{scattered into the} \\ -\mu \text{ hemisphere} \\ \text{(backward if } \mu'>0\text{)}}} \quad [\text{where } \mu \text{ is now } \oplus.]$$

$$f(\mu') = 1 - b(\mu') \qquad b(\mu')$$

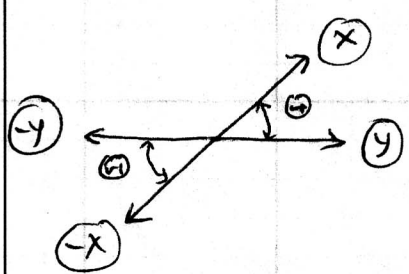

For two arbitrary directions X, Y,

$$p(X,Y) = p(Y,X) = p(-X,-Y) = p(-Y,-X)$$

if p depends only on Θ.

So

(change signs) ↓ (exchange μ, μ') ↓

$$b(\mu') = \frac{1}{2}\int_0^1 p(-\mu,\mu')\,d\mu = \frac{1}{2}\int_0^1 p(\mu,-\mu')\,d\mu = \frac{1}{2}\int_0^1 p(-\mu',\mu)\,d\mu$$

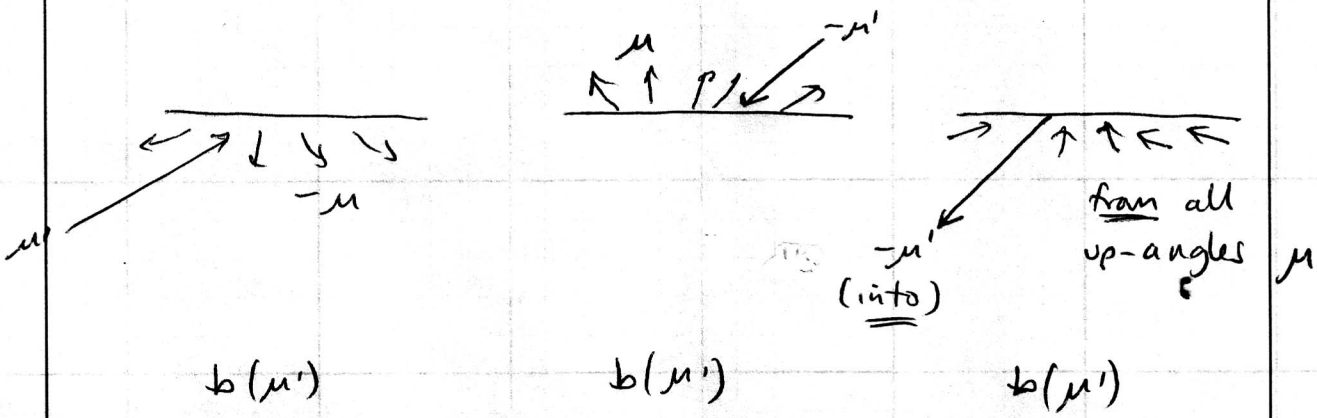

b is related to g, as discussed by Wiscombe & Grams, 1976: J Atmos Sci. 33, 2440.

A simple relation between b and g can be obtained by considering two streams vertically upward or downward. Then $\cos\Theta$ is either +1 or −1 for each scattering event:

I^- ↓ / ↑ I^+

$$g = (+1)\,f + (-1)\,b = (1-b) - b = 1 - 2b$$

so $\boxed{b = \frac{1-g}{2}}$. We will use this below, as does Bohren, 1987: Am. J. Phys 55, 524–533

Fig 3.67 Simple representation of backscatter b

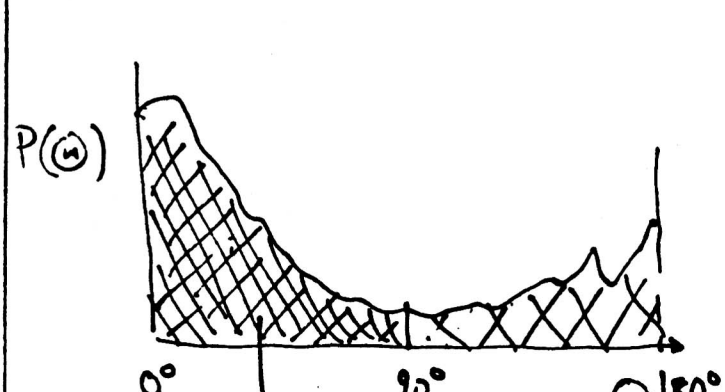

Forward scatter

$$f = \frac{1}{4\pi}\int_0^{2\pi}\int_0^{1} p(\cos\Theta)\sin\Theta\, d\Theta\, d\phi$$

Backscatter

$$b = \frac{1}{4\pi}\int_0^{2\pi}\int_{-1}^{0} p(\cos\Theta)\sin\Theta\, d\Theta\, d\phi$$

Normalization

$$f + b = 1$$

Assume simple form of $P(\Theta)$

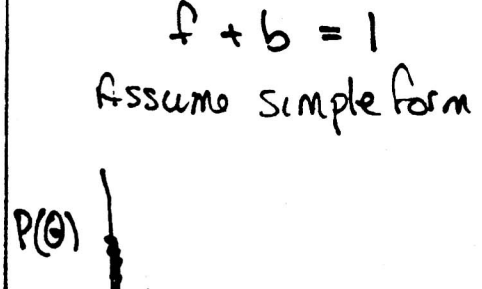

Then by definition

$$g = (+1)f + (-1)b$$

and

$$b = (1-g)/2$$

$$f = (1+g)/2$$

32.

3.2. Derivation of twostream equations, including direct beam

(following Liou)

The procedure will be to average (11) over the upward hemisphere and over the downward hemisphere, to obtain two equations: for I^+ and for I^-

First consider what happens to S_d.

In the equation for I^+, before averaging over μ, S_d will be

$$S_d = \frac{\tilde{\omega}}{2}\int_{-1}^{1} d\mu' \, p(\mu,\mu') \, I(\tau,\mu')$$

$$= \frac{\tilde{\omega}}{2}\int_{0}^{1} d\mu' \, p(\mu,\mu') \, I(\tau,\mu') + \frac{\tilde{\omega}}{2}\int_{-1}^{0} d\mu' \, p(\mu,\mu') \, I(\tau,\mu')$$

$$= \frac{\tilde{\omega}}{2} I^+ \int_0^1 d\mu' \, p(\mu,\mu') + \frac{\tilde{\omega}}{2} I^- \int_0^1 d\mu' \, p(-\mu,\mu')$$

$$\boxed{S_d = \tilde{\omega} I^+ (1 - b(\mu)) + \tilde{\omega} I^- b(\mu)} \qquad (\text{in } I^+ \text{ eqn}, \mu > 0)$$

Similarly in the I^- eqn:

$$\boxed{S_d = \tilde{\omega} I^- (1 - b(\mu)) + \tilde{\omega} I^+ b(\mu)} \qquad (\text{in } I^- \text{ eqn}, \mu < 0)$$

(16)

This is also seen in the diagram:

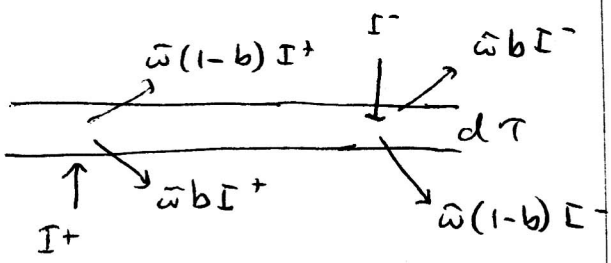

Now to average (11) over the upward hemisphere, apply $\int_0^1 d\mu$ to (11)

Define $\bar{b} \equiv \int_0^1 b(\mu)\, d\mu$, the average value of b,

so $\int_0^1 S_s\, d\mu = \tilde{\omega}\, I^+ (1-\bar{b}) + \tilde{\omega}\, I^- \bar{b}$.

Also note that $\int_0^1 \mu\, d\mu = \frac{1}{2}$;

$\frac{1}{2}\int_0^1 p(\mu, \mu_0)\, d\mu = b(\mu_0)$; $\int_0^1 I(\tau, \mu)\, d\mu = I^+(\tau)$

Then

$$\frac{1}{2}\frac{dI^+(\tau)}{d\tau} = I^+(\tau) - \tilde{\omega}\, I^+ (1-\bar{b}) - \tilde{\omega}\, I^- \bar{b} - \frac{\tilde{\omega}}{2\pi} F^s e^{-\tau/\mu_0} b(\mu_0)$$

or

$$\boxed{\frac{1}{2}\frac{dI^+(\tau)}{d\tau} = (1-\tilde{\omega})\, I^+(\tau) + \tilde{\omega}\bar{b}\,(I^+ - I^-) - \frac{\tilde{\omega}}{2\pi} F^s e^{-\tau/\mu_0} b(\mu_0)} \qquad (17)$$

Similarly, averaging over the downward hemisphere, apply $\int_{-1}^0 d\mu$ to (11):

$$\boxed{-\frac{1}{2}\frac{dI^-(\tau)}{d\tau} = (1-\tilde{\omega})\, I^-(\tau) - \tilde{\omega}\,\bar{b}\,(I^+ - I^-) - \frac{\tilde{\omega}}{2\pi} F^s e^{-\tau/\mu_0}\,(1-b(\mu_0))} \qquad (18)$$

These are equivalent to Eqs 4a, 4b of Wiscombe & Grams but with different sign convention for I^+, I^-.

The procedure to solve eqns (17) and (18) is to add and subtract them, obtaining eqns for $(I^+ + I^-)$ and $(I^+ - I^-)$. Then differentiate one or the other to get a second-order differential equation that can be solved. Liou gives the results.

3.3 Solution for diffuse incidence

In order to simplify the two-stream equations to illustrate results, we ignore the direction of the solar beam. We set the direct beam to zero, and instead specify isotropic diffuse incidence at Top-of-Atmosphere. This is just equivalent to saying b is independent of μ_0.

We also set $b = \frac{1-g}{2}$ as on page 74.

Then (17) & (18) become

$$\frac{1}{2}\frac{dI^+}{d\tau} = (1-\tilde{\omega})I^+ + \frac{\tilde{\omega}(1-g)}{2}(I^+ - I^-) \tag{19}$$

$$-\frac{1}{2}\frac{dI^-}{d\tau} = (1-\tilde{\omega})I^- - \frac{\tilde{\omega}(1-g)}{2}(I^+ - I^-) \tag{20}$$

Add and subtract (19) and (20) to obtain

$$\frac{1}{2}\frac{d}{d\tau}(I^+ - I^-) = (1-\tilde{\omega})(I^+ + I^-) \tag{21}$$

$$\begin{aligned}\frac{1}{2}\frac{d}{d\tau}(I^+ + I^-) &= (1-\tilde{\omega})(I^+ - I^-) + \tilde{\omega}(1-g)(I^+ - I^-) \\ &= (1-\tilde{\omega}+\tilde{\omega}-\tilde{\omega}g)(I^+ - I^-) \\ &= (1-\tilde{\omega}g)(I^+ - I^-)\end{aligned} \tag{22}$$

These are two coupled first-order differential equations. To uncouple them, differentiate them:

$$\frac{d^2}{d\tau^2}(I^+ + I^-) = 2(1-\tilde{\omega}g)\frac{d}{d\tau}(I^+ - I^-) \qquad (23)$$

$$= 4(1-\tilde{\omega}g)(1-\tilde{\omega})(I^+ + I^-)$$

Also $$\frac{d^2}{d\tau^2}(I^+ - I^-) = 4(1-\tilde{\omega}g)(1-\tilde{\omega})(I^+ - I^-) \qquad (24)$$

(23) and (24) are mathematically the same equation; abbreviate the dependent variable as Y: $\frac{d^2Y}{d\tau^2} = \Gamma^2 Y$

where $\Gamma \equiv 2\sqrt{1-\tilde{\omega}}\sqrt{1-\tilde{\omega}g}$.

The solution is $Y = \alpha e^{\Gamma\tau} + \beta e^{-\Gamma\tau}$

so the solutions for I^+, I^- are also sums of exponentials:

$$I^+(\tau) = Ae^{\Gamma\tau} + Be^{-\Gamma\tau} \qquad (25)$$

$$I^-(\tau) = Ce^{\Gamma\tau} + De^{-\Gamma\tau} \qquad (26)$$

where A, B, C, D are coefficients to be determined.

The coefficients are related; only 2 are independent:

substitute (25) and (26) into (19):

$$\frac{dI^+}{d\tau} = 2(1-\tilde{\omega})(Ae^{\Gamma\tau} + Be^{-\Gamma\tau}) + \tilde{\omega}(1-g)\left[(A-C)e^{\Gamma\tau} + (B-D)e^{-\Gamma\tau}\right] \qquad (27)$$

But from (25) we also have

$$\frac{dI^+}{d\tau} = A\Gamma e^{\Gamma\tau} - B\Gamma e^{-\Gamma\tau} \qquad (28)$$

Setting (27) = (28) and grouping terms $e^{\Gamma\tau}$, $e^{-\Gamma\tau}$:

$$\left[2(1-\tilde{\omega})A + \tilde{\omega}(1-g)(A-C) - A\Gamma\right] e^{\Gamma\tau} = \left[-B\Gamma - 2(1-\tilde{\omega})B - \tilde{\omega}(1-g)(B-D)\right] e^{-\Gamma\tau}$$

In order that this ~~eqn~~ hold for all τ, the two groups of coefficients must separately $= 0$. The result is a relation between A, B, C, D:

$$\frac{C}{A} = \frac{B}{D} = \frac{2-\tilde{\omega}-\tilde{\omega}g-\Gamma}{\tilde{\omega}(1-g)} = \frac{\sqrt{1-\tilde{\omega}g} - \sqrt{1-\tilde{\omega}}}{\sqrt{1-\tilde{\omega}g} + \sqrt{1-\tilde{\omega}}} \equiv \rho_\infty$$

Thomas abbreviates this ratio ρ_∞; it will turn out to be the reflectance of a semi-infinite atmosphere.

So $C = \rho_\infty A$; $B = \rho_\infty D$. And (25) & (26) became

$$I^+(\tau) = A e^{\Gamma\tau} + \rho_\infty D e^{-\Gamma\tau} \qquad (29)$$

$$I^-(\tau) = \rho_\infty A e^{\Gamma\tau} + D e^{-\Gamma\tau} \qquad (30)$$

Next: apply boundary conditions, to evaluate A, D.

Top boundary condition.

$I^-(0) = I_0$, the average incident intensity at top.

[Incident flux is $F^s \mu_0$, so $I_0 = \frac{F^s \mu_0}{\pi}$.]

Bottom boundary condition.

Lambertian surface with reflectivity (albedo) r_s:

$$I^+(\tau^*) = r_s I^-(\tau^*)$$

Inserting these conditions into (29), (30):

$$\left\{ \begin{aligned} & I_0 = \rho_\infty A + D \\ & A e^{\Gamma\tau^*} + \rho_\infty D e^{-\Gamma\tau^*} = r_s \left[\rho_\infty A e^{\Gamma\tau^*} + D e^{-\Gamma\tau^*} \right] \end{aligned} \right\}$$ These two equations are solved for A, D.

Then substitute A, D into (29), (30) to get the general solution for intensity at any level τ

$$\frac{I^+(\tau)}{I_0} = \frac{\rho_\infty (1 - r_s \rho_\infty) e^{\Gamma(\tau^* - \tau)} - (\rho_\infty - r_s) e^{-\Gamma(\tau^* - \tau)}}{(1 - r_s \rho_\infty) e^{\Gamma\tau^*} - \rho_\infty (\rho_\infty - r_s) e^{-\Gamma\tau^*}} \qquad (31)$$

$$\frac{I^-(\tau)}{I_0} = \frac{(1 - r_s \rho_\infty) e^{\Gamma(\tau^* - \tau)} - \rho_\infty (\rho_\infty - r_s) e^{-\Gamma(\tau^* - \tau)}}{(1 - r_s \rho_\infty) e^{\Gamma\tau^*} - \rho_\infty (\rho_\infty - r_s) e^{-\Gamma\tau^*}} \qquad (32)$$

If the lower boundary is black ($r_s = 0$), the solution simplifies to

$$I^+(\tau) = \frac{\rho_\infty I_0}{e^{\Gamma\tau^*} - \rho_\infty^2 e^{-\Gamma\tau^*}} \left\{ e^{\Gamma(\tau^* - \tau)} - e^{-\Gamma(\tau^* - \tau)} \right\} \tag{33}$$

$$I^-(\tau) = \frac{I_0}{e^{\Gamma\tau^*} - \rho_\infty^2 e^{-\Gamma\tau^*}} \left\{ e^{\Gamma(\tau^* - \tau)} - \rho_\infty^2 e^{-\Gamma(\tau^* - \tau)} \right\} \tag{34}$$

The flux-reflectance (r) and flux-transmittance (t) are:

$$r = \frac{\pi I^+(0)}{\pi I^-(0)} = \frac{I^+(0)}{I_0} = \frac{\rho_\infty \left[e^{\Gamma\tau^*} - e^{-\Gamma\tau^*} \right]}{e^{\Gamma\tau^*} - \rho_\infty^2 e^{-\Gamma\tau^*}} \tag{35}$$

$$t = \frac{\pi I^-(\tau^*)}{\pi I^-(0)} = \frac{I^-(\tau^*)}{I_0} = \frac{1 - \rho_\infty^2}{e^{\Gamma\tau^*} - \rho_\infty^2 e^{-\Gamma\tau^*}} \tag{36}$$

The following examples will assume $r_s = 0$.

3.4 Examples of results

3.4.1 Semi-infinite medium. $\tau^* \to \infty$

(33) and (34) became

$$I^+(\tau) = I_0 \rho_\infty e^{-\Gamma\tau}$$

$$I^-(\tau) = I_0 e^{-\Gamma\tau}$$

Albedo

$$\text{Albedo at TOA} = \frac{\pi I^+(0)}{\pi I^-(0)} = \rho_\infty = \frac{\sqrt{1-\tilde{\omega}g} - \sqrt{1-\tilde{\omega}}}{\sqrt{1-\tilde{\omega}g} + \sqrt{1-\tilde{\omega}}}$$

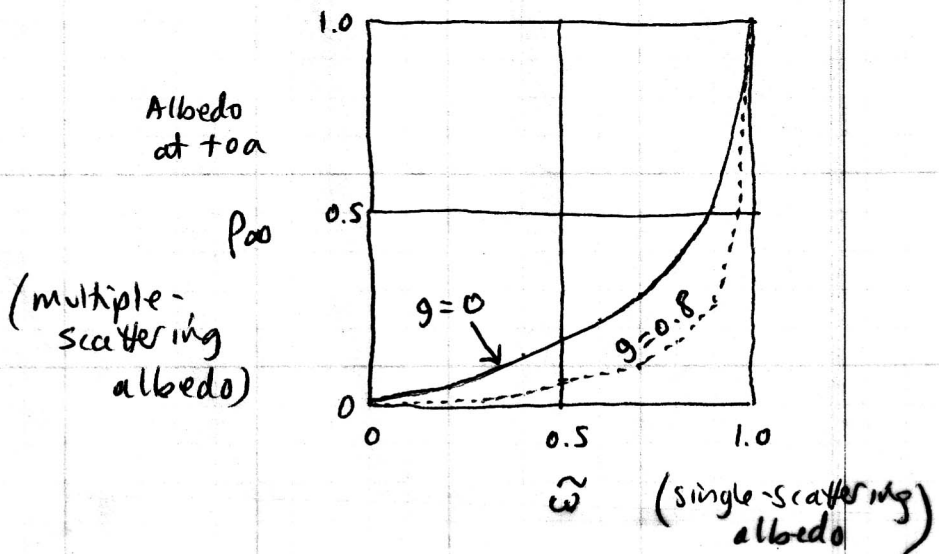

Net flux

$$F = \text{net flux} = \pi(I^+ - I^-) = -\pi I_0 (1-\rho_\infty) e^{-\Gamma\tau}$$

The net flux is negative because $I^- > I^+$.
I^-, I^+, and F all decay away from the irradiated surface exponentially but with an effective optical depth $\Gamma\tau$ instead of the true optical depth τ. This "flux optical depth" $\Gamma\tau$ is $2\sqrt{1-\tilde{\omega}}\sqrt{1-\tilde{\omega}g}\,\tau$.
As $\tilde{\omega}$ increases, Γ decreases, and radiation can penetrate deeply by scattering.

In the limit of pure absorption, $\tilde{\omega} = 0$, $\Gamma \to 2$, and flux is attenuated by

$$e^{-\Gamma\tau} = e^{-2\tau} = e^{-\tau/\bar{\mu}} \quad \text{where } \bar{\mu} = 1/2, \text{ as expected.}$$

If $\tilde{\omega} \neq 0$, flux is attenuated more slowly.

3.4.2. Conservative scattering, $\tilde{\omega} = 1$ (cloud at visible wavelengths)

If $\tilde{\omega} = 1$ is substituted into (31) and (32), the equations reduce to $I^+(\tau) = \frac{0}{0}$. It is necessary therefore to take the limit as $\tilde{\omega} \to 1$. But an easier way to proceed is to start with (21) and (22) again using $\tilde{\omega} = 1$ from the start, and redo the derivation. (21) becomes

$$\frac{1}{2}\frac{d}{d\tau}(I^+ - I^-) = 0.$$

This gives, on integration,

$$I^+ - I^- = \text{constant.} \qquad \text{But } I^+ - I^- \text{ is } F/\pi,$$

so F is the constant net flux to be determined by boundary conditions.

$$I^+ - I^- = F/\pi \tag{37}$$

(22) becomes

$$\frac{d}{d\tau}(I^+ + I^-) = 2(1-g)(I^+ - I^-) = \frac{2F}{\pi}(1-g) .$$

This integrates to

$$I^+ + I^- = \frac{2F\tau}{\pi}(1-g) + k \qquad (38)$$

The constants of integration F & k are to be determined by the boundary conditions.

Solving (37) and (38) for I^+ and I^- gives

Add: $$I^+ = \frac{F}{2\pi}(1 + 2\tau(1-g)) + k/2 \qquad (39)$$

Subtract: $$I^- = \frac{-F}{2\pi}(1 - 2\tau(1-g)) + k/2 \qquad (40)$$

Applying the boundary conditions $I^+(\tau^*) = 0$ and $I^-(0) = I_0$ in (39) and (40) gives (for non reflecting surface)

$$\frac{k}{2} = I_0 + F/2\pi \quad \text{and} \quad F = \frac{-\pi I_0}{1 + \tau^*(1-g)} , \text{ the net flux.}$$

The general solution for intensity is then (for non-reflecting lower surface)

$$I^+(\tau) = \frac{I_0(1-g)(\tau^* - \tau)}{1 + \tau^*(1-g)} \qquad I^-(\tau) = \frac{I_0[1 + (1-g)(\tau^* - \tau)]}{1 + \tau^*(1-g)} \qquad (41)$$

Transmittance: $$t = \frac{I^-(\tau^*)}{I^-(0)} = \frac{1}{1 + (1-g)\tau^*} \qquad (42)$$

Reflectance (albedo): $$r = 1 - t = \frac{(1-g)\tau^*}{1 + (1-g)\tau^*} \qquad (43)$$

Addendum to page 85. (85a)

Reflecting lower boundary with albedo r_s:

Eqs (41) are for $r_s = 0$ and $\tilde{\omega} = 1$. For $r_s \neq 0$:

$$I^+(\tau) = \frac{I_0 \left[r_s + (1-r_s)(1-g)(\tau^* - \tau) \right]}{1 + (1-r_s)\tau^*(1-g)}$$

$$I^-(\tau) = \frac{I_0 \left[1 + (1-r_s)(1-g)(\tau^* - \tau) \right]}{1 + (1-r_s)\tau^*(1-g)}$$

Albedo. $$\frac{\pi I^+}{\pi I^-} = \frac{r_s + (1-r_s)(1-g)(\tau^* - \tau)}{1 + (1-r_s)(1-g)(\tau^* - \tau)}$$

Albedo at top $$\frac{\pi I^+(0)}{\pi I^-(0)} = \frac{r_s + (1-r_s)(1-g)\tau^*}{1 + (1-r_s)(1-g)\tau^*}$$

These equations reduce to eqs (41) and (43) for $r_s = 0$.

"transmittance" $$\frac{\pi I^-(\tau^*)}{\pi I^-(0)} = \frac{1}{1 + (1-r_s)(1-g)\tau^*}$$

This "transmittance", plus albedo at top, add to more than 1 if $r_s > 0$. Do you understand why? (see pp 89-90)

K+E SEMI-LOGARITHMIC 4 CYCLES X 70 DIVISIONS
KEUFFEL & ESSER CO. MADE IN U.S.A.

46 6010

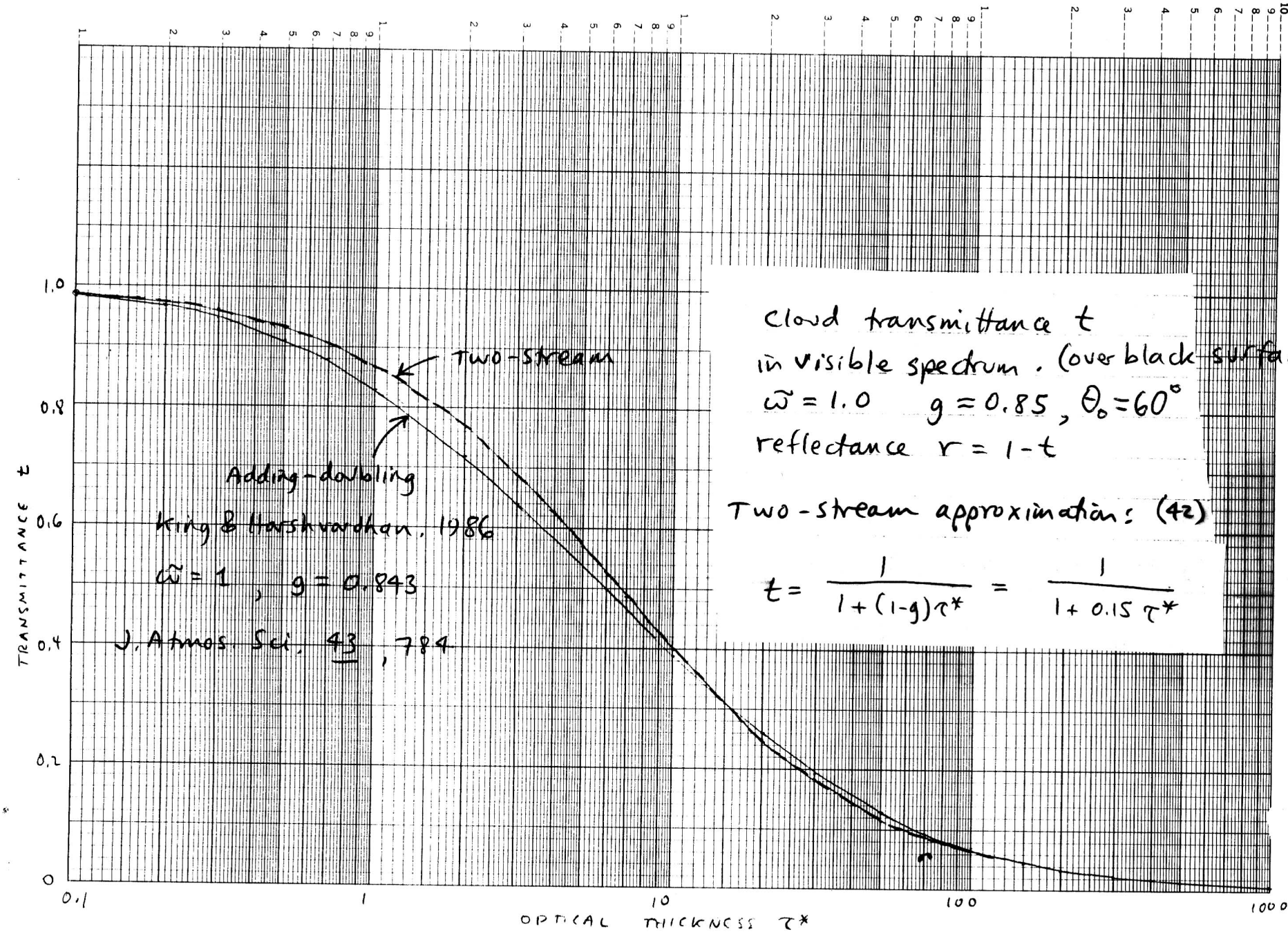

Cloud transmittance t
in visible spectrum. (over black surface)
$\tilde{\omega} = 1.0$ $g = 0.85$, $\theta_0 = 60°$
reflectance $r = 1 - t$

Two-stream approximation: (42)

$$t = \frac{1}{1 + (1-g)\tau^*} = \frac{1}{1 + 0.15\,\tau^*}$$

For isotropic scattering, g=0, and $t = \frac{1}{1+\tau^*}$ So for conservative scattering the flux is not depleted exponentially. This is a famous result obtained by Schuster in 1905.

Equations 42 and 43 were derived for diffuse incidence. For direct incidence, Coakley and Chylek derived equations for the albedo and transmittance of a non-absorbing cloud as functions of solar zenith cosine μ_0:

$$r(\mu_0) = \frac{\tau^*(1-g)}{2\mu_0 + \tau^*(1-g)}, \text{ and } \quad t(\mu_0) = \frac{2\mu_0}{2\mu_0 + \tau^*(1-g)} \tag{44}$$

(Coakley, J.A. Jr., and P. Chylek, 1975: The two-stream approximation in radiative transfer: including the angle of the incident radiation. *J. Atmos. Sci., 32,* 409-418.)

Eq. 44 reduces to (43) for θ_0=60°. It is quite accurate, so it is a very useful approximation for clouds at solar wavelengths.

Eqs. 42, 43, and 44 show that the relevant variable for determining albedo of a nonabsorbing cloud is τ^*(1-g). This has been called a "scaled optical depth". For example, a typical marine stratocumulus water-cloud with g=0.85 and τ^*=20 will have scaled optical depth = 3. So a real cloud with g=0.85 and τ^*=20 will have the same albedo as an isotropically-scattering cloud with τ^*=3.

Alternative derivation of the effect of surface reflection

If we are interested only in reflectance, absorptance, and transmittance of the atmosphere (and not intensities or fluxes within the atmosphere), then we can just apply a correction to the results we derived for a black underlying surface, for reflectance r and transmittance t. (eqs. 35, 36).

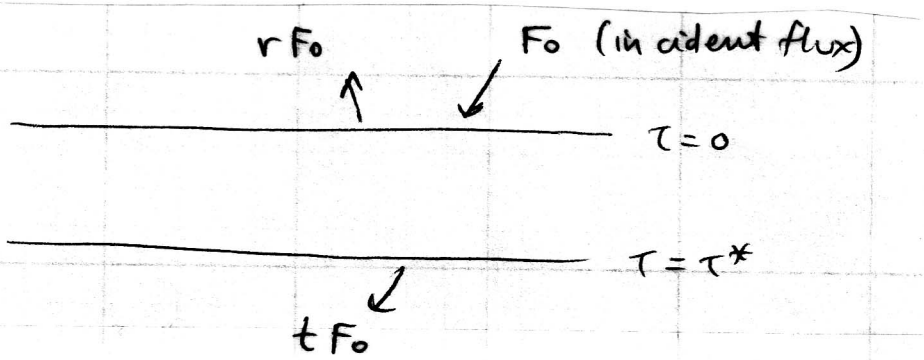

Because they were derived for a non-interacting lower boundary, these are "inherent" properties of the atmosphere. The "apparent" transmittance will be larger than t if $r_s > 0$, and the reflectance of the surface-atmosphere system (the "planetary albedo") will be larger than r.

To derive the effect of a reflecting lower boundary, we use a "multiple bounce" model:

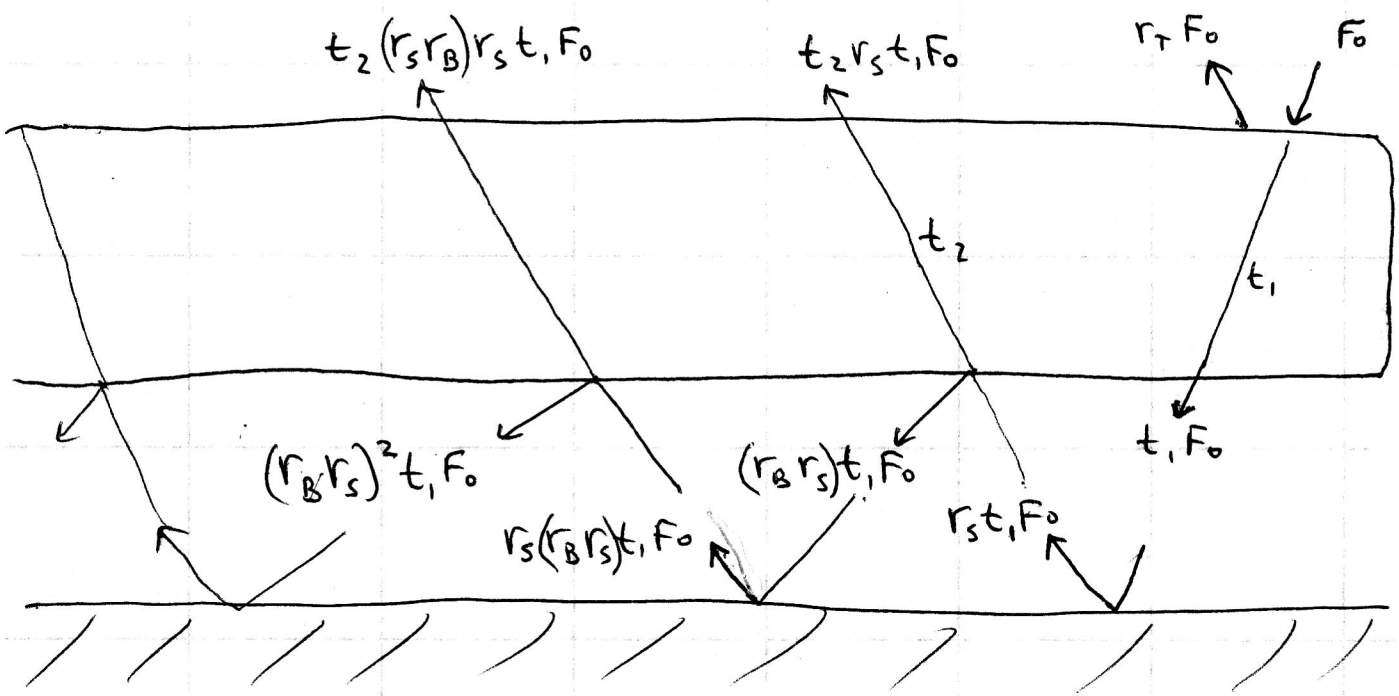

Downward flux at surface: $F_s = t_1 F_0 \left[1 + r_B r_s + (r_B r_s)^2 + (r_B r_s)^3 + \cdots\right]$

$$F_s = t_1 F_0 \frac{1}{1 - r_B r_s} \quad \text{because} \quad 1 + x + x^2 + x^3 + \cdots = \frac{1}{1-x} \text{ for } |x| < 1$$

Apparent transmittance of atmosphere (cloud) is $\frac{F_s}{F_0} = \frac{t_1}{1 - r_B r_s}$.

If $r_s = 0$, $\frac{F_s}{F_0} = t_1$. If $r_s > 0$, $\frac{F_s}{F_0} > t_1$.

89a

ILLUSTRATED GLOSSARY OF SNOW AND ICE

BY

TERENCE ARMSTRONG
BRIAN ROBERTS
CHARLES SWITHINBANK

Published with the support of
UNESCO

Second edition

PRINTED FOR THE
SCOTT POLAR RESEARCH INSTITUTE
CAMBRIDGE
1973

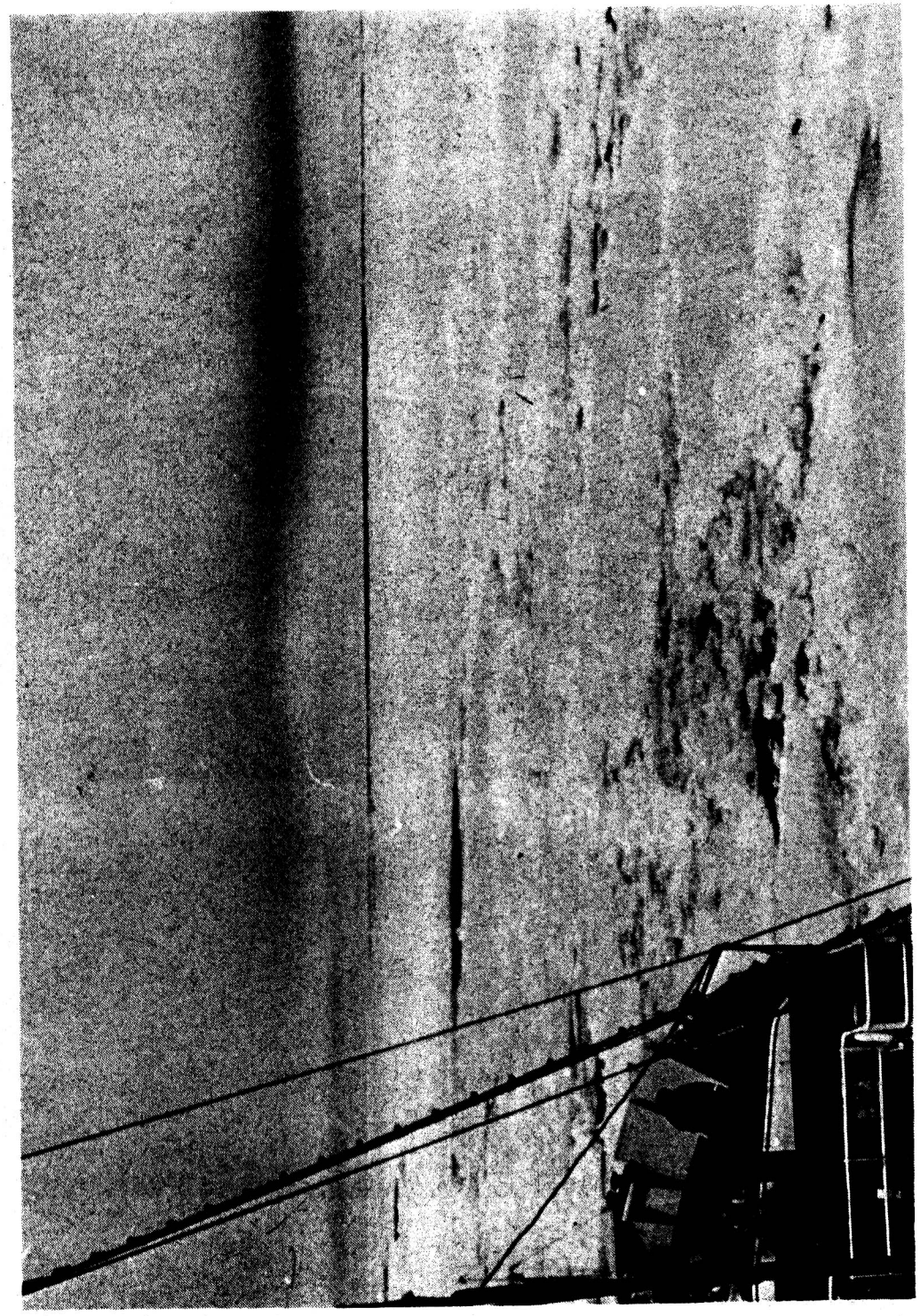

Fig. 27. WATER SKY.

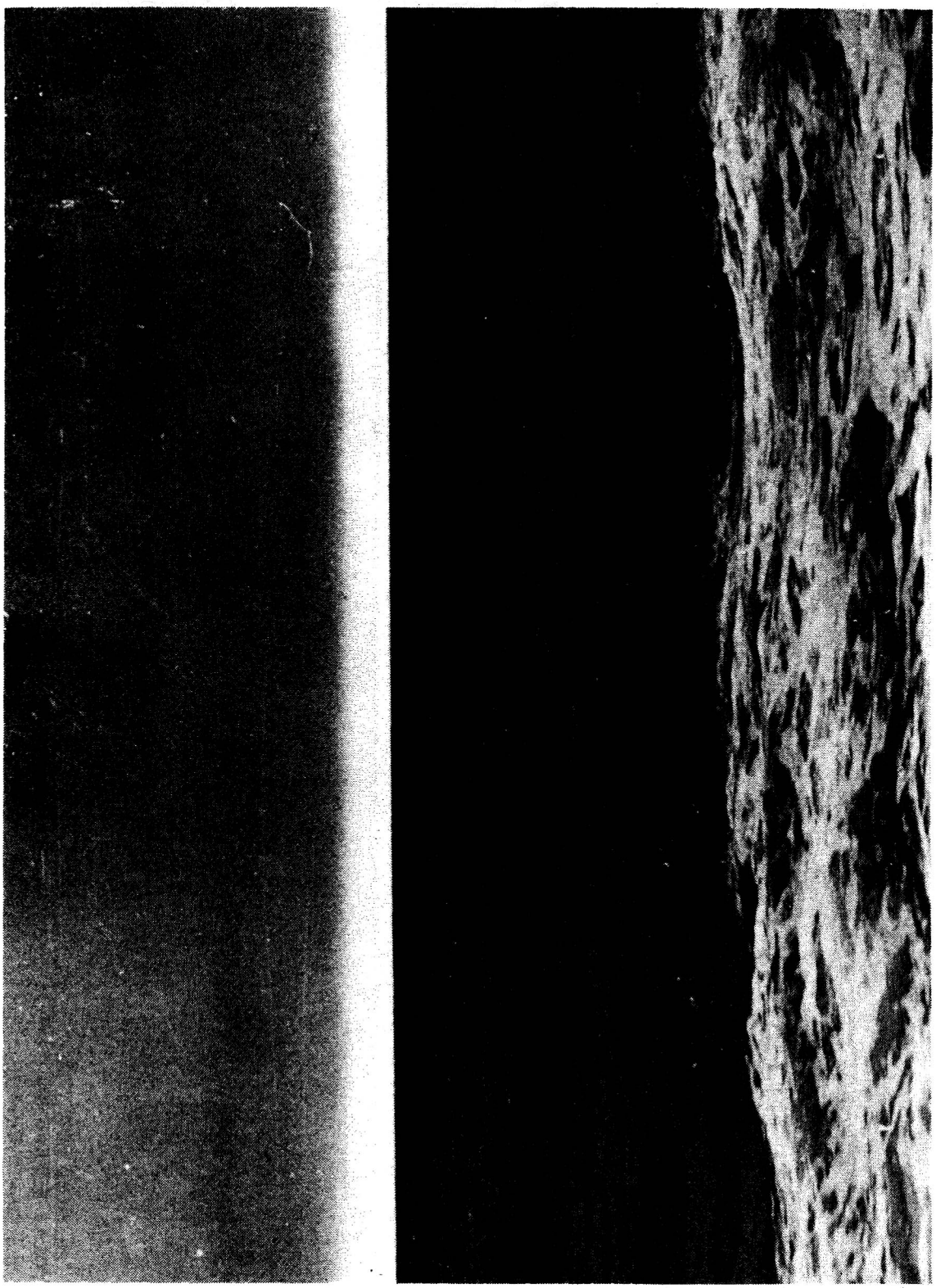

Fig. 28. ICE BLINK.

Upward flux at TOA (or TOC), F_r:

$$F_r = F_0 r_T + F_0 t_1 t_2 r_S \left[1 + r_S r_B + (r_S r_B)^2 + \cdots\right]$$

$$= F_0 \left[r_T + \frac{t_1 t_2 r_S}{1 - r_B r_S} \right] \quad \cdot \qquad \frac{F_r}{F_0} = \frac{r_T - r_T r_B r_S + t_1 t_2 r_S}{1 - r_B r_S}.$$

$\frac{t_1 t_2 r_S}{1 - r_B r_S}$ $\begin{cases} = 0 & \text{if } r_S = 0 \\ > 0 & \text{if } r_S > 0 \end{cases}$

i.e. a reflecting surface below the cloud augments planetary albedo

Special cases for downward flux:

① Non-absorbing cloud (i.e. visible wavelengths):

$t_1 = 1 - r_T$, so $F_S = F_0 \cdot \frac{1 - r_T}{1 - r_B r_S}$

② Non-absorbing cloud over $r_S = 1$
(snow at visible wavelengths; see p. 66):

$$F_S = F_0 \frac{1 - r_T}{1 - r_B}$$

If $r_T = r_B$ then $F_S = F_0$

If $r_B > r_T$ then $F_S > F_0$ (!)

ATMS 533 notes

References:

116 E.P. Shettle and J.A. Weinman, 1970: The transfer of solar irradiance through inhomogeneous turbid atmospheres evaluated by Eddington's approximation. *J. Atmos. Sci., 27*, 1048-1055.

124 W.J. Wiscombe and J.H. Joseph, 1977: The range of validity of the Eddington approximation. *Icarus, 32*, 362-377.

139a J.F. Potter, 1970: The delta function approximation in radiative transfer theory. *J. Atmos. Sci., 27*, 943-949. (*excerpts*)

140 J.H. Joseph, W.J. Wiscombe and J.A. Weinman, 1976: The delta-Eddington approximation for radiative flux transfer. *J. Atmos. Sci., 33*, 2452-2459.

148 M.D. King and Harshvardhan, 1986: Comparative accuracy of selected multiple scattering approximations. *J. Atmos. Sci., 43*, 784-801.

166 Harshvardhan, and M.D. King, 1993: Comparative accuracy of diffuse radiative properties computed using selected multiple scattering approximations. *J. Atmos. Sci., 50,* 247-259. (*excerpts*)

KING. JAS 1981 38 2031

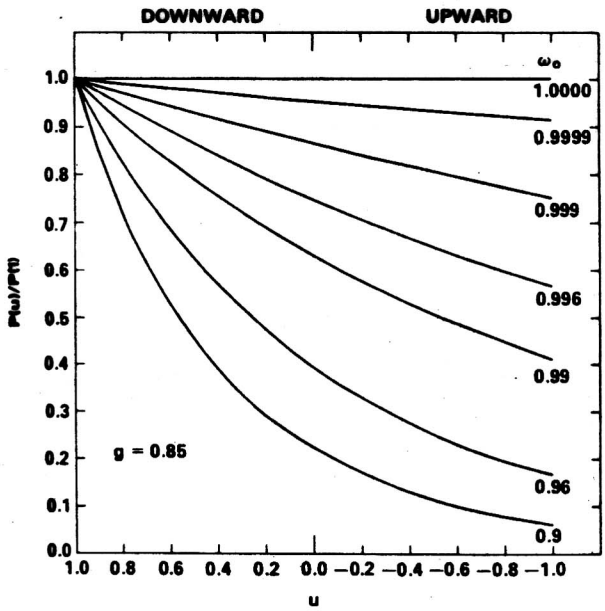

FIG. 1. Diffusion pattern as a function of the cosine of the zenith angle u for a Henyey-Greenstein phase function with $g = 0.85$ and for seven values of the single scattering albedo. All curves are normalized to unity for downwelling photons from the zenith.

$\tau^* = \infty$?

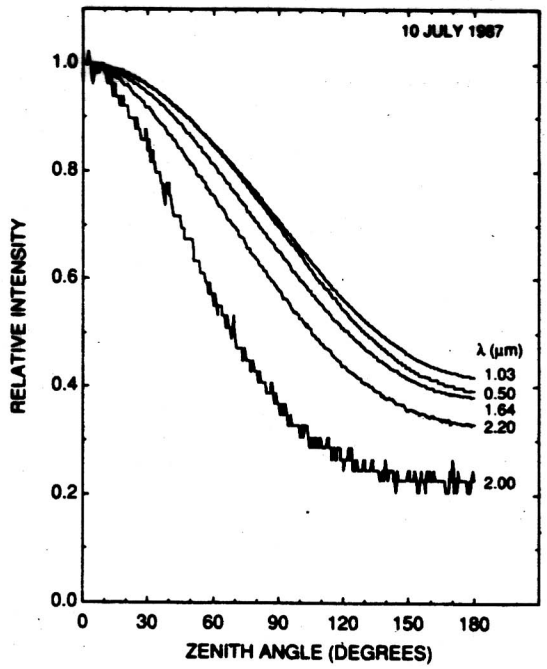

FIG. 6. Relative intensity as a function of zenith angle and wavelength for internal scattered radiation measurements obtained with the cloud absorption radiometer at 0937 PDT.

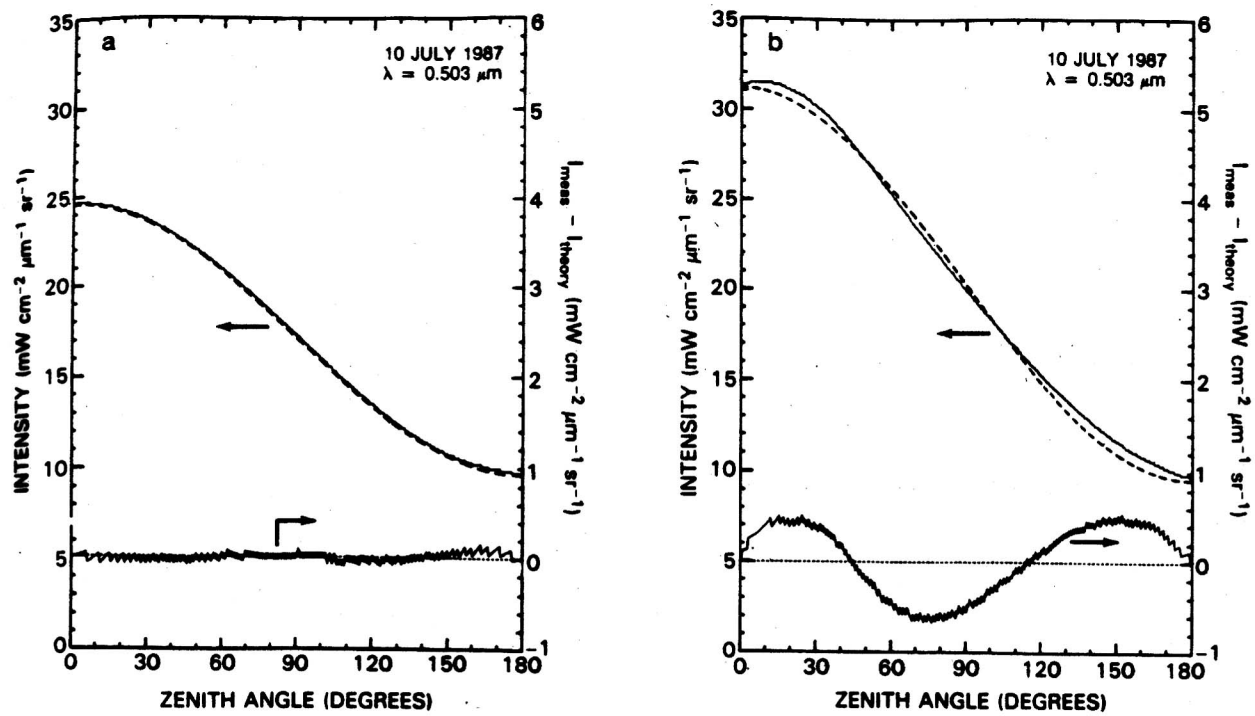

FIG. 8. Intensity as a function of zenith angle for two scans of the cloud absorption radiometer. Superimposed on the measurements (continuous curve) is the theoretical cosine function (dashed curve) necessary for the measurements to be within the diffusion domain. The right-hand scale applies to the deviations between measurements and theory, illustrated in the lower portion of each panel. The scan on the left (a) satisfies all conditions of the diffusion domain criteria (dashed and continuous curves coincide), whereas the scan on the right (b) fails to satisfy these criteria. All measurements were made at $\lambda = 0.503$ μm.

NOTES ON EDDINGTON METHOD

with reference to Shettle & Weinman, 1970: ("SW")
J. Atmos. Sci. 27, 1048-1055.

Start with eq. 15 on p. 72, but change the sign of μ, because SW use the convention

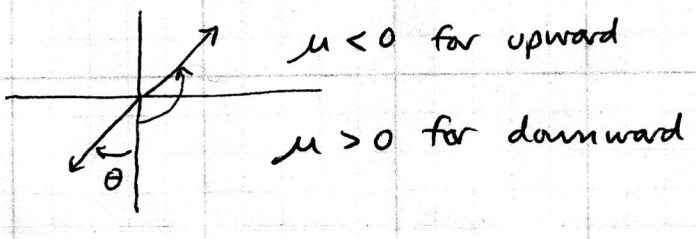

$$\mu \frac{dI(\tau,\mu)}{d\tau} = -I(\tau,\mu) + \frac{\tilde{\omega}}{2}\sum_{l=0}^{\infty}(2l+1)\chi_l P_l(\mu)\int_{-1}^{1} d\mu' P_l(\mu') I(\tau,\mu')$$

$$+ \frac{\tilde{\omega}}{4\pi} F^S e^{-\tau/\mu_0} \sum (2l+1)\chi_l P_l(\mu) P_l(+\mu_0) \qquad (15')$$

The Eddington approximation is that I is linear in μ, as $I = a + b\mu$, or in SW notation $I = I_0 + I_1 \mu$

$$I(\tau,\mu) = I_0(\tau) + I_1(\tau)\cdot\mu$$

First apply this approximation to S_d:

$$S_d = \frac{\tilde{\omega}}{2}\int_{-1}^{1}\sum_{l=0}^{\infty}(2l+1)\chi_l P_l(\mu) P_l(\mu')\left[I_0(\tau) + I_1(\tau)\mu'\right] d\mu'$$

$P_0(\mu') = 1$ $\qquad$ $P_1(\mu') = \mu'$

only $l=0, l=1$ terms will survive the integration because $\int_{-1}^{1} P_n(\mu') P_m(\mu') d\mu' = 0$ for $m \neq n$.

So $\sum_{\ell=0}^{\infty} (2\ell+1)\chi_\ell P_\ell(\mu) P_\ell(\mu') \longrightarrow \sum_{\ell=0}^{1}$

$= 1 \cdot 1 \cdot 1 \cdot 1 + 3\chi_1 \cdot \mu \cdot \mu'$

$= 1 + 3g\mu\mu'$ because $\chi_1 = g$ (from p. 59)

This is equivalent to keeping only the first two terms in $P(\cos\Theta)$:

$P(\cos\Theta) \approx 1 + 3g\cos\Theta$

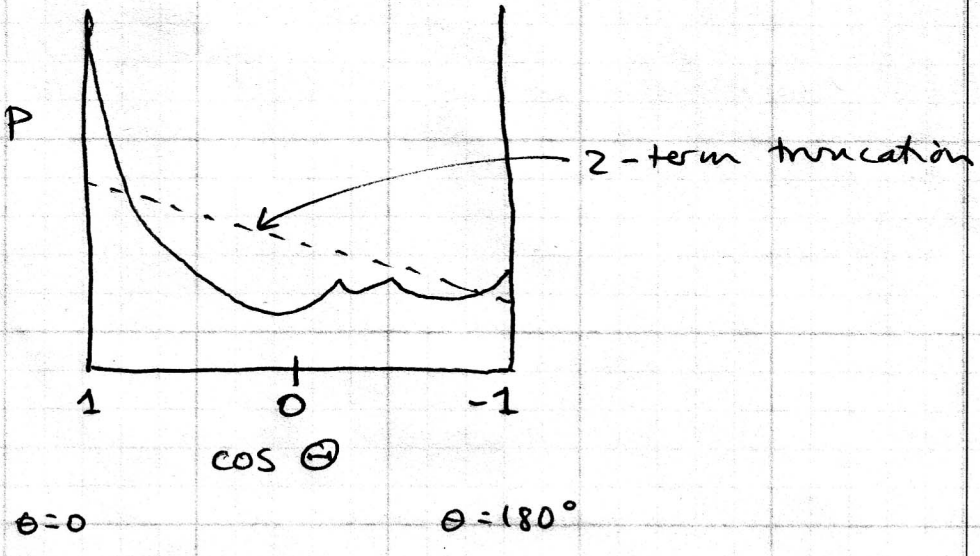

The Eddington method is inaccurate because the phase function has a large narrow forward peak (as we will see), so that the 2-term truncation is a poor approximation.

$$S_d = \frac{\tilde{\omega}}{2}\int_{-1}^{1}(1+3g\mu\mu')\left(I_0(\tau)+I_1(\tau)\mu'\right)d\mu'$$

$$= \frac{\tilde{\omega}}{2}\int_{-1}^{1}\left[I_0(\tau) + 3g\mu\mu' I_0(\tau) + I_1(\tau)\mu' + 3g\mu\mu'^2 I_1(\tau)\right]d\mu'$$

($3g\mu\mu' I_0(\tau) \to 0$, $I_1(\tau)\mu' \to 0$)

$$= \frac{\tilde{\omega}}{2}\left[2I_0(\tau) + 3g\mu I_1(\tau)\underbrace{\int_{-1}^{1}\mu'^2 d\mu'}_{2/3}\right]$$

$$= \tilde{\omega}\left[I_0(\tau) + \mu g I_1(\tau)\right].$$

This is S_d. Now using the same 2-term truncation of the phase function also in S_{solar}:

$$\sum_{l=0}^{1}(2l+1)\chi_l P_l(\mu)P_l(+\mu_0) = 1\cdot 1\cdot 1\cdot 1 + 3\chi_1\cdot\mu\cdot\mu_0$$
$$= 1 + 3g\mu\mu_0$$

$S_0(15')$ becomes

$$\mu\frac{d}{d\tau}(I_0+\mu I_1) = \underbrace{-I_0 - \mu I_1 + \tilde{\omega}\left[I_0+\mu g I_1\right]}_{\text{This is eq. (5) of SW, They use } \underline{a} \text{ for } \underline{\tilde{\omega}}.} + \frac{\tilde{\omega}}{4\pi}F^s e^{-\tau/\mu_0}(1+3g\mu\mu_0)$$

group terms in I_0 and in I_1

$$-I_0(1-\tilde{\omega}) - \mu(1-\tilde{\omega}g)I_1.$$

Now our objective is to solve for the τ-dependence of I_0 & I_1.

We solve this equation by taking zeroth and first moments of r.t.e., and getting two equations:

(1) apply $\frac{1}{2}\int_{-1}^{1} d\mu$ (zeroth moment; an averaging operator)

(2) apply $\frac{1}{2}\int_{-1}^{1} \mu\, d\mu$ (first moment)

Note that

$$\tfrac{1}{2}\int_{-1}^{1} d\mu = 1 \qquad \tfrac{1}{2}\int_{-1}^{1} \mu\, d\mu = 0$$

$$\tfrac{1}{2}\int_{-1}^{1} \mu^2 d\mu = \tfrac{1}{3} \qquad \tfrac{1}{2}\int_{-1}^{1} \mu^3 d\mu = 0$$

, so only even powers of μ will survive.

$\frac{1}{2}\int d\mu$: $\quad 0$

$$\mu \frac{d}{d\tau}(I_0 + \mu I_1) = -I_0(1-\tilde{\omega}) - \mu(1-\tilde{\omega}g) I_1 + \frac{\tilde{\omega}}{4\pi} F^S e^{-\tau/\mu_0}\left[1 + 3g\mu\mu_0\right]$$

$\frac{1}{2}\int \mu\, d\mu$: $\quad 0$ $\qquad$ 0 $\qquad$ 0

So $\frac{1}{2}\int d\mu$ gives $\quad \frac{1}{3}\frac{dI_1}{d\tau} = -I_0(1-\tilde{\omega}) + \frac{1}{4}\tilde{\omega}\frac{F^S}{\pi} e^{-\tau/\mu_0}$ $\qquad$ (SW 6)

$\frac{1}{2}\int \mu\, d\mu$ gives $\quad \frac{1}{3}\frac{dI_0}{d\tau} = -\frac{1}{3}(1-\tilde{\omega}g) I_1 + \frac{1}{4}\tilde{\omega}\frac{F_S}{\pi} e^{-\tau/\mu_0} \cdot \frac{3g\mu_0}{3}$ $\qquad$ (SW 7)

Note that SW (6) and SW (7) can be written ($I_0 \to x$; $I_1 \to y$) as

$$\left.\begin{aligned} \frac{dy}{d\tau} &= ax + b e^{-\tau/\mu_0} \\ \frac{dx}{d\tau} &= cy + f e^{-\tau/\mu_0} \end{aligned}\right\}$$ Two coupled differential equations

← Differentiate this, and get a second order differential equation.

$$\frac{d^2x}{d\tau^2} = c\frac{dy}{d\tau} - \frac{f}{\mu_0} e^{-\tau/\mu_0}$$

$$= c\left[ax + b e^{-\tau/\mu_0}\right] - \frac{f}{\mu_0} e^{-\tau/\mu_0}$$

so $\boxed{\frac{d^2x}{d\tau^2} = sx + q e^{-\tau/\mu_0}}$, where s and q are two new constants: $s = ca$; $q = cb - \frac{f}{\mu_0}$.

Solutions to this inhomogeneous second order differential equation:

$$x = c_1 e^{-k\tau} + c_2 e^{k\tau} + \underbrace{c_3 e^{-\tau/\mu_0}}$$

because $\frac{d^2}{d\tau^2} e^{-\tau/\mu_0} \propto e^{-\tau/\mu_0}$

So I_0 and I_1 have this form.

The result is given by SW as their eq. 12

(on p. 97 here)

SW assume the atmosphere is composed of a series of homogeneous layers. g and $\tilde{\omega}$ are constant within a layer, but different for different layers.

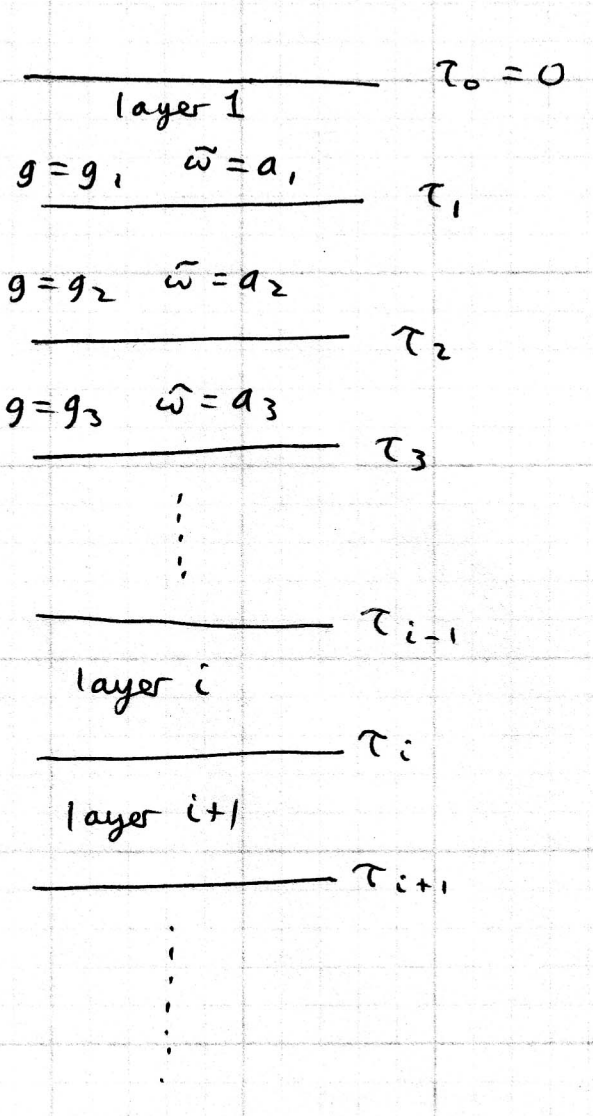

SW eq. 12, for the $\underline{i}$th atmospheric layer:

$$I_0^i(\tau) = C_1^i e^{-k_i\tau} + C_2^i e^{+k_i\tau} - \alpha_i e^{-\tau/\mu_0}$$

$$I_1^i(\tau) = P_i\left(C_1^i e^{-k_i\tau} + C_2^i e^{+k_i\tau}\right) - \beta_i e^{-\tau/\mu_0}$$

where $k_i = \sqrt{3(1-\bar{\omega}_i)(1-\bar{\omega}_i g_i)}$

The solution has $e^{-k_i\tau}$, $e^{+k_i\tau}$. In 2-stream we had $e^{-\Gamma\tau}$, $e^{+\Gamma\tau}$. This k_i looks like Γ.

Recall $\Gamma = 2\sqrt{1-\bar{\omega}}\sqrt{1-\bar{\omega}g}$

so Γ has 2 instead of $\sqrt{3}$

↓	↓
$\bar{\mu} = 1/2$	$\bar{\mu} = 1/\sqrt{3}$
$\bar{\theta} = 60°$	$\bar{\theta} = 55°$
2-stream	Eddington

and $-P_i = \sqrt{\dfrac{3(1-\bar{\omega}_i)}{1-\bar{\omega}_i g_i}}$ (Misprint in SW has wrong sign $+P_i$)

$$\alpha_i = \frac{3\bar{\omega}_i F^S \mu_0^2 \left[1 + g_i(1-\bar{\omega}_i)\right]}{\pi 4 (1-k_i^2\mu_0^2)}$$

$$\beta_i = \frac{3\bar{\omega}_i F^S \mu_0 \left[1 + 3g_i(1-\bar{\omega}_i)\mu_0^2\right]}{4\pi(1-k_i^2\mu_0^2)}$$

For N layers we need 2N boundary conditions to specify C_1^i, C_2^i.

We have 2 from top and bottom, but the top and bottom boundary conditions are on I not on I_0 & I_1.

SW put the boundary condition on diffuse flux F at top and bottom: (recall $\searrow \downarrow \swarrow$ $\mu > 0$; $\nearrow \uparrow \nwarrow$ $\mu < 0$)

$$F^{\downarrow} = \int I \mu \, d\omega = 2\pi \int_0^1 I \mu \, d\mu$$

$$F^{\downarrow,\uparrow}(\tau) = 2\pi \int_0^{\pm 1} \left[I_0(\tau) + \mu I_1(\tau) \right] \mu \, d\mu$$

$$= \pi \left[I_0(\tau) \pm \tfrac{2}{3} I_1(\tau) \right]$$

Boundary conditions:

$$F^{\downarrow}(0) = \pi \left[I_0(0) + \tfrac{2}{3} I_1(0) \right] = 0 .$$ No diffuse incidence at top.

$$F^{\uparrow}(\tau^*) = \pi \left[I_0(\tau^*) - \tfrac{2}{3} I_1(\tau^*) \right] = A \left[F^{\downarrow}(\tau^*) + \text{direct flux} \right]$$

↑ Lambert albedo of ground.

$$= A\pi \left[I_0(\tau^*) + \tfrac{2}{3} I_1(\tau^*) + \mu_0 \frac{F^s}{\pi} e^{-\tau^*/\mu_0} \right]$$

This is where the remaining direct flux gets diffused

Now we have two boundary conditions from top and bottom.

For the internal boundary conditions we require

I_0, I_1 to be continuous at layer-interfaces.

$$\text{for } i = 1, \dots, N-1 \begin{cases} I_0^i(\tau_i) = I_0^{i+1}(\tau_i) & \leftarrow (N-1) \text{ internal b.c.s} \\ I_1^i(\tau_i) = I_1^{i+1}(\tau_i) & \leftarrow (N-1) \text{ internal b.c.s} \end{cases}$$

So we have $2N$ equations

in the $2N$ unknowns C_1^i, C_2^i.

They are solved by matrix methods.

Delta-eddington approximates the phase function as the sum of two parts: A delta function for the forward peak, plus the remainder. So the approximation is that the photons deflected only slightly on scattering are not deflected at all. The remainder of the phase function has asymmetry factor $g < 0.5$, i.e. in a range where the Eddington method is accurate.

$$P(\cos\Theta) \approx P_{\delta Edd}(\cos\Theta) = f\left[2\delta(1-\cos\Theta)\right] + (1-f)\left[1+3g'\cos\Theta\right].$$

The two quantities in square brackets are two phase functions; each normalized, as we will see.

(f) will be the fraction of photons scattering into the forward peak. The remainder is approximated as a two-term Legendre expansion, because higher order terms will drop out when we apply the Eddington approximation.

(g') will be the asymmetry factor of the truncated phase function. Both f and g are as yet unspecified.

① Show that g' is the asym. factor of the truncated P:

$$\text{asym. fac.} = \int_{4\pi} \left[1 + 3g'\cos\theta\right]\cos\theta \,\frac{d\omega}{4\pi} = g' \qquad \checkmark$$

② Show that $P_{\delta edd}$ is normalized. Let $u \equiv \cos\Theta$.

$$\int P \frac{d\omega}{4\pi} = \frac{1}{2}\int_{-1}^{1} P(u)\,du = \frac{1}{2}\cdot 2f\cdot 1 + \frac{(1-f)}{2}\underbrace{\int_{-1}^{1}(1+3g'u)\,du}_{2}$$

$$= f + (1-f)$$

Note that the δ-function integrated to f. This is the fraction going into the forward peak.

③ How to specify f and g':

(a) Require $P_{\delta edd}$ to have the same asymmetry factor as the true phase function.

Let $g \equiv$ asym. factor of true phase function.

$$g = \text{Asym. fac. of } P_{\delta edd} = \frac{1}{2}\int_{-1}^{1} u\,du\,[2f\,\delta(1-u) + (1-f)(1+3g'u)]$$

$$= \frac{2f}{2}\cdot 1 + (1-f)\frac{3g'}{2}\underbrace{\int_{-1}^{1} u^2\,du}_{2/3}$$

$$= f + (1-f)g'$$

So $g = f + (1-f)g'$

and $g' = \dfrac{g-f}{1-f}$

(b) Require <u>second</u> moments equal for P_{HG} and $P_{Eddington}$.

nth moment is

$$\int_{4\pi} \frac{1}{4\pi} P(\cos\theta)\, P_n(\cos\theta)\, d\omega = \frac{1}{2}\int_{-1}^{1} P(u)\, P_n(u)\, du$$

$u \equiv \cos\theta$

$P_0(u) = 1$

$P_1(u) = u$

$P_2(u) = \frac{1}{2}(3u^2-1)$

The expansion of P_{HG} (Henyey-Greenstein) in Legendre polynomials is

$$P_{HG}(u) = \frac{1-g^2}{(1+g^2-2gu)^{3/2}} = \sum_{l=0}^{\infty} (2l+1)\, g^l\, P_l(u)$$

The normalization of Legendre polynomials is

$$\frac{1}{2}\int_{-1}^{1} P_l(x)\, P_l(x)\, dx = \frac{1}{2l+1}$$

So the nth moment of P_{HG} is

$$\chi_n = \frac{1}{2}\int_{-1}^{1} P_{HG}(u)\, P_n(u)\, du = (2n+1)\, g^n \left(\frac{1}{2n+1}\right) = g^n$$

so the second moment of P_{HG} is $\underline{\underline{g^2}}$.

what is the second moment of $P_{Eddington}$?

Second moment of $P_{\delta Edd}$:

$$\chi_2 = \frac{1}{2}\int_{-1}^{1} P_2(u) P_{\delta Edd}(u)\, du = \frac{1}{2}\int_{-1}^{1} \frac{1}{2}(3u^2-1)\, du \left[2f\delta(1-u) + (1-f)(1+3g^2u)\right]$$

$$= f$$

So set $f = g^2$ for δEddington.

(Typical cloud droplet has $g = 0.85$; $g^2 = 0.72$).

Then $g' = \dfrac{g-f}{1-f} = \dfrac{g-g^2}{1-g^2} = \dfrac{g}{1+g}$

So if $0 < g < 1$ then $0 < g' < 0.5$, i.e. in the range where the Eddington method is accurate (Wiscombe & Joseph, 1977: Icarus, 32, 362-377).

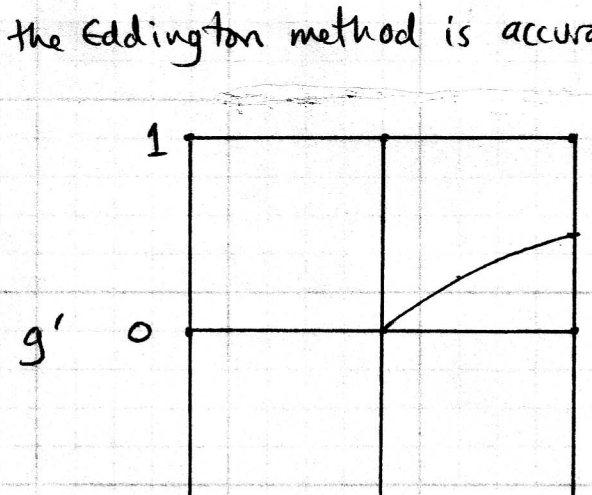

In summary, we approximated the true phase function as a weighted average of two phase functions, P_f and P_r:

$$P(\cos\Theta) \approx P_{\delta\epsilon}(\cos\Theta) = f \cdot \underbrace{\left[2\delta(1-\cos\Theta)\right]}_{P_f \text{ "forward"}} + (1-f)\underbrace{\left[1+3g'\cos\Theta\right]}_{P_r \text{ "remainder"}}$$

Both P_f and P_r are phase functions normalized to an average value of 1. To specify f and g', we required:

(a) Match zeroth moment to true P: $\frac{1}{4\pi}\int P\, d\omega = 1$

(b) Match first moment to true P: $g' = \frac{g-f}{1-f}$

(c) Match second moment to P_{HG}: $f = g^2$, so $g' = \frac{g}{1+g}$

For use in the azimuthally-averaged r.t.e., we will need the azimuthally-averaged $P_{\delta\epsilon}$; to do this we first need to express P_f in terms of (μ, μ', ϕ, ϕ'):

$$P_f = 2\delta(1-\cos\Theta) = 4\pi\delta(\mu-\mu')\delta(\phi-\phi'). \quad [\text{Eq (11) of Joseph et al.}]$$

Let's check that the normalization is correct: $\frac{1}{4\pi}\int_{4\pi} P_f \, d\omega = 1$.

Substitute $u \equiv \cos\Theta$.

LHS

$$\frac{1}{4\pi}\int_{4\pi} P_f \, d\omega = \frac{1}{4\pi}\int 2\delta(1-u)\, d\omega = \frac{1}{4\pi}\cdot 2\int_0^{2\pi} d\phi \int_{-1}^{1} \delta(1-u)\, du$$

$$= \frac{2\cdot 2\pi}{4\pi}\int_{-1}^{1}\delta(1-u)\, du = 1$$

RHS

$$\frac{1}{4\pi}\int_{4\pi} P_f \, d\omega = \frac{4\pi}{4\pi}\underbrace{\int_0^{2\pi}\delta(\phi-\phi')\, d\phi}_{1}\underbrace{\int_{-1}^{1}\delta(\mu-\mu')\, d\mu}_{1} = 1.$$

Now derive the azimuthally-averaged phase function:

$$\overline{P}_{\delta\epsilon}(\mu,\mu') = \frac{1}{2\pi}\int P_{\delta\epsilon}\, d\phi$$

$$= \frac{1}{2\pi}\int d\phi \left[f\cdot 4\pi\delta(\mu-\mu')\delta(\phi-\phi')\right]$$

$$+ \frac{1}{2\pi}\int_0^{2\pi} d\phi\,(1-f)\left\{1+3g'\left[\mu\mu' + (1-\mu^2)^{1/2}(1-\mu'^2)^{1/2}\underbrace{\cos(\phi-\phi')}_{\text{integrates to zero.}}\right]\right\}$$

$$\overline{P}_{\delta\epsilon} = 2f\,\delta(\mu-\mu') + (1-f)(1+3g'\mu\mu')$$

Now put the azimuthally-averaged delta-Eddington phase function into the r.t.e.

Azimuthally-averaged r.t.e:

$$\mu \frac{dI}{d\tau} = -I + \frac{\tilde{\omega}}{2} \int_{-1}^{1} \bar{P}(\mu, \mu') I(\mu') d\mu'$$

In the source-function integral $\int P \cdot I \, d\mu'$, the δ-function part becomes:

$$\frac{\tilde{\omega}}{2} \int_{-1}^{1} 2f \delta(\mu - \mu') I(\mu') d\mu' = \tilde{\omega} f I(\mu)$$

The r.t.e. becomes

$$\mu \frac{dI}{d\tau} = -\underbrace{I(1-\tilde{\omega}f)}_{\text{i.e. attenuation not as rapid.}} + \frac{(1-f)\tilde{\omega}}{2} \int_{-1}^{1} (1 + 3g'\mu\mu') I(\mu') d\mu'$$

substitute $d\tau = \frac{d\tau'}{1-\tilde{\omega}f}$, τ' is an adjusted optical-depth coordinate.

$$\frac{d}{d\tau} = (1-\tilde{\omega}f) \frac{d}{d\tau'}$$

Then divide the whole equation by $(1-\tilde{\omega}f)$:

so

$$\mu \frac{dI}{d\tau'} = -I + \frac{(1-f)\tilde{\omega}}{(1-\tilde{\omega}f)} \frac{1}{2} \int_{-1}^{1} (1+3g'\mu\mu') I(\mu') d\mu'.$$

call this $\tilde{\omega}'$

Summary.

with the substitutions $g' = \frac{g}{1+g}$

$$d\tau' = (1-\tilde{\omega}f)\, d\tau$$

$$\tilde{\omega}' = \frac{1-f}{1-\tilde{\omega}f} \tilde{\omega}$$

then the r.t.e. looks exactly like Shettle & Weinman's.

With the δ-ϵ adjustment, the total optical depth of a homogeneous medium is

$$\tau^{*\prime} = (1-\tilde{\omega}f)\tau^*$$

To Steve Warren,
Warren

N.T.I.S. No. PB270618

NCAR/TN-121+STR
NCAR TECHNICAL NOTE

July 1977

The Delta-Eddington Approximation for a Vertically Inhomogeneous Atmosphere

W. J. Wiscombe

ATMOSPHERIC ANALYSIS AND PREDICTION DIVISION

NATIONAL CENTER FOR ATMOSPHERIC RESEARCH
BOULDER, COLORADO

Discrete Ordinates Method (very brief outline)

Developed by Chandrasekhar.

Reliable, stable, computer routines developed by Stamnes & Wiscombe.

Consider Eq (8) on p. 68. Evaluation of S_d:

$$S_d(\tau,\mu,\phi) = \frac{\tilde{\omega}}{4\pi}\int_0^{2\pi} d\phi' \int_{-1}^{1} d\mu' P(\mu,\phi,\mu',\phi') I(\tau,\mu',\phi') \quad (1)$$

Represent $I(\tau,\mu,\phi) \approx \sum_{m=0}^{N} I^m(\tau,\mu)\cos[m(\phi_0-\phi)]$.

(a Fourier cosine series at each μ. ϕ_0 is solar azimuth)

Represent phase function as a Legendre series:

$$P(\cos\Theta) = \sum_{l=0}^{N} (2l+1)\chi_l P_l(\cos\Theta).$$

Using orthogonality of Legendre polynomials as on pp 71-72, Chandrasekhar shows that we can get a separate equation not just for the azimuthally averaged intensity I^0, but for each harmonic order I^m. (Ch. sec 48.1, TS eq 6.35, Liou eq 6.1.5):

$$\mu\frac{dI^m(\tau,\mu)}{d\tau} = I^m(\tau,\mu) - \frac{\tilde{\omega}}{2}\sum_{l=m}^{N}(2l+1)\chi_l^m P_l^m(\mu)\int_{-1}^{1} d\mu' P_l^m(\mu') I^m(\tau,\mu') - S_s \quad (2)$$

where $\chi_l^m = 2\chi_l \frac{(l-m)!}{(l+m)!}$ — Associated Legendre Function (p. 71)

i.e. all harmonic orders are uncoupled: I^m on lhs, I^m on rhs

For $m=0$ (azimuthal average) this is the same as eq 15 on p. 72.

Quadrature of the S_d integral:

Approximate the integral over μ' as a sum.

$$\int_{-1}^{1} d\mu'\, P_\ell^m(\mu') I^m(\tau,\mu') \approx \sum_{\substack{j=-n \\ j\neq 0}}^{n} a_j\, P_\ell^m(\mu_j)\, I^m(\mu_j)$$

a_j: weights; μ_j: Quadrature points "discrete ordinates"

e.g. for 4-stream:

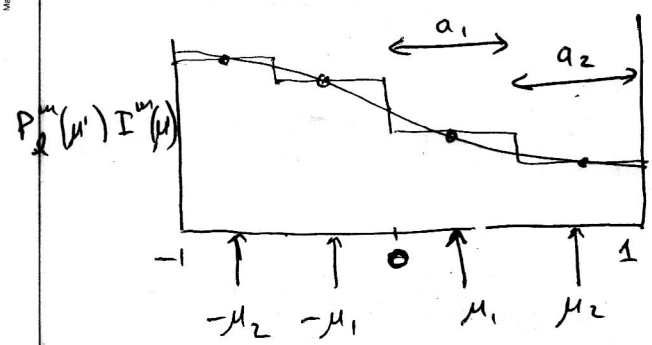

(also TS pp 281-287)

Chandrasekhar shows that the best choice of quadrature points μ_j is "Gaussian quadrature". The weights a_j are determined by the choice of quadrature points μ_j: $\{\mu_j\} \Rightarrow \{a_j\}$.

Theorem of Gaussian quadrature.

To best approximate the integral of a function $f(\mu)$ as a sum of m terms; i.e,

$$\int_{-1}^{1} f(\mu)\,d\mu \approx \sum_{j=1}^{m} a_j f(\mu_j),$$

take the quadrature points μ_j as roots of the Legendre polynomial $P_m(\mu)$

and weights $$a_j = \frac{1}{P_m'(\mu_j)} \int_{-1}^{1} \frac{P_m(\mu)}{\mu - \mu_j}\,d\mu .$$

For example, if $m=4$ then use P_4.

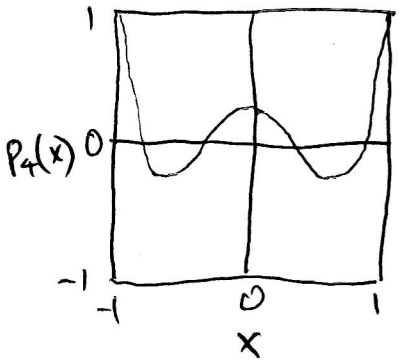

Then if $f(\mu)$ is a polynomial of degree $(2m-1)$ or less, the sum will evaluate the integral exactly; i.e. a sum of only m terms can match the integral of a polynomial of degree $2m-1$.

Notes

(1) We're not matching the function; we're matching the integral.

(2) Only P_m is used, not all P_i up to P_m.

(3) The weights a_j are evaluated once and for all when the μ_j are specified.

Number of Legendre orders is $2n$:

	Legendre expansion of P uses
2-stream :	P_0, P_1
4-stream :	P_0, P_1, P_2, P_3

The r.t.e. (2) can be written in matrix notation as

$$\mu \frac{dI^m(\mu_i)}{d\tau} = C_{ij} I^m(\mu_j) + D$$

where I^m is $\begin{bmatrix} I_0^m \\ I_2^m \\ \vdots \end{bmatrix}$ and C is $\begin{bmatrix} C_{ij} \\ \text{(dimension } 2n\text{)} \end{bmatrix}$

This to solve for the (μ, τ)-dependence of one Fourier component of the ϕ-dependence.

Trial solutions to the differential equation are of the form $I^m(\mu_j) = g^m e^{-k\tau}$ for each harmonic order m.

Putting this into (2) results in an eigenvalue equation for the allowed exponents k, as a function of $\bar{\omega}, \mu_i, a_i$:

$$\{\bar{\omega}, \mu_i, a_i\} \Rightarrow k$$

There are $2n$ values of k: $\pm k_1, \pm k_2, \cdots, \pm k_n$.

i.e. the number of k's is the same as the number of quadrature points.

For 2-stream we had $e^{+\Gamma\tau}$, $e^{-\Gamma\tau}$ i.e. $k_1 = \Gamma$, $k_{-1} = -\Gamma$.

The coefficients $g(\mu_j, k_\alpha)$ turn out to be of the form $\frac{L_\alpha Q}{1+\mu_j k_\alpha}$,

where Q is a polynomial in μ and L_α are coefficients to be determined by boundary conditions.

For example, the intensity in the four-stream version is

$$I^m(\mu_j, \tau) = \frac{L_1 Q e^{-k_1\tau}}{1+\mu_j k_1} + \frac{L_2 Q e^{-k_2\tau}}{1+\mu_j k_2} + \frac{L_{-1} Q e^{+k_1\tau}}{1-\mu_j k_1} + \frac{L_{-2} Q e^{+k_2\tau}}{1-\mu_j k_2}$$

$$+ \text{solar term } (\mu_0, \phi_0).$$

Boundary conditions lead to a set of linear equations to be solved for the coefficients $L_{I\alpha}$ (by inverting a matrix).

(If there is no solar term; i.e. if diffuse incidence or only emission sources, then the intensity has azimuthal symmetry and consists only of the $m=0$ component.)

"DISORT" code is available. Program and documentation are available by anonymous FTP

ftp://climate1.gsfc.nasa.gov/wiscombe/Multiple_Scatt/

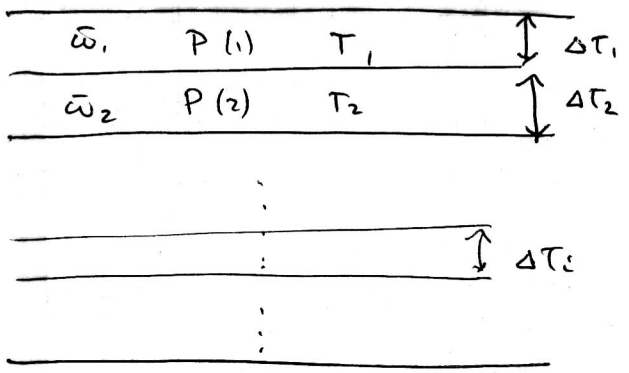

where phase function P is supplied as the set of moments $\{\chi_i,\ i = 1, \cdots 2n-1\}$

Specify distribution of incident radiation at top. Specify $\tilde{\omega}$, P, T for each layer of optical thickness $\Delta\tau_i$ (emission is also allowed).

Specify lower boundary condition as Lambertian or an arbitrary BRDF.

The program computes fluxes at any level and intensities in any direction, $I(\tau, \mu, \phi)$ (not just at quad. angles), at any level including top, bottom.

Solar direction μ_0 does not have to be at a quadrature angle μ_i.

(113)

Reprinted from Applied Optics, Vol. 27 page 2502, June 15, 1988
Copyright © 1988 by the Optical Society of America and reprinted by permission of the copyright owner.

Numerically stable algorithm for discrete-ordinate-method radiative transfer in multiple scattering and emitting layered media

Knut Stamnes, S-Chee Tsay, Warren Wiscombe, and Kolf Jayaweera

We summarize an advanced, thoroughly documented, and quite general purpose discrete ordinate algorithm for time-independent transfer calculations in vertically inhomogeneous, nonisothermal, plane-parallel media. Atmospheric applications ranging from the UV to the radar region of the electromagnetic spectrum are possible. The physical processes included are thermal emission, scattering, absorption, and bidirectional reflection and emission at the lower boundary. The medium may be forced at the top boundary by parallel or diffuse radiation and by internal and boundary thermal sources as well. We provide a brief account of the theoretical basis as well as a discussion of the numerical implementation of the theory. The recent advances made by ourselves and our collaborators—advances in both formulation and numerical solution—are all incorporated in the algorithm. Prominent among these advances are the complete conquest of two ill-conditioning problems which afflicted all previous discrete ordinate implementations: (1) the computation of eigenvalues and eigenvectors and (2) the inversion of the matrix determining the constants of integration. Copies of the FORTRAN program on microcomputer diskettes are available for interested users.

I. Introduction

The discrete ordinate method for radiative transfer is commonly ascribed to Chandrasekhar.[1] Computer implementations of that method were, however, plagued by numerical difficulties[2] to such an extent that researchers made little use of it. The purpose of this paper is to alert the community to a new numerical implementation of the discrete ordinate method for vertically inhomogeneous layered media which is free of these difficulties and to give a summary of its equations and its various advanced features. The resulting computer code represents the culmination of years of effort[3-9] on the part of ourselves and our collaborators to make it the finest algorithm available. Our intent is that the code be so well documented, so versatile, and so error-free that other researchers can easily and safely use it both in data analysis and as a component of large models.

Knut Stamnes is with University of Tromsø, Institute of Mathematical & Physical Sciences, Auroral Observatory, N-9001 Tromsø, Norway; W. Wiscombe is with NASA Goddard Space Flight Center, Greenbelt, Maryland 20771; the other authors are with University of Alaska—Fairbanks, Physics Department & Geophysical Institute, Fairbanks, Alaska 99775-0800.

Received 7 August 1987.

The problem to be solved is the transfer of monochromatic radiation in a scattering, absorbing, and emitting plane-parallel medium with a specified bidirectional reflectivity at the lower boundary. Section II summarizes the equations and boundary conditions. Section III discusses the numerical implementation of the theory, in particular, (a) how to compute eigenvalues and eigenvectors reliably and efficiently and (b) how to avoid fatal overflows and ill-conditioning in the matrix inversion needed to determine the constants of integration. Reference 9 provides a more detailed account as well as documentation, test problems, and a listing of the FORTRAN code.

II. Theory

A. Basic Equations

The purpose of this section is to present the basic radiative transfer formulas with a minimum of definition and explanation to establish notation and conventions. (For more comprehensive discussions of the subject, the reader is referred to textbooks[1,10] and review articles.[11-15])

The equation describing the transfer of monochromatic radiation at frequency ν through a plane-parallel medium is given by[1]

$$\mu \frac{du_\nu(\tau_\nu,\mu,\phi)}{d\tau} = u_\nu(\tau_\nu,\mu,\phi) - S_\nu(\tau_\nu,\mu,\phi), \quad (1)$$

δ-M method. (A generalization of δ-Eddington)

Truncation of phase function for use in D.O., doubling methods, where M is the number of quadrature points per hemisphere. ref. Wiscombe 1977 JAS 34 1408.

Expand phase function as a series of Legendre polynomials P_n:

$$P(\cos\Theta) \approx \sum_{n=0}^{N} (2n+1)\,\chi_n\,P_n(\cos\Theta)$$

Written this way, the χ_n are the moments of P w.r.t. Legendre polynomials.

$$n\text{th moment} \equiv \frac{1}{2}\int_{-1}^{1} P(\cos\Theta)\,P_n(\cos\Theta)\,d(\cos\Theta)$$

$$= \frac{1}{2}\int_{-1}^{1} P(u)P_n(u)\,du = \frac{1}{2}(2n+1)\chi_n \cdot \frac{2}{2n+1} = \chi_n$$

Approach:

1. Find moments χ_n of the true phase function, $n=0,\ldots,N$ up to $N>2M$, where $2M$ is the number of quadrature points (M in each hemisphere).
2. Define an approximate phase function P^* which contains a δ- part:

$$P^*(u) = 2f\,\delta(1-u) + (1-f)\sum_{n=0}^{2M-1} (2n+1)\,\chi_n^*\,P_n(u)$$

where M is the number of quadrature points in hemisphere:

$M=1$	$n=0,1$	2-stream (or Eddington)
$M=2$	$n=0,1,2,3$	4-stream

13-782 500 SHEETS, FILLER 5 SQUARE
42-381 50 SHEETS EYE-EASE® 5 SQUARE
42-382 100 SHEETS EYE-EASE® 5 SQUARE
42-389 200 SHEETS EYE-EASE® 5 SQUARE
42-391 100 SHEETS RECYCLED WHITE 5 SQUARE
42-392 200 RECYCLED WHITE 5 SQUARE
42-399 200 RECYCLED WHITE 5 SQUARE
Made in U.S.A.
National® Brand

③ Find moments of P^* :

m^{th} moment of P^* is $\frac{1}{2}\int_{-1}^{1} P^*(u)\,P_m(u)\,du$

$$= \underbrace{\frac{1}{2}\int_{-1}^{1} 2f\,\delta(1-u)\,P_m(u)\,du}_{\substack{P_m(1)=1 \\ \frac{1}{2}(2f)(1)(1)}} + \underbrace{\frac{1}{2}\int_{-1}^{1}(1-f)\left[\sum_{n=0}^{2M-1}(2n-1)\,\chi_n^*\,P_n(u)\right]P_m(u)\,du}_{\substack{=0 \text{ for } n\neq m \\ =\chi_m^*(1-f) \text{ for } n=m}}$$

$$= \begin{cases} f + (1-f)\,\chi_m^* & , \; m \le 2M-1 \\ f & , \; m \ge 2M \end{cases}$$

④ Require that low-order moments of P^* match those of P.

$$\chi_m = f + (1-f)\,\chi_m^* \;\; ; \;\; \chi_m^* = \frac{\chi_m - f}{1-f}, \quad m = 0, \cdots, 2M-1$$

$$f = \chi_m \text{ for } m \ge 2M. \qquad (\text{recall } g' = \tfrac{g-f}{1-f} \text{ for } \delta\text{-Eddington})$$

This determines f nonuniquely. For consistency with δ-Eddington, and because it's more important to get low-order moments correct than high-order moments, we choose to set $\boxed{f = \chi_{2M}}$

(recall $f = g^2$ for δE). The χ decrease with increasing m, so f is smaller as the number of quadrature points increases.

⑤ τ & $\tilde{\omega}$ are altered exactly as in δ-Eddington.

$$d\tau' = (1-\tilde{\omega}f)\,d\tau \qquad \tilde{\omega}' = \frac{1-f}{1-\tilde{\omega}f}\,\tilde{\omega}$$

13-782 500 SHEETS FILLER 5 SQUARE
42-381 50 SHEETS EYE-EASE® 5 SQUARE
42-382 100 SHEETS EYE-EASE® 5 SQUARE
42-389 200 SHEETS EYE-EASE® 5 SQUARE
42-392 100 RECYCLED WHITE 5 SQUARE
42-399 200 RECYCLED WHITE 5 SQUARE
Made in U.S.A.
National® Brand

ATMS 533 notes

Cloud optical properties

Cloud optical depth: Computation from liquid water content and dropsize distribution.

Define extinction efficiency $Q_{ext} \equiv \frac{\text{extinction cross-section}}{\text{geometric cross-section}} = \frac{C_{ext}}{\pi r^2}$

so $C_{ext} = \pi r^2 Q_{ext}$. $\quad 0 \lesssim Q_{ext} \lesssim 6$ from Mie theory.

$Q_{ext} \to 2$ for $r \gg \lambda$.

optical depth $\tau = \int \sigma_{ext}\, dz = \int (\sigma_{abs} + \sigma_{scat})\, dz$

σ_{ext} = linear extinction coefficient (m^{-1})

$\sigma_{ext} = C_{ext} N$

where C_{ext} = extinction cross-section (m^2 / particle)

N = number-density (particles / m^3)

so σ_{ext} has units $\frac{m^2}{m^3}$ or <u>cross-sectional area per unit volume</u>

so $\tau = \int \sigma_{ext}\, dz = \int C_{ext} N\, dz = \int Q_{ext} \pi r^2 N\, dz$ (1)

This is for a "monodispersion".

For a size distribution

see next page.

where $\int n(r)\, dr = N$

– continued –

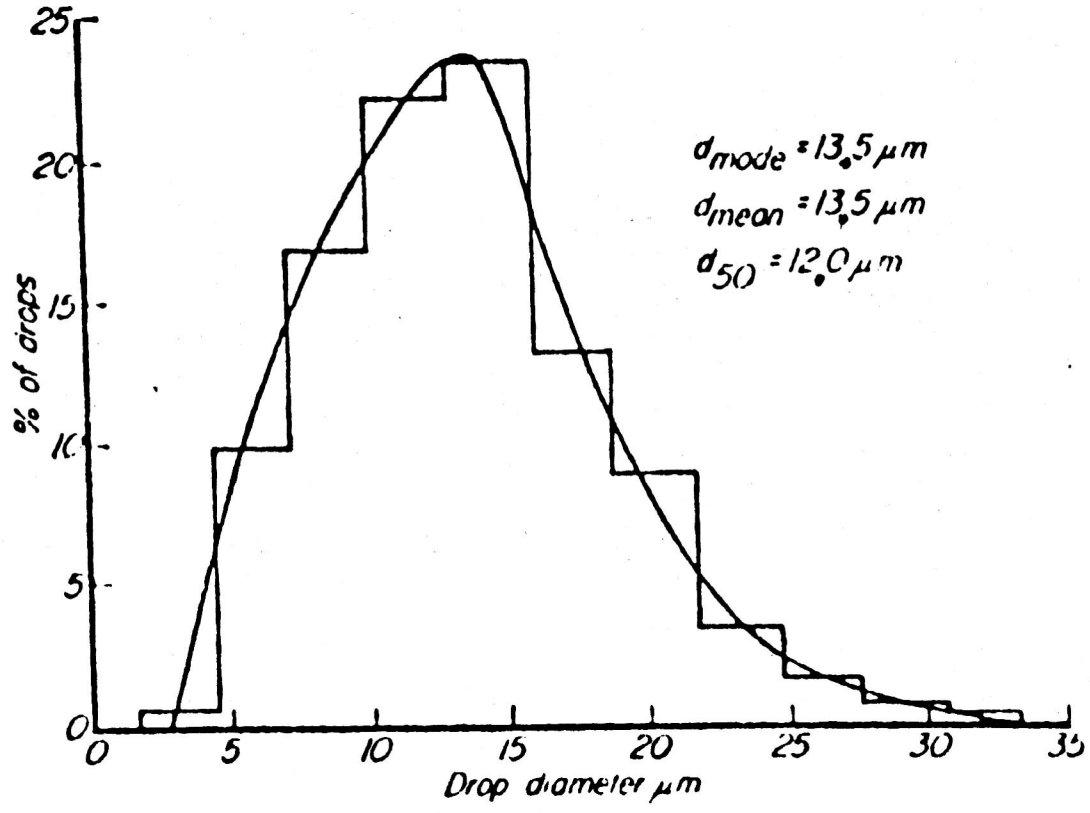

FIG. 5. --- Average drop size spectrum for the arctic stratus clouds.

Jayaweera & Ohtake, 1973.

J. Rech. Atmos. 7, 199-207.

For a size-distribution integrate over r.

$$\tau(z) = \int_z^{top} \int_0^{\infty} Q_{ext}(r)\, \pi r^2\, n(r, z')\, dr\, dz' \qquad (2)$$

Now to simplify this formula.

(a) Define some moments of the size-distribution:

number-mean radius (average radius) $\qquad \dfrac{\int r\, n(r)\, dr}{\int n(r)\, dr} = \dfrac{\int r\, n(r)\, dr}{N}$

area-mean radius $\qquad \dfrac{\int r \cdot r^2\, n(r)\, dr}{\int r^2\, n(r)\, dr}$ = "effective radius" r_{eff} (3)

$\begin{pmatrix}\text{volume}\\ \text{mass}\end{pmatrix}$-mean radius $\qquad \dfrac{\int r \cdot r^3\, n(r)\, dr}{\int r^3\, n(r)\, dr}$

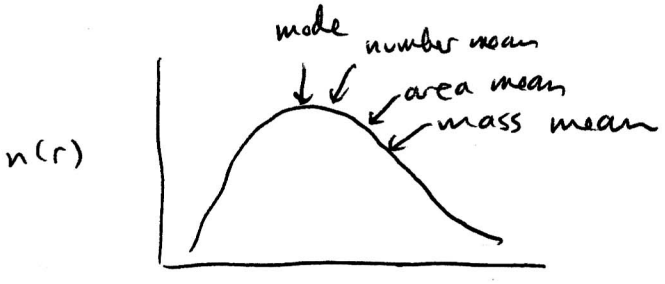

(b) Liquid water content LWC (g/m^3)

(1) for monodispersion

$$LWC = \underbrace{N}_{\frac{\text{particles}}{m^3}} \cdot \underbrace{\frac{4}{3}\pi r^3 \rho_w}_{\frac{g}{\text{particle}}}$$

ρ_w: $1.0\ g\ cm^{-3} = 10^6\ g\ m^{-3}$

(2) for size distribution

$$LWC = \frac{4}{3}\rho_w \pi \int r^3 n(r)\, dr \qquad (4)$$

(c) so $$\frac{LWC}{r_{eff}} = \frac{4}{3}\rho_w \pi \int r^2 n(r)\, dr \qquad \text{from (3,4)} \qquad (5)$$

so $$\int \pi r^2 n(r,z')\, dr = \frac{3}{4}\frac{LWC(z')}{r_{eff}(z')\rho_w} \qquad (6)$$

(d) Assume $r >> \lambda$ so $Q_{ext} \approx 2$ (7)

(e) Putting (7) into (2)

next page

we obtain

$$\tau(z) = \int_z^{top} 2 \underbrace{\int_0^{\infty} \pi r^2 n(r,z')\, dr}\, dz'$$

↓ replace from (6), and assume r_{eff} constant with height

$$\tau(z) = \frac{3}{2} \frac{1}{r_{eff}\, \rho_w} \int_z^{top} LWC(z')\, dz'$$

This is optical depth measured from top of cloud down to level z.

The total optical thickness of the cloud, τ^*, is then

$$\tau^* = \frac{3}{2} \frac{1}{r_{eff}\, \rho_w} \underbrace{\int_{bottom}^{top} LWC(z')\, dz'}$$

This is the "vertically-integrated LWC", or "Liquid-water path" LWP. (g/m^2)

SO $\boxed{\tau^* = \frac{3}{2} \frac{LWP}{r_{eff}\, \rho_w}}$ Derived by Stephens (JAS 1978)

or

$$\tau^* = \frac{3}{4} \frac{LWP \cdot Q_{ext}}{r_{eff} \cdot \rho_w}$$

where (eg) LWP is in $g\, m^{-2}$,

r_{eff} is in μm,

and $\rho_w = 10^6\, g\, m^{-3} = 1\, g\, m^{-2}\, \mu m^{-1}$

so for constant LWP, τ^* varies inversely with r_{eff}.

S. Twomey, 1977: Atmospheric Aerosols p. 289.

Nonabsorbing cloud over a black surface. $\theta_0 = 0°$

N = number-density of CCN. r = droplet radius

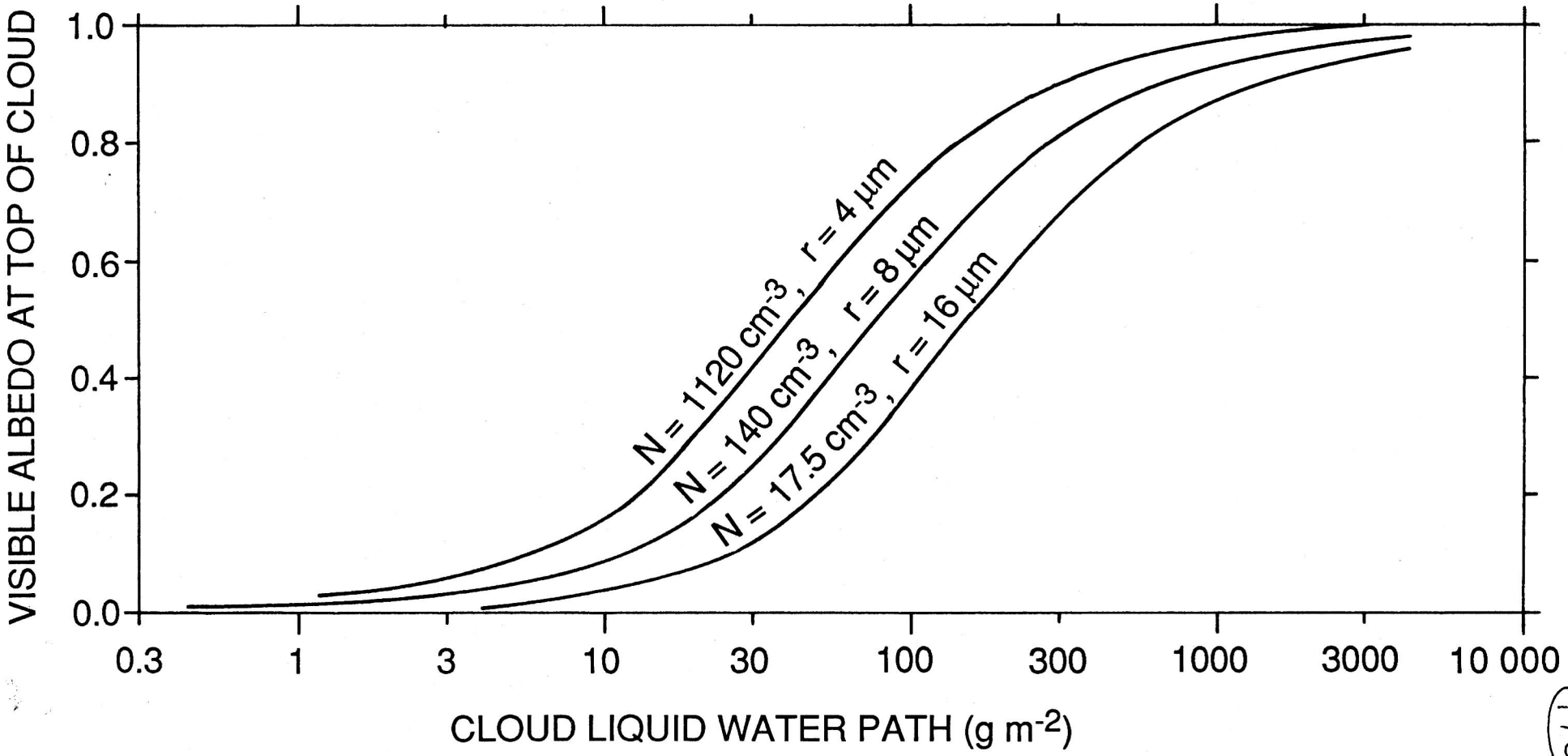

J. ATMOS. SCI. 41 1336–1355

(177)

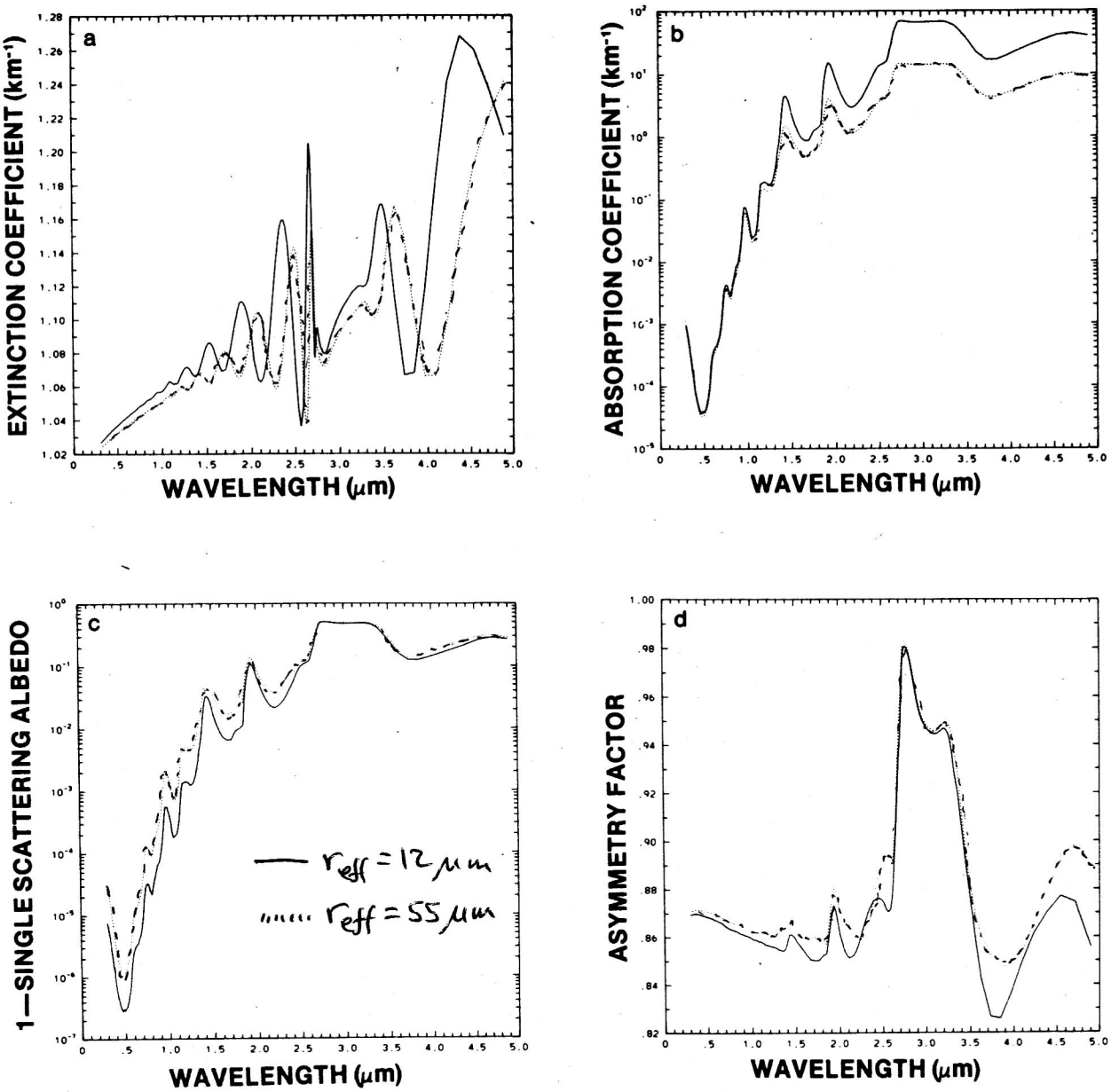

ω
0
0.9
0.99
0.999
0.9999
0.99999
0.999999

FIG. 2. Mie computations as a function of wavelength for the normal (solid line) and large (dotted line) drop distributions. (a) Extinction coefficient normalized to $W/r_{\text{eff}} = 1/1500$, where W is liquid water content and r_{eff} is effective drop radius. (b) Absorption coefficients normalized to $W = 1$ g m^{-3}. (c) $1 - \omega_0$, where ω_0 is the single scattering albedo. (d) Asymmetry factor g.

In Fig. 2b, both distributions are normalized to have the same water content $W = 1$ g m^{-3}, or, equivalently, the same *volume*. With this normalization, both curves for absorption coefficient are practically identical in the main part of the solar spectrum (0.2–1.5 μm).

If the surface-area normalization had been used in Fig. 2b, the absorption curves would have separated by more than an order of magnitude. Figure 2c, in which the "co-albedo" or absorption-to-extinction-coefficient ratio is plotted, shows this. (Since the extinction coefficient ≈ 1 when $W/r_{\text{eff}} = 1/1500$, Fig. 2c is nearly a plot of absorption coefficient when both drop distributions have equal surface areas.)

What Figs. 2a and 2b imply is that *the shortwave optical properties of a cloud cannot depend on just a single moment of the drop distribution.* Drop distribution variability can only be accounted for if *two* moments are known: namely, W and r_{eff}, or W and W/r_{eff}. Knowing only one moment, say W, fixes the absorption coefficient (almost independent of drop distribution) from some relative of Fig. 2b; but the extinction coefficient will be able to vary dramatically,

SNOW

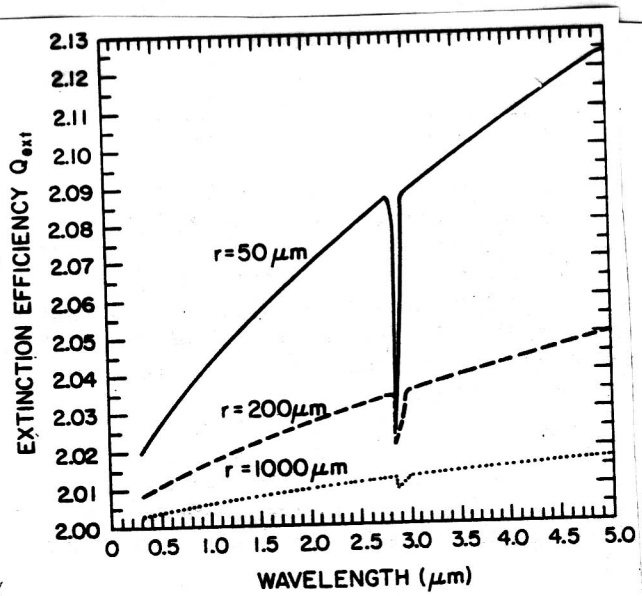

FIG. 2. Extinction efficiency (Q_{ext}) for ice spheres of various radii, as a function of wavelength.

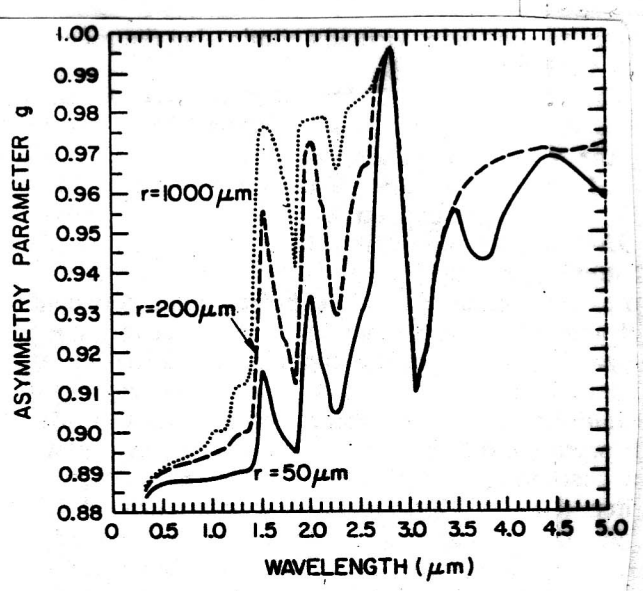

FIG. 4. Asymmetry factor g for ice spheres of various radii, as a function of wavelength.

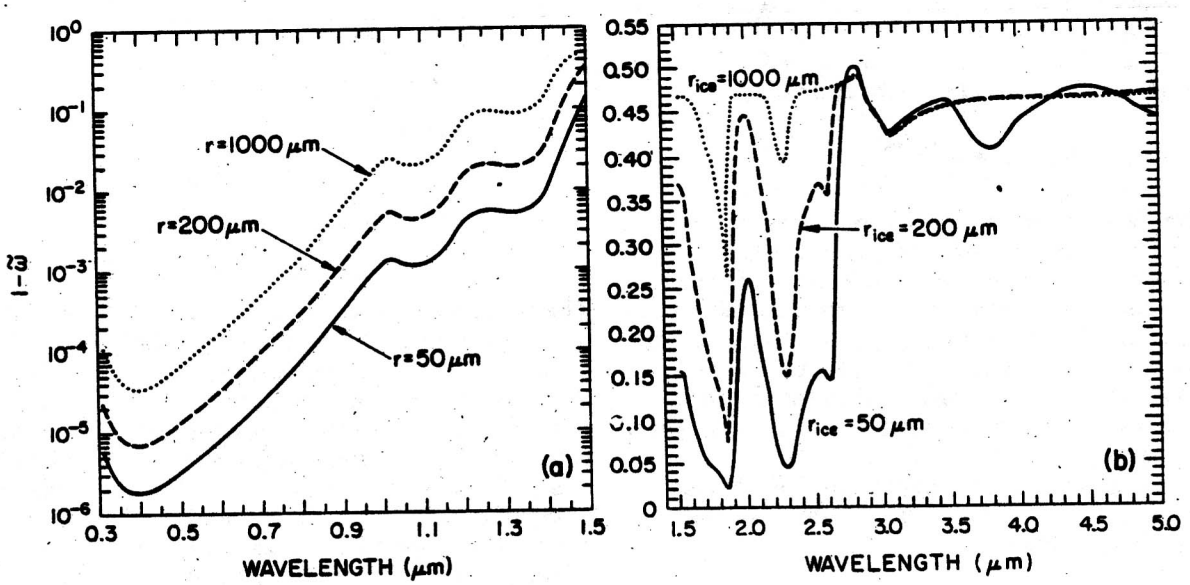

FIG. 3. Single-scattering coalbedo ($1 - \tilde{\omega}$) for ice spheres of various radii, as a function of wavelength.

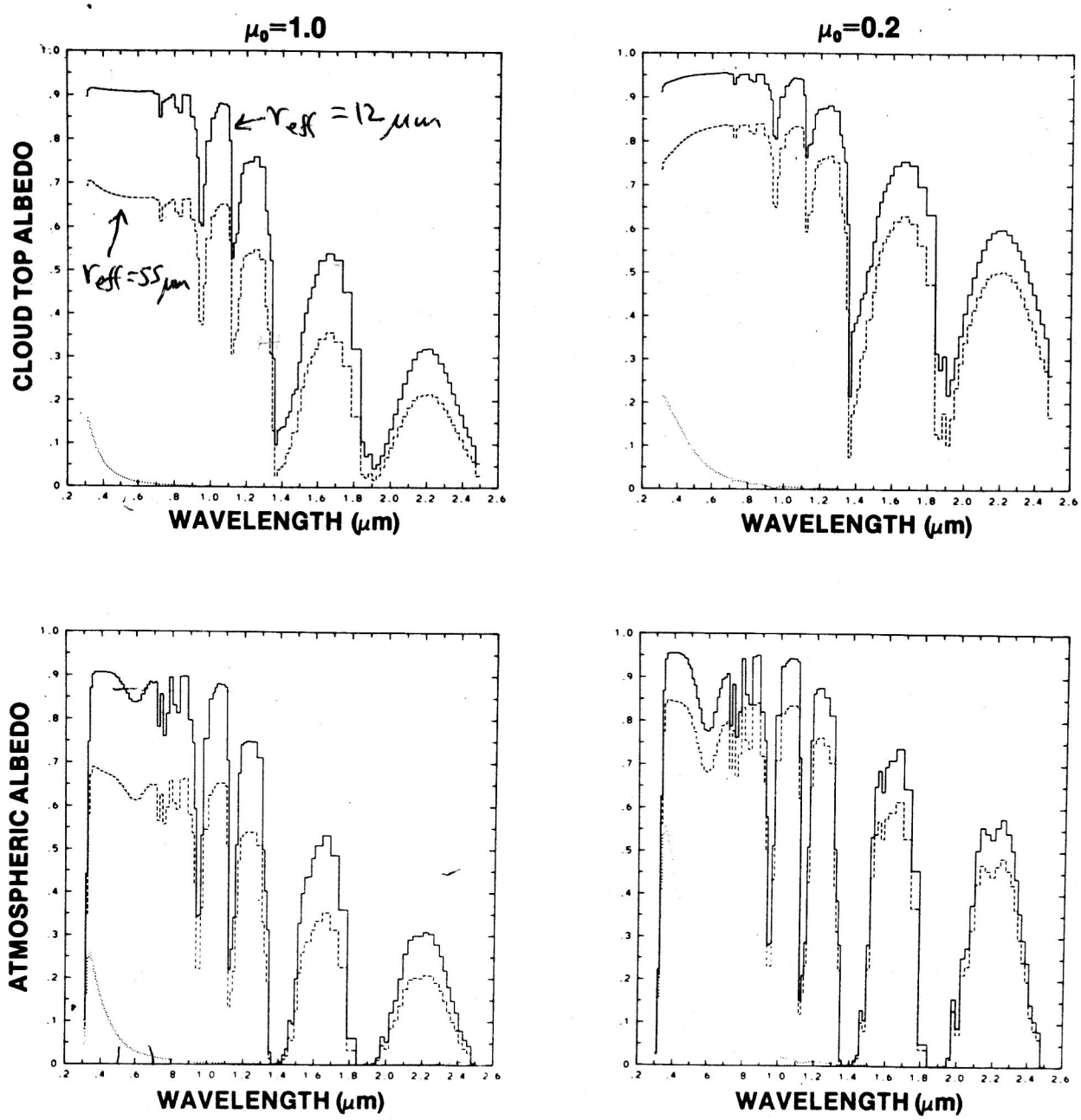

FIG. 7. Spectral albedo as a function of wavelength (0.3–2.5 μm) for two values of solar zenith angle. Cloud thickness is 2 km. The first row shows values of spectral albedo, as would be measured by an aircraft immediately above the cloud; the second column shows these values as they would be measured by a satellite. Solid and dashed lines are for normal and large drop distributions, respectively; dotted line is for the clear atmosphere (with Rayleigh scattering). For further explanation see text.

reflected radiation passes through the ozone layer for a second time.

The effect of adding very large drops to the drop spectrum is far from uniform across all wavelengths. It has its main effect in the aforementioned 1.5–1.8 μm window, a somewhat lesser effect in the range 1.1–1.35 μm, and a still lesser effect near 0.95 μm. Elsewhere, it has practically no effect. In particular, in the 2.0–2.4 μm region, there is a marked insensitivity to drop distribution (Fig. 9).

d. Vertical heating rate

Finally, the vertical distributions of solar heating are shown in Fig. 10, integrating the results given in Figs. 8 and 9. For the overhead sun case, very large

EFFECT OF SNOW GRAIN SIZE

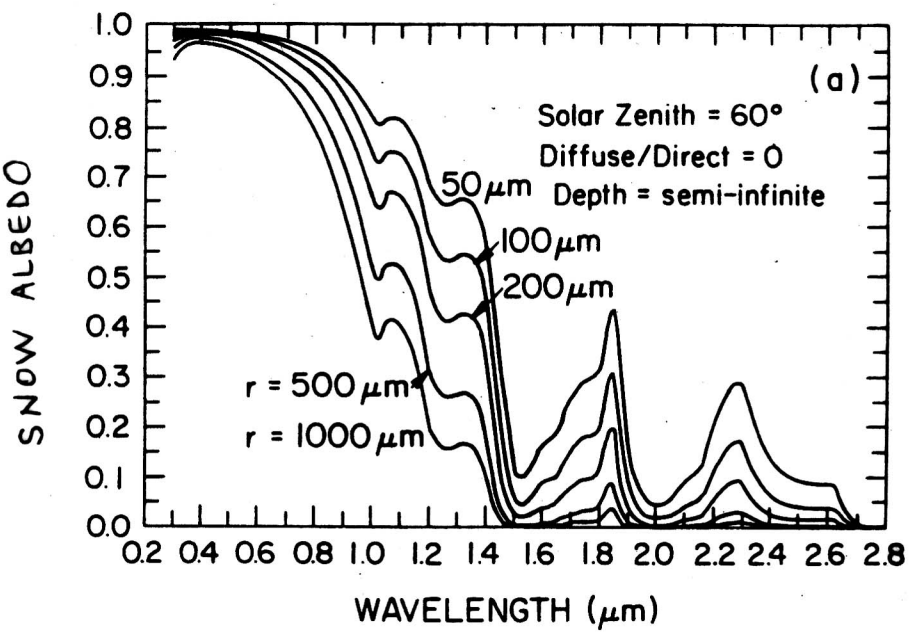

Wiscombe & Warren 1980

JAS 37 2712

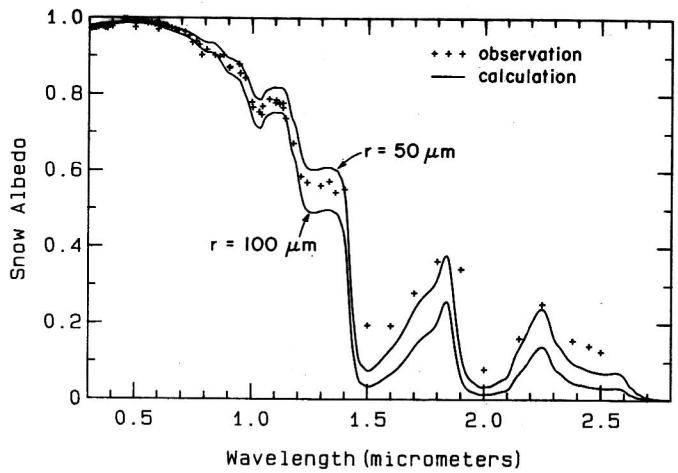

Points (plus signs): Spectral albedo of the snow surface measured 600 meters "northeast" (045° grid) from the clean-air facility at the South Pole on 23 January 1986 under diffuse light (thick overcast). Solid curves: Calculations of spectral albedo for homogeneous snowpacks of uniform grain radius r = 50 micrometers and r = 100 micrometers. The experimental points match theoretical calculations for r < 50 micrometers at wavelength λ > 1.5 micrometers and 50–100 micrometers for shorter wavelengths. At the shorter wavelengths, the light penetrates more deeply into the snow, so the albedo is sensitive to grains beneath the surface; whereas at the longer wavelengths, the albedo is influenced only by the grains very close to the surface. The observed albedos can thus be explained by an increase of grain size with depth. ("μm" denotes "micrometer.")

Warren et al 1986 Antarctic J.U.S. 21 247

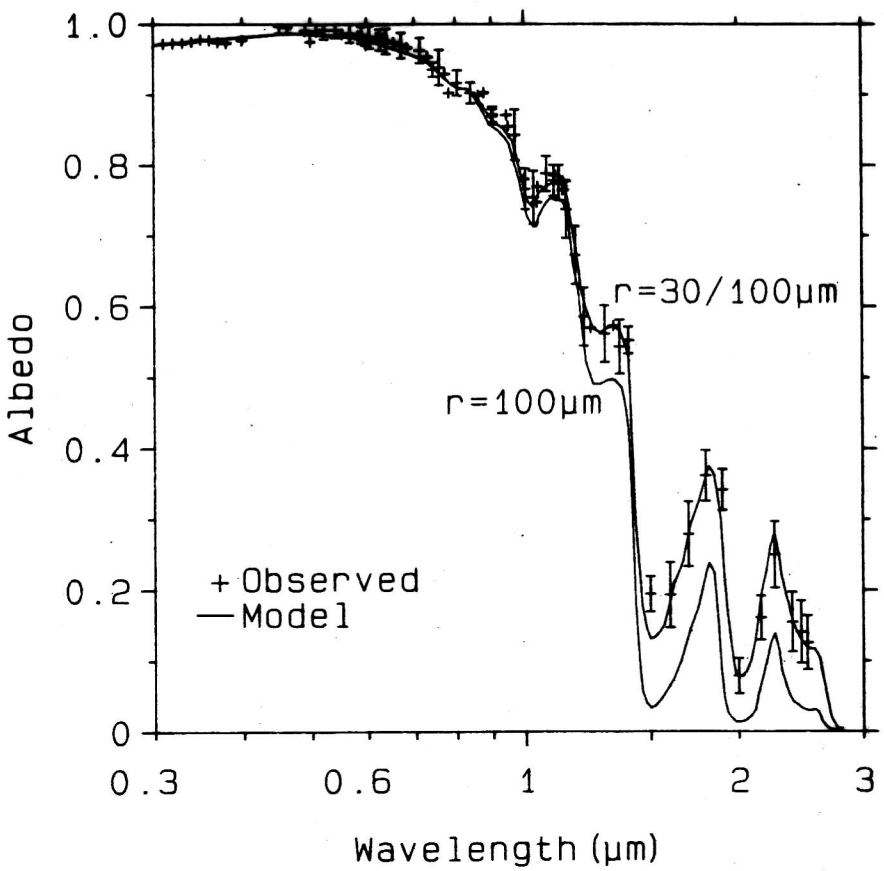

Figure 4. The observed spectral albedo for diffuse incident radiation versus wavelength for January 23, 1986, near South Pole Station [$\langle\alpha\rangle$ = 0.83]. The error bars show the standard deviation of three scans. Where they are not shown, the standard deviation is smaller than the height of the symbol. The solid lines are model results for a homogeneous layer with a grain radius of 100 μm [$\langle\alpha\rangle$ = 0.81] and for a two-layer model with a 0.25-mm thick layer of 30-μm grains over a thick layer of 100-μm grains [$\langle\alpha\rangle$ = 0.83]. NOAA's average albedo for this day was $\langle\alpha\rangle$ = 0.839.

GRENFELL, WARREN, MULLEN 1994

JGR 99, 18669

JGR 90 3773-3779 (182)

TABLE 1. Preliminary Estimate of Average Percent Sky Covers for Each of Six Cloud Classes for the Northern Hemisphere Summer (S. G. Warren, private communication, 1984)

Cloud Type	North Latitude					
	0-15	15-30	30-45	45-60	60-75	75-90
Altostratus/ altocumulus	31	19	20	30	27	30
Stratus/ stratocumulus	19	18	24	40	40	55
Nimbostratus	5	3	4	8	11	16
Cumulus	15	12	9	6	4	2
Cumulonimbus	9	6	4	6	6	3

These preliminary values may differ somewhat from the more accurate values that will be available on completion of the cloud climatology.

Hemisphere since Southern Hemispheric data are not sufficiently complete for detailed calculations. However, the available data suggest little difference exists between the hemispheres in total liquid water.

In order to convert this information to liquid water mass, it is necessary to have the geographic area which corresponds to the given percent sky cover, and the mean liquid water mass per unit area for each of the cloud types. The latter quantity is determined from estimates of the mean cloud liquid water concentration and depth of the various cloud types. The geographic areas employed are determined by assuming that the percent sky cover is equivalent to percent ground cover. Sky cover will actually be somewhat larger than ground cover to the extent that sides as well as bottoms of clouds near the horizon contribute to the sky cover a seen by the observer. However, this projection bias will only be appreciable for convective clouds, because of their large height-to-width ratio. To compensate for this effect, an ad hoc reduction of 0.8 has been made to the observed sky covers of convective clouds (cumulus and cumulonimbus) to obtain geographic extent.

The values of mean cloud liquid water concentration and depth are estimated from a literature survey. The values employed are listed in Table 2. Only five cloud types are shown since

TABLE 2. Mean Cloud Thicknesses (ΔH) and Liquid Water Contents (LWC) Derived From a Literature Survey

Cloud Type	ΔH, km	LWC, g m^{-3}	Column Density, kg m^{-2}	SMMR, kg m^{-2}
Cumulus	2.0	0.4	0.8	1.0
Cumulonimbus				
Tropical	5.0	1.0	5.0	
Trade wind	2.0	1.5	3.0	
Midlatitude	2.5	1.5	3.75	1.6-8
Polar	2.0	1.5	3.0	
Altostratus/ altocumulus	0.5	0.1	0.05	0-1.0
Stratus/ stratocumulus	1.0	0.2	0.2	0-1.0
Nimbostratus	3.0	0.1	0.3	0-1.0

The main references employed were Ludlum [1980], Mason [1972], Pruppacher and Klett [1978], Sartor [1978], Spencer et al. [1983], Jeck [1983], and Churchill [1982]. Mean column densities (ΔHxLWC) derived from the survey data are also shown together with limited scanning multichannel microwave radiometer measurements from Seasat and Nimbus 7 [Katsaros, 1983; Spencer et al., 1983].

(183)

Reprinted from JOURNAL OF THE ATMOSPHERIC SCIENCES, Vol. 43, No. 4, 15 February 1986
American Meteorological Society

Comments on "The Effects of Very Large Drops on Cloud Absorption. Part I: Parcel Models"

DEAN A. HEGG

Atmospheric Sciences Department, University of Washington, Seattle, WA 98195

29 April 1985 and 13 September 1985

TABLE 1. Values of r_{eff} calculated from cloud-droplet spectra over the size range 2–4500 μm diameter obtained on 10 research flights in the western portion of Washington State during 1984. Ranges of values for a particular flight are based on at least six different in-cloud samples. Each sample represents an ~400 m spatial average.

Date (1984)	Cloud type	Johnson-Williams LWC (g m^{-3})	r_{eff} (μm)
4 January	Sc	0.5	9–41
23 January	Sc	0.2	6–21
25 January	Sc-Cu	0.5	11–275
9 February	Sc	0.3	5–23
13 February	Cu	0.4	6–232
24 February	Cu	0.4	13–51
18 April	Cu	0.6	6–62
20 April	Cu	0.4	$\approx$6
30 April	Sc	0.5	$\approx$7
10 May	Sc	0.4	50–80

JGR 94 8623-8632

(184)

TABLE 3. Composition of Stratocumulus Clouds Measured in the Eastern Pacific

Date Sample Taken	Soot Concentration,* ng g^{-1} cloud water	Liquid water,† g m^{-3}	r_{eff},‡ μm	Cloud depth,§ m	τ^* ‖
June 30, 1987	23 ± 14	0.30	7.8	240	14
July 2, 1987	79 ± 47	0.28	6.5	365	24
July 7, 1987	<3	0.24	6.9	425	22
July 13, 1987	54 ± 32	0.31	5.0	240	22
July 16, 1987	25 ± 15	0.28	7.4	485	28

*Calculated concentration of soot in sampled cloud water; explained in more detail in section 4 of the text.
†Average cloud liquid water content during the sampling period, as measured by the Johnson-Williams probe.
‡Average "effective" droplet radius, or surface-area-weighted mean radius [*Hansen and Travis*, 1974] during the sampling period.
§Approximate cloud depth; determined from visual in-flight observations of cloud base and cloud top.
‖ Cloud optical thickness τ^*; calculated from liquid water, r_{eff}, and cloud depth columns, and the appropriate extinction efficiency, Q_{ext} (approximately 2.1 for these clouds), for the measured dropsize distributions.

determining absorption effects of soot within clouds or snow, a substantial amount of variation exists in the properties of atmospheric soot itself. Factors which are not usually directly measured, such as refractive index, shape, and porosity, also will affect the absorption cross section and therefore the effectiveness of soot particles at reducing cloud albedo. These properties may be at least as important as the internal/external mixture problem, and their uncertainties should be kept in mind. As will become evident in section 6, however, even a factor of 5 change in the absorption cross section of soot is unlikely to substantially change our conclusion about the climatic effects of soot in clouds.

The radiative properties of clouds are controlled by the size distribution of droplets. However, *Hansen and Travis* [1974] showed that knowledge of the ratio of two moments of the droplet size distribution, the surface-area-weighted radius or "effective radius," r_{eff}, is usually sufficient to predict extinction efficiency, phase function, and single-scattering albedo. The effective radius was calculated and averaged for each sampling period from the cloud droplet size distribution measured by the FSSP probe and is given by

$$r_{eff} = \sum_{i=1}^{M} r_i^3 n_i \left[\sum_{i=1}^{M} r_i^2 n_i \right]^{-1}$$

where M is the total number of size categories of the Knollenberg FSSP probe and r_i and n_i are the surface-area-weighted mean radius and the number of droplets per unit volume, respectively, in the ith size category. Since droplets with radii greater than about 30 μm are not detected by the FSSP, calculated r_{eff} values given in Table 3 may be slightly lower than actual values (a point considered later in the interpretation of our results). Droplet size distributions used in the Mie calculations were taken to be almost monodisperse at r_{eff}, broadened just enough to average over oscillations in the scattering efficiency (since r_{eff} alone determines the effect of the droplet size distribution on single-scattering albedo, ω [*Hansen and Travis*, 1974]). The refractive index, m, used for water at 0.475 μm was $1.336–0.935 \times 10^{-9}i$, as given by *Hale and Querry* [1973]. All soot particles, whether interstitial or within droplets, were assumed to be spheres with radii 0.1 μm and $m = 2.0 - 0.66i$, as recommended by *Bergstrom* [1972]. For consistency with our earlier assumed k value of 10 m^2 g^{-1}, a soot density of 1.183 g cm^{-3} was used. (Whether or not these values are representative of the soot that was actually sampled does not affect our radiative results; they were chosen for convenience in order to convert a measurement (or calculation) of absorption into an equivalent mass concentration of soot. Since both the measurements and the radiative calculations were of absorption, it was not necessary to know the exact conversion between absorption and soot mass). Using the Mie program of *Wiscombe* [1980], single-scattering quantities were calculated individually for pure water and for soot and then combined to obtain values for ω, asymmetry factor, and extinction efficiency. Multiple-scattering calculations used the Delta-eddington approximation [*Joseph et al.*, 1976], assuming an ocean surface albedo of 0.07. In order to estimate the typical climatic influence of soot on cloud albedo, calculations assumed a global average solar zenith angle of 60°, rather than the zenith angles that actually occurred during the experiment.

6. Radiative Transfer Results

The calculated effect of soot on the albedo (at $\lambda = 0.475$ μm) of clouds with different effective radii is shown in Figures 1 and 2. The r_{eff} values were chosen to cover the range occurring in real clouds reported by *Hegg* [1986] (5–275 μm), as well as some of the grain sizes in snow [*Wiscombe and Warren*, 1980] (50–1000 μm). Figure 1 represents a semi-infinite cloud (optical thickness $\tau^* = \infty$), with the shaded area signifying the range of soot concentrations under consideration. In the following discussion all concentrations are given units of ng soot g^{-1} cloud water, unless otherwise stated. The concentration at the left boundary of the shaded region represents the maximum calculated inside the droplets themselves (79), doubled (to 160) to account for the higher absorption of an internal mixture. The maximum value, 590, is the sum of the same cloud droplet soot concentration (160) and the maximum interstitial soot concentration possible from our measurements (430). The curves represent different r_{eff} values. The albedo without soot (left side of the graph) is lower for clouds of larger droplets, but the point we wish to emphasize is that soot causes a greater reduction of albedo in a cloud of large droplets. In the words of *Warren and Wiscombe* [1980, p. 2738], this is because radiation penetrates more deeply in a cloud of large droplets than in a cloud of small droplets with the same liquid water content and thus encounters more absorbing material before it can reemerge from the top of the cloud. If a r_{eff} of 10 μm (slightly larger than the ones calculated to compensate for the possible underestimation of this parameter by the FSSP) is assumed, the change in the

JGR 94 8629
1989

185

albedo of this semi-infinite cloud due to the range of soot concentrations in the shaded area is −0.014 to −0.029.

Our results are generally consistent with earlier calculations of *Chýlek et al.* [1984], but their calculations emphasized much larger concentrations of soot. Using a range of realistic droplet distributions, they calculated that a volume fraction of internally mixed soot of between 5×10^{-6} and 1×10^{-5} would be required to reduce the albedo (at $\lambda = 0.5$ μm) of an optically thick cloud to 0.80. This is approximately equivalent to between 5×10^3 and 1×10^4 in our units (in units of ng soot g^{-1} cloud water), more than 10 times greater than the maximum concentration we found in clouds.

A simple convenient expression for optical thickness is given by *Stephens* [1978, equation (7)] as

$$\tau^* \approx \frac{3}{4} \frac{Q_{ext} W}{r_{eff} \rho}$$

where the extinction efficiency, Q_{ext}, is approximately 2, W is the vertically integrated liquid water content (in g m^{-2}) and ρ is the density of water (1 g cm^{-3}). The clouds observed during FIRE in the eastern Pacific (Table 3) had calculated τ^* values between 14 and 28 (liquid water contents ≈ 0.3 g m^{-3} and depths of 240–485 m). Figure 1, which depicts a semi-infinite cloud, is not therefore representative of the clouds we sampled. In Figure 2 we show the results of albedo calculations at $\lambda = 0.475$ μm for more realistic clouds, with $\tau^* = 30$, slightly larger than the maximum thickness we observed. Comparing this with Figure 1, we see that the albedos of the $\tau^* = 30$ clouds are noticeably lower than those of the semi-infinite clouds. They

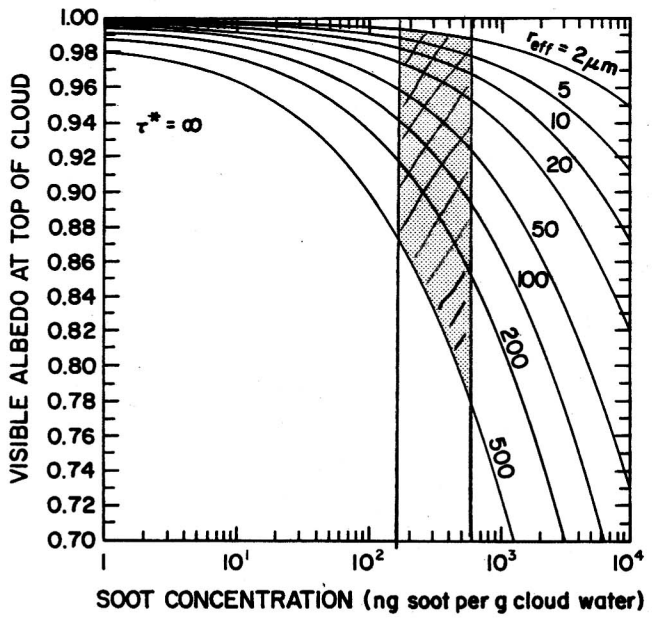

Fig. 1. The calculated effect of different concentrations of soot on the albedo of a semi-infinite cloud (optical thickness $\tau^* = \infty$) at $\lambda = 0.475$ μm, with curved lines representing different values of effective droplet radii (r_{eff}) in micrometers. Stratocumulus clouds sampled in the eastern Pacific had r_{eff} values of 5.0–7.8 μm. The shaded area represents the range of concentrations under consideration: from 160, which assumes the only soot in the cloud is the maximum amount measured inside droplets, to 590, which includes the maximum possible value for interstitial soot as well. In order to show the combined effects of both types of particles in the same figure, the inside-droplet concentration has been doubled to account for the enhanced absorption of soot inside water droplets. (All calculations modeled soot as an external mixture.)

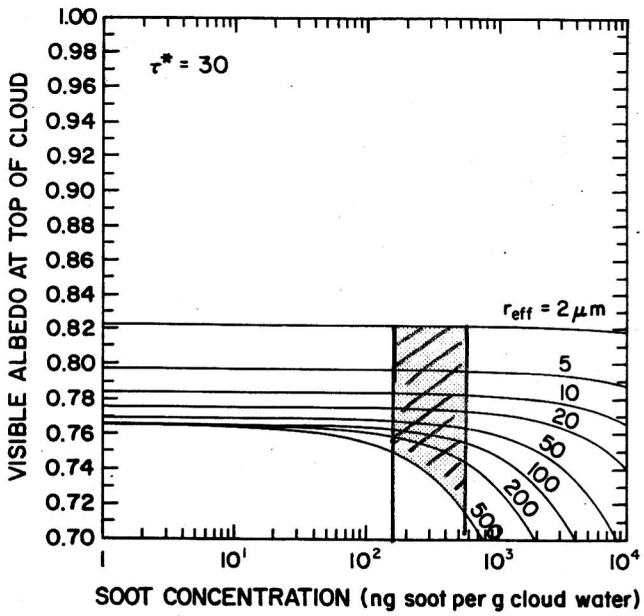

Fig. 2. Same as Figure 1, except for a cloud with a more realistic optical thickness of 30, similar to the thickness of stratocumulus clouds sampled in the eastern Pacific.

are still high relative to spectrally averaged values, however, since absorption by liquid water and water vapor is very weak at this visible wavelength. Since water is more absorptive in the near-infrared than in the visible, absorption in the near-infrared by a water droplet containing soot is largely due to the water and not the soot. Reductions in spectrally averaged albedo due to soot will therefore be approximately half as large (see Figure 2 of *Warren and Wiscombe* [1985]) as those calculated here. Comparison of Figures 1 and 2 shows that soot has a smaller effect on albedo as optical thickness decreases; therefore the albedos of the clouds like those in FIRE with $\tau^* < 30$ should be slightly less affected than those represented in Figure 2.

If we evaluate the same range of soot concentrations as for the semi-infinite cloud, the maximum reduction in albedo of a $\tau^* = 30$ cloud is only 0.001 for $r_{eff} = 10$ μm. Thus much higher contaminant levels or much larger droplets would be necessary to significantly alter the albedo of a realistic cloud like this: a soot concentration of about 2×10^4 ng soot g^{-1} cloud water for a $r_{eff} = 10$ μm (or a r_{eff} of about 500 μm, that is raindrop size, for a soot concentration of 340 ng g^{-1}) would be required to reduce the albedo of a $\tau^* = 30$ cloud by 0.03 at the most sensitive wavelength. (An albedo change of about 0.03 is probably the minimum detectable by most methods.) An average soot concentration in urban areas, based on published measurements of atmospheric fine particles, is about 2.9 μg m^{-3} [*Heintzenberg*, 1989], which, assuming it all was present inside a cloud, corresponds to a concentration of about 1×10^4 in our units. Therefore it is possible that in highly polluted urban areas, soot could have some effect on cloud albedo at sensitive wavelengths.

For snow, by contrast, the same reduction of albedo could be achieved by a soot concentration of only 10–60, depending on snow grain size (see Figure 2 of *Warren and Wiscombe* [1985]). These concentrations are within the range of those actually measured in snow in the Arctic (Table 2*b*). This important contrast between clouds and snow, that about 1000 times higher concentrations of soot are needed

2. Cloud albedo

For a plane-parallel cloud in the visible wavelengths, the figure shows that, for global average zenith angle $\theta_0 = 60°$; $\cos\theta_0 = \mu_0 = 0.5$, cloud albedo of 0.4 results from optical thickness $\tau^* \approx 4$.

The global average cloud optical thickness has to be greater than this to produce global average cloud albedo of 0.4, because (a) clouds are horizontally inhomogeneous and (b) clouds absorb in near-IR. (This figure is for visible.)

OSPHERIC SCIENCES VOL. 43, NO. 8

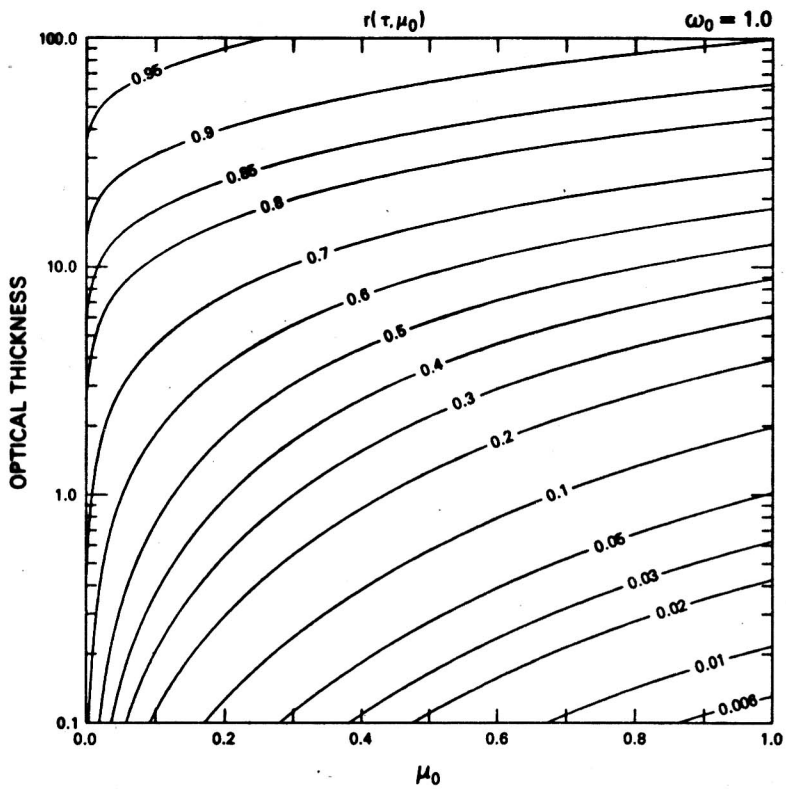

King & Harshvardhan

FIG. 2. Computations of the plane albedo as a function of optical thickness and cosine of the solar zenith angle for a FWC phase function with conservative scattering ($\omega_0 = 1.0$).

Measured cloud albedos: (From many different lines of evidence, average cloud albedo is ~ 0.4-0.5)

a) from aircraft.

1) Salomonson & Marlatt 1968 J. Appl. Meteor. 7 475 - 483

Table 1 column 12, top 3 entries are for marine stratus off California, for total solar spectrum.

column 10 is for visible

albedo { 34 - 44% average solar spectrum
45 - 56 % visible.

2) Griggs 1968 J. Appl. Meteor. 7 1012 - 1017

Figs 2, 3 show albedos 10 - 90%.

b) From satellite AVHRR - channel 1 (visible).

Coakley & Davies 1986. J. Atmos. Sci. 43 1025 - 1035

using only fully-filled pixels (left hand side of scatter-diagrams in Figs 3d, 4d, 5d) and applying zenith-angle correction to go from bidirectional reflectance to albedo, gives

equator	(Fig 5d)	albedo 25-65%
30°N	(Fig 3d)	30-60
45°N	(Fig 4d)	40-60

(c) From Earth-radiation-budget computation

Global average albedo is 0.3 (Stephens et al. 1981, JGR 86, 9739)

Earth is 64% covered with clouds (Warren et al. 1995, J. Climate 8, 1429)

Planetary albedo without clouds ("minimum albedo") is ~0.17 (ERBE)

So cloud albedo α_c must satisfy this equation:

$\alpha_c f_c + \alpha_s(1-f_c) = \langle\alpha\rangle$,

where f_c is cloud cover fraction, α_s is is clear-sky albedo, and $\langle\alpha\rangle$ is average albedo.

Putting $\langle\alpha\rangle=0.3$, $\alpha_s=0.17$, $f_c=0.64$,

we obtain $\alpha_c= 0.37$

Reprinted from Nature, Vol. 326, No. 6114, pp. 655-661, 16 April 1987
© Macmillan Journals Ltd., 1987

189

Oceanic phytoplankton, atmospheric sulphur, cloud albedo and climate

Robert J. Charlson*, James E. Lovelock†, Meinrat O. Andreae‡ & Stephen G. Warren*

* Department of Atmospheric Sciences AK-40, University of Washington, Seattle, Washington 98195, USA
† Coombe Mill Experimental Station. Launceston, Cornwall PL15 9RY, UK
‡ Department of Oceanography, Florida State University, Tallahassee, Florida 32306, USA

The major source of cloud-condensation nuclei (CCN) over the oceans appears to be dimethylsulphide, which is produced by planktonic algae in sea water and oxidizes in the atmosphere to form a sulphate aerosol. Because the reflectance (albedo) of clouds (and thus the Earth's radiation budget) is sensitive to CCN density, biological regulation of the climate is possible through the effects of temperature and sunlight on phytoplankton population and dimethylsulphide production. To counteract the warming due to doubling of atmospheric CO_2, an approximate doubling of CCN would be needed.

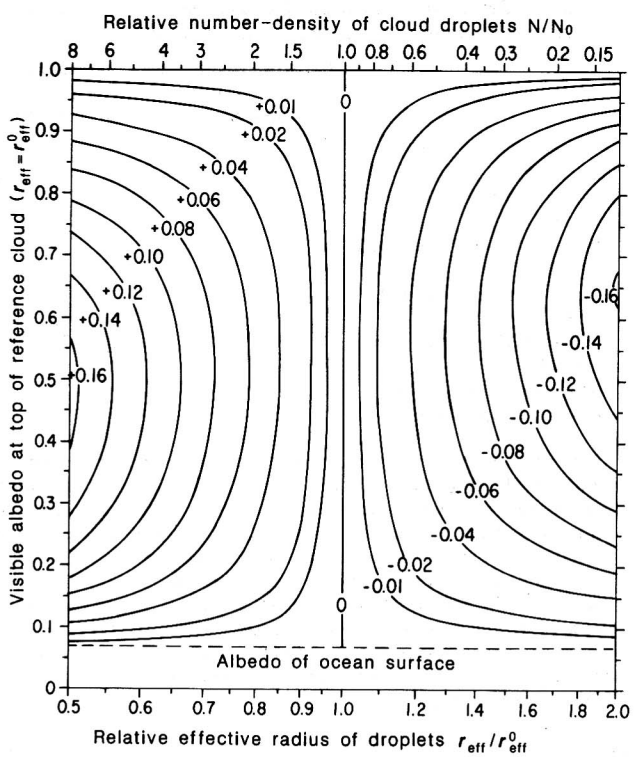

Fig. 1 Change (Δa) of visible albedo (0.6-μm wavelength) at cloud top caused by changing droplet number-density N while holding vertically integrated liquid water content (liquid water path, LWP) constant. Δa is plotted as a function of the albedo of the reference cloud and the effective radius (r_{eff}, the surface-area-weighted mean radius[65]) of the dropsize distribution relative to that of the reference cloud (r^0_{eff}). The corresponding change in top-of-atmosphere albedo (needed for estimating the effect on Earth radiation budget) can be obtained approximately by multiplying these values by 0.8, as described in footnote of Table 1. The different albedos for the reference cloud (vertical axis) correspond to different values of LWP. When LWP and the shape of the dropsize distribution are held fixed, the number-density of cloud droplets N is related to r_{eff} by $N/N_0 = (r_{eff}/r^0_{eff})^{-3}$, shown on the scale at the top of the figure. These calculations used $r^0_{eff} = 8$ μm, but the figure also is approximately valid for other reference clouds: the plotted values of Δa are in error by less than 20% if albedo <0.9 and $4 \leq r^0_{eff} \leq 500$ μm (that is, anywhere in the range of r_{eff} found in real clouds by Hegg[66]). The size distributions used for the calculations are almost monodisperse, broadened just enough to average over the oscillations in the Mie-scattering quantities. However, the calculations are also valid for any realistic size distributions with the same r_{eff}, as Hansen and Travis[65] showed that the scattering properties of a cloud are controlled essentially by r_{eff}, with very little influence from other moments of size distribution. These calculations assume a direct solar beam at the global average zenith angle $\theta_0 = 60°$, incident on a cloud of spherical droplets of pure water, above an ocean surface. The albedo of an ocean surface under a cloud is essentially independent of wavelength and averages 0.06–0.08 (refs 67–69); these calculations assumed 0.07 (dashed horizontal line). The computation of phase function, single-scattering albedo and extinction efficiency for individual cloud droplets used the Mie program of Wiscombe[70] assuming the refractive index for water is $1.332-1.09+10^{-8}i$ at 0.6 μm wavelength[71]. The computation of radiative transfer in the cloud used the delta-Eddington approximation[72]. This leads to absolute errors in albedo (for water-clouds at visible wavelengths and $\theta_0 = 60°$) of 0.00 to 0.03 depending on cloud optical thickness (Fig. 8 of ref. 73), but the error in albedo differences plotted here is much smaller, generally by a factor of 10.

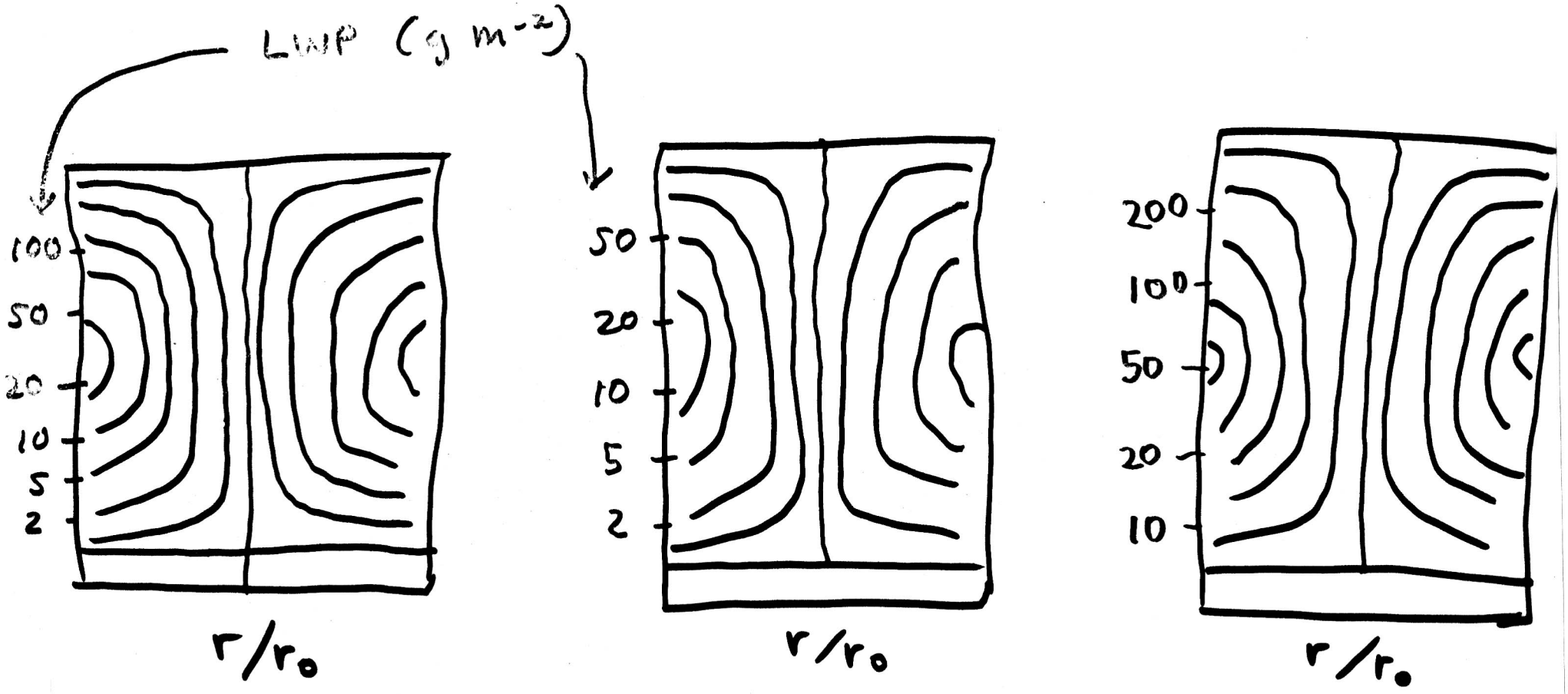

$r_0 = 8\ \mu m$
$\theta_0 = 60°$

$r_0 = 4\ \mu m$
$\theta_0 = 60°$

$r_0 = 8\ \mu m$
$\theta_0 = 0°$